Effective Field Theory for Large-Scale

大尺度有效场论

Structure

结构

Mikhail M. Ivanov

米哈伊尔·M. 伊万诺夫

Contents

目录

Introduction. 214

引言. 214

Why Does the EFT of LSS Work? 216

为什么大尺度结构有效场论成立? 216

A Wrong but Useful Model: Pressureless Perfect Fluid. 217

一个错用但有用的模型: 无压理想流体. 217

Linear Theory. 218

线性理论. 218

Non-linear Perturbation Theory 222

非线性微扰理论 222

IR and UV Singularities. 225

红外与紫外奇点. 225

Physical IR Effects. 229

物理红外效应. 229

Physical UV Effects 231

物理紫外效应 231

Lessons. 233

结论. 233

Large-Scale Structure as an Effective Fluid. 234

作为有效流体的大尺度结构. 234

The Stress Tensor and Time (Non)-locality 235

应力张量与时间 (非) 定域性 235

Stochasticity. 237

随机性. 237

One-Loop Power Spectrum in the EFTofLSS 238

大尺度结构有效场论中的单圈功率谱 238

Power Counting and the Scaling Universe. 240

幂次计数与标度宇宙. 240

Path Integral Methods: Time-Sliced Perturbation Theory 241

路径积分方法: 时间切片微扰理论 241

Generating Functional for Large-Scale Structure 242

大尺度结构生成泛函 242

Soft Limits and IR Safety 246

软极限与红外安全性 246

IR Resummation 247

红外重求和 247

UV Renormalization 249

紫外重整化 249

Comparison with Data 254

与实验数据对比 254

Galaxy Bias and Redshift Space Distortions 254

星系偏置与红移空间畸变 254

Galaxies in the EFT. 255

有效场论中的星系 255

Redshift Space Distortions 255

红移空间畸变 255

Summary and Outlook. 256

总结与展望 256

References 257

参考文献 257

M. M. Ivanov ( )

M. M. 伊万诺夫 ( )

Institute for Advanced Study, Princeton, NJ, USA

美国新泽西州普林斯顿高等研究院

e-mail: ivanov@ias.edu

电子邮箱:ivanov@ias.edu

This chapter is a non-expert introduction to the effective field theory of large-scale structure. First, we give a detailed pedagogical explanation of why previous attempts to build non-linear cosmological perturbation theory failed. After that, we introduce the description of dark matter as an effective non-ideal fluid and show how it corrects the shortcomings of the previous approaches. Finally, we develop a formulation of the effective field theory of large-scale structure from a non-equilibrium field theory perspective, called time-sliced perturbation theory. We show how this framework can be used for a consistent renormalization of cosmological correlation functions and a systematic resummation of large infrared effects relevant for the baryon acoustic oscillations.

本章为非专业人士介绍大尺度结构有效场论。首先，我们以教学角度详细解释了为何过往构建非线性宇宙学微扰论的尝试均告失败。随后，我们引入将暗物质描述为有效非理想流体的方法，并展示该方法如何解决了过往方法的缺陷。最后，我们从非平衡场论视角构建了大尺度结构有效场论的表述，称为时间切片微扰论。我们展示了如何利用该框架对宇宙学关联函数进行一致重整，并对与重子声学振荡相关的大红外效应进行系统重求和。

Keywords

关键词

Large-scale structure - Cosmological perturbation theory - Effective field theory - Renormalization - Baryon acoustic oscillations

大尺度结构-宇宙扰动理论-有效场论-重整化-重子声学振荡

Introduction

简介

Cosmology is a rapidly evolving branch of modern physics. Over the last few decades, cosmology has metamorphosed from a speculative field into a highly precise and predictive science. As of now, we have established a coherent picture of our universe and its evolution, with typical agreement between theory and observations at the percent level [2].

宇宙学是现代物理学中发展迅速的一个分支。过去几十年间，宇宙学已经从一个推测性领域转变为一门高度精确、具备预测能力的科学。截至目前，我们已经建立了关于宇宙及其演化的连贯图景，理论与观测的契合度通常达到百分位数水平 [2]。

These spectacular advances have been driven, to a large extent, by the measurements of the cosmic microwave background (CMB) anisotropies. These anisotropies are small fluctuations in temperature and polarization of the photons that were left over when first atoms were formed. The CMB anisotropies trace cosmological density fluctuations produced in a very early universe during a process called ”inflation.” Inflation may have happened when typical energies in the universe could be as high as 10^{16}GeV . The cosmological fluctuations, thus, offer a unique way to probe physics at these high energies.

这些惊人的进展在很大程度上是由宇宙微波背景 (CMB) 各向异性的测量推动的。这些各向异性是宇宙第一批原子形成时遗留下来的光子, 其温度和偏振存在微小涨落。CMB 各向异性追踪了极早期宇宙在被称为“暴胀”的过程中产生的宇宙密度涨落。暴胀可能发生在宇宙的典型能量高达 10^{16}GeV 的阶段。因此，宇宙涨落为探索这些高能下的物理提供了独一无二的途径。

Importantly, the observed cosmological fluctuations also carry information about other dynamical stages of our universe. Hence, the entire cosmic history can be inferred from them. In particular, the CMB fluctuations are a sensitive probe of dark matter (DM), dark energy, etc.

重要的是，观测到的宇宙涨落还承载着宇宙其他动力学阶段的信息。因此，我们可以从中推导出完整的宇宙演化史。具体而言，CMB 涨落是探测暗物质 (DM)、暗能量等的灵敏探针。

A crucial advantage of cosmological fluctuations is that they are small perturbations on top of a homogeneous and isotropic background. This means that they can be systematically described within linear cosmological perturbation theory. That is a major reason why the study of the CMB has been so successful.

宇宙涨落的一个关键优势在于，它们是均匀各向同性背景之上的小扰动，这意味着我们可以在宇宙学线性微扰理论框架内对其进行系统描述，这也是 CMB 研究如此成功的主要原因。

Despite significant progress made with the CMB, there are many questions that remain unanswered. The most pressing ones are the physical nature of dark matter, dark energy, and inflation. In order to elucidate these questions and thus continue making progress in cosmology, we have to measure more cosmological fluctuations. This may be problematic with the CMB as its information content is getting more and more exhausted. However, there is another source of cosmological information independent from the CMB, which is becoming more important now. This is cosmic large-scale structure, i.e., the distributions of mass and luminous objects (e.g., galaxies), which also trace primordial perturbations. At face value, large-scale structure offers orders of magnitude more information than the CMB as its distribution is intrinsically three-dimensional. In contrast, individual observables (Fourier modes) accessible with the CMB are distributed across a two-dimensional celestial sphere.

尽管 CMB 研究已经取得了重大进展，仍有许多问题悬而未决。最紧迫的问题包括暗物质、暗能量和暴胀的物理本质。为了阐明这些问题，推动宇宙学继续发展，我们需要对更多宇宙涨落进行测量。CMB 在这里可能存在局限，因为它的信息含量已经被挖掘得越来越充分。不过，还存在另一个独立于 CMB 的宇宙信息来源，如今它的重要性正不断提升，这就是宇宙大尺度结构，即物质和发光天体 (比如星系) 的分布，它们同样可以追踪原初扰动。从表面上看，大尺度结构提供的信息量比 CMB 高出好几个数量级，因为它的分布本质上是三维的，而 CMB 能获取的独立观测量 (傅里叶模态) 分布在二维天球上。

The main drawback of large-scale structure though is that it is a non-linear tracer of cosmological fluctuations, and thus linear cosmological perturbation theory is insufficient for their study. There have been many attempts to build a non-linear cosmological perturbation theory for large-scale structure. But these attempts have not been successful because they were based on unjustified assumptions, such as that dark matter behaves as a pressureless perfect fluid in the non-linear regime.

但大尺度结构的主要缺点在于，它是宇宙涨落的非线性示踪剂，线性宇宙学微扰理论不足以支撑相关研究。人们已经做了许多尝试，试图为大尺度结构构建非线性宇宙学微扰理论，但这些尝试都不成功，因为它们都基于不合理的假设，比如假设暗物质在非线性区表现为无压理想流体。

A major breakthrough has been made after applying particle physics ideas to large-scale structure. The key observation is that the large-scale distribution features several distance scales with a large hierarchy between them. In particular, the complicated phenomena associated with fully non-linear collapse of matter and galaxy formation happen on scales $\sim$ 5Mpc . This is much smaller than the typical galaxy separations of interest $\sim$ 100Mpc . This means that one is working practically in a large-scale limit, where the dynamical evolution should be representable in a simple way. In this limit, it is sufficient to use only the degrees of freedom that are active on large scales, while all effects of unknown short-scale physics can be systematically parameterized by a set of effective operators built out of these long-distance degrees of freedom. In particle physics, this phenomenon is called decoupling. Using this key principle, one can describe the distribution of galaxies on large scales even without a detailed knowledge of the galaxy formation physics. This idea has been formalized in a framework called the effective field theory of large-scale structure (EFTofLSS) [9, 23, 33] (see [6, 18] for recent reviews). By construction, EFTofLSS is a rigorous program of successive approximations that can be carried out to arbitrary accuracy. This can be contrasted with phenomenological models, which

are constructed to merely mimic aspects of structure formation, but are not large-scale structure theories in the strict sense.

将粒子物理学思想应用到大尺度结构研究后，领域取得了重大突破。核心发现是，大尺度分布存在多个特征距离尺度，且尺度之间层级分明。具体来说，与物质完全非线性坍缩、星系形成相关的复杂过程都发生在尺度 ~ 5Mpc 上，这远小于我们关注的典型星系间距 ~ 100Mpc 。也就是说，我们的研究实际上处于大尺度极限下，在该极限下动力学演化应当可以用简单的方式表示。在这个极限下，我们只需要保留大尺度上活跃的自由度，所有未知小尺度物理的效应都可以通过一组由长程自由度构造的有效算符进行系统参数化。在粒子物理学中，这种现象被称为退耦。利用这个核心原理，哪怕不掌握星系形成物理的细节，我们也可以描述大尺度上的星系分布。这一思想已经在大尺度结构有效场论 (EFTofLSS) [9, 23, 33] 框架中得到形式化 (最新综述见 [6, 18])。从构造上来说，EFTofLSS 是一套严谨的逐次逼近方案，可以将精度提升至任意要求，这和唯象模型形成了鲜明对比——唯象模型仅仅是为了模拟结构形成的部分特征而构建，严格来说并不算是大尺度结构理论。

In this chapter, we give a non-specialist introduction to the effective field theory of large-scale structure. After giving a brief qualitative picture of structure formation in section ”Why Does the EFT of LSS Work?,” we present a detailed pedagogical description of a pressureless perfect fluid model (PPFM) for structure formation in section ”A Wrong but Useful Model: Pressureless Perfect Fluid.” This model is ultimately wrong, but it will give us many valuable lessons. In particular, we will see how IR and UV singularities in PPFM are related to physical effects of large-scale bulk flows and short-scale backreaction. We introduce the EFTofLSS in terms of Eulerian hydrodynamics in section ”Large-Scale Structure as an Effective Fluid,” where we show in detail how this approach corrects the shortcomings of PPFM. In section ”Path Integral Methods: Time-Sliced Perturbation Theory,” we present a path integral formulation for the EFTofLSS, which proved particularly convenient for the study of baryon acoustic oscillations. In section ”Comparison with Data,” we compare the predictions of the EFTofLSS for the dark matter power spectrum with N-body simulation data and find perfect agreement on mildly non-linear scales. We briefly discuss extensions to galaxy bias and redshift space distortions in section ”Galaxy Bias and Redshift Space Distortions.” We draw conclusions in section ”Summary and Outlook.”

本章我们将为非专业读者介绍大尺度结构有效场论 (EFTofLSS)。在“为什么 LSS 的 EFT 是成立的?”一节中，我们先给出结构形成的定性概览，随后在“一个错误但有用的模型: 无压理想流体”一节中，详细教学讲解描述结构形成的无压理想流体模型 (PPFM)。该模型本质上并不正确，但仍能为我们带来诸多宝贵启示。具体而言，我们会看到 PPFM 中的红外与紫外奇点如何对应大尺度整体流和小尺度反作用的物理效应。我们在“作为有效流体的大尺度结构”一节中基于欧拉流体力学引入 EFTofLSS，在此我们将详细说明该方法如何修正 PPFM 的缺陷。在“路径积分方法: 时间切片微扰论”一节中，我们给出 EFTofLSS 的路径积分表述，该表述已被证明对研究重子声学振荡尤其方便。在“与数据对比”一节中，我们将 EFTofLSS 对暗物质功率谱的预言与 N 体模拟数据进行对比，发现在弱非线性尺度上二者完全符合。我们在“星系偏置与红移空间畸变”一节中简要讨论了该理论对星系偏置和红移空间畸变的推广。我们在“总结与展望”一节中给出本章结论。

Why Does the EFT of LSS Work?

大尺度结构有效场论 (EFT of LSS) 为何成立?

Large-scale structure of the universe is the distribution of matter and galaxies on large cosmological scales. This distribution has been observed for a very long time, much before the CMB. The galaxies are clearly not distributed randomly. In fact, the structure of our universe on large scales is a result of cosmological evolution that depends on the initial conditions and constituents of our universe. This distribution is approximately homogeneous and isotropic on very large scales, which suggests that its proper description should be in terms of small fluctuations around a smooth cosmological background. This matches observable properties of other cosmological fields, such as the CMB temperature fluctuations.

宇宙大尺度结构指的是宇宙学大尺度上的物质与星系分布。远在人们观测宇宙微波背景 (CMB) 之前，就已经对该分布开展了长期观测。星系显然不是随机分布的。实际上，宇宙大尺度的结构是依赖宇宙初始条件与组分的宇宙学演化的结果。在极大尺度上，该分布近似均匀且各向同性，这说明对它的恰当描述应当围绕平滑宇宙学背景的小涨落展开。这与其他宇宙学场的可观测性质一致，比如 CMB 温度涨落。

The CMB temperature fluctuations are very small, $\delta T/T \sim 10^{-5}$, and hence they can be accurately described by means of relativistic linear cosmological perturbation theory. Just like the CMB, galaxies represent fluctuations in the cosmological density field. However, unlike the CMB, they cannot be described with linear theory. Galaxies are produced by complicated astrophysical processes taking place on the background of collapsing matter. This collapse produces halos where galaxies reside. As a result, galaxies probe the underlying matter distribution indirectly, i.e., galaxies are tracers of matter. The clustering of matter is also non-linear as it subject to the Jeans instability.

CMB 温度涨落非常小，$\delta T/T \sim 10^{-5}$ ，因此可以用相对论线性宇宙学微扰理论精确描述。和 CMB 一样，星系对应宇宙学密度场中的涨落。但和 CMB 不同，星系无法用线性理论描述。星系是坍缩物质背景下发生的复杂天体物理过程的产物。坍缩形成了星系寄居的暗物质晕。因此，星系是间接探测底层物质分布的，也就是说，星系是物质的示踪体。物质成团同样是非线性的，因为它会受到金斯不稳定性的影响。

In order to obtain a simple physical picture of matter clustering, we can think of matter as a collection of collisionless particles. These particles move with certain velocities set by the initial conditions in our universe, and if they get sufficiently close to one another, they virialize and form bound structures - halos; see Fig. 1. In this simplified picture, DM particles move in a mean gravitational potential until they stick together by gravity forces at short scales.

为了得到物质成团的简洁物理图像，我们可以将物质视为无碰撞粒子的集合。这些粒子以宇宙初始条件给定的特定速度运动，如果它们彼此足够靠近，就会发生维里化并形成束缚结构——暗物质晕；见图 1。在这个简化图像中，暗物质 (DM) 粒子在平均引力势中运动，直到在小尺度上被引力结合在一起。

There are two relevant scales in this problem: the Hubble horizon scale $l_H \sim \mathcal{H}^{-1} \sim 3h^{-1}$Gpc and the halo virial radius $R_{\rm vir} \sim 3h^{-1}$Mpc . These scales correspond to different physics: at the horizon, the relativistic effects become important, and one has to use general relativity to describe motions on these scales. At the scales of the halo radius, the fully non-linear processes of gravitational collapse take place, which are hard (if possible) to model analytically. However, there is a wide range of scales r ,

这个问题存在两个特征尺度: 哈勃视界尺度 $l_H \sim \mathcal{H}^{-1} \sim 3h^{-1}$Gpc 和暗物质晕维里半径 $R_{\rm vir} \sim 3h^{-1}$Mpc 。这两个尺度对应不同物理: 在视界尺度上，相对论效应变得重要，必须用广义相对论描述该尺度下的运动。在暗物质晕半径尺度上，引力坍缩的完全非线性过程发生，很难 (即便有可能) 进行解析建模。不过，存在很宽的尺度范围 r ,

$$R_{\rm vir} \ll r \ll l_H \tag{1}$$

where one can build a systematic analytic description of the non-linear galaxy distribution in terms of the distance (derivative) expansion. These scales are called quasi-linear, because their description is formulated in terms of a perturbation theory over the linear theory result. On one end, physics operating on these scales is essentially Newtonian, since the relativistic corrections are suppressed by powers of r/l_H . On the other end, the fully non-linear effects of halo formation and virialization are suppressed by powers of $R_{\rm vir}/r$. In the EFT jargon, the halo formation physics "decouples" from the large-scale physics. The typical galaxy separations that are relevant for galaxy surveys are $r \sim (10-100)\,h^{-1}$Mpc , so that the relativistic effects can be ignored. However, the non-linear effects associated with the expansion in $R_{\rm vir}/r$ are very important in practice. The EFTofLSS is a systematic framework that allows to compute the galaxy distribution perturbatively, effectively expanding in powers of the small parameter $R_{\rm vir}/r$.

我们可以在这个范围内，以距离 (导数) 展开的方式构建非线性星系分布的系统解析描述。这些尺度被称为准线性尺度，因为它的描述是在线性理论结果基础上做微扰论构建的。一方面，该尺度上的物理本质上是牛顿引力的，因为相对论修正被 r/l_H 的幂次压低。另一方面，暗物质晕形成与维里化的完全非线性效应被 $R_{\rm vir}/r$ 的幂次压低。用有效场论的术语来说，暗物质晕形成的物理过程和大尺度物理“退耦”了。星系巡天中关联的典型星系间距处于 $r \sim (10-100)\,h^{-1}$Mpc 范围，因此相对论效应可以忽略。不过，和 $R_{\rm vir}/r$ 展开相关的非线性效应在实际中非常重要。大尺度结构有效场论 (EFTofLSS) 是一个系统化框架，它允许我们微扰地计算星系分布，有效按小参数 $R_{\rm vir}/r$ 的幂次做展开。

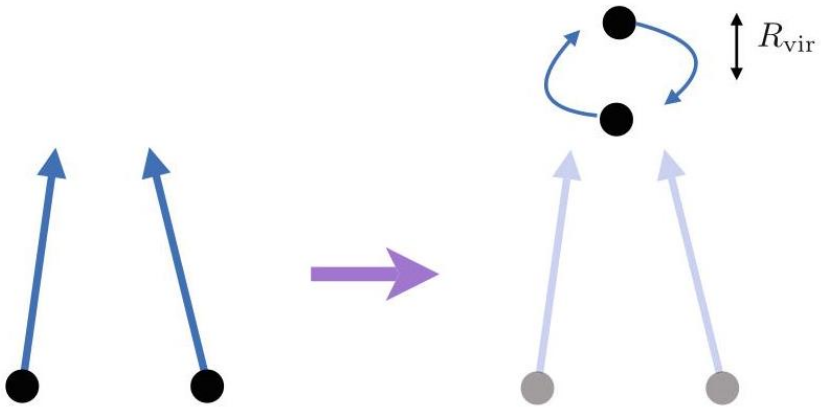

Fig. 1 Cartoon of the DM clustering. Left panel: Collapse of DM particles. When the particles approach each other sufficiently close, they "stick" together by gravity and form a virialized object, DM halo (Right panel). $R_{\rm vir}$ is the typical virial radius of the halo

图 1 DM 成团示意图。左图:DM 粒子坍缩。当粒子彼此足够靠近时，引力将它们“结合”在一起，形成维里化天体 DM 晕 (右图)。$R_{\rm vir}$ 是暗物质晕的典型维里半径

In this chapter, we give an introduction into this subject, focusing on the physical intuition behind this approach and the most important technical aspects. In what follows, we assume that the reader possess basic knowledge of cosmological perturbation theory and quantum field theory.

在本章中，我们将介绍这一领域，聚焦该方法背后的物理直觉和最重要的技术要点。在下文中，我们假设读者已经掌握宇宙学微扰论和量子场论的基础知识。

A Wrong but Useful Model: Pressureless Perfect Fluid

一个错误但有用的模型: 无压理想流体

There are three key empirical facts about dark matter:

关于暗物质有三个关键经验事实:

1. DM behaves like dust on large scales, i.e., its pressure is vanishingly small.

1. 暗物质在大尺度上表现得像尘埃，即它的压力极小，几乎可以忽略。

2. DM perturbations are small on large scales.

2. 暗物质的大尺度扰动幅度很小。

3. The initial conditions for structure formation in our universe are Gaussian to a very good accuracy.

3. 我们宇宙结构形成的初始条件，在极高精度下服从高斯分布。

These three facts are consistent with linear cosmological perturbation theory, where DM fluctuations are described as a pressureless perfect fluid. Therefore, it seems reasonable to extend this description to the fully non-linear level. Historically, this had been the traditional approach before the EFTofLSS. The pressureless perfect fluid approach is wrong, but however, it gives us many useful lessons and important technical tools. Thus, in this section, we will consider the pressureless perfect fluid hydrodynamics as a toy model for matter clustering. This approach is also known as standard perturbation theory [10]. Our main variables will be the peculiar velocity field v^i and the overdensity field

这三个事实与线性宇宙学扰动理论自洽，该理论将暗物质涨落描述为无压理想流体。因此，将这个描述推广到完全非线性阶段看起来是合理的。从历史上看，这是大尺度结构有效场论 (EFTofLSS) 提出之前的传统方法。无压理想流体方法本身是错误的，但它给我们留下了许多有用的经验和重要的技术工具。因此，我们在本节将无压理想流体流体力学作为物质成团的玩具模型进行讨论。这个方法也被称为标准微扰论 [10]。我们的核心变量是本动速度场 v^i 和 overdensity 场

$$\delta(\tau, \mathbf{x}) = \frac{\rho(\tau, \mathbf{x}) - \rho_0(\tau)}{\rho_0(\tau)}, \tag{2}$$

where ρ_0 is the background density and τ is the conformal time. The naive perturbation theory assumption is that δ and $|\mathbf{v}|$ are small parameters.

其中 ρ_0 是背景密度，τ 是共形时间。朴素微扰论的假设是 δ 和 $|\mathbf{v}|$ 都是小参数。

The equations of motion for dust on the cosmological background in the Newtonian approximation (modes are sufficiently inside the horizon) are given by

牛顿近似下 (模式充分处在视界以内)，宇宙学背景下尘埃的运动方程由下式给出

$$\frac{\partial}{\partial\tau}\delta + \partial_i\left[(1+\delta)\,v^i\right] = 0, \tag{3}$$

$$\frac{\partial}{\partial\tau}v^i + \mathcal{H}v^i + v^j\partial_j v^i = -\partial_i\Phi,$$

where the perturbed gravitational potential satisfies the Poisson equation

其中扰动引力势满足泊松方程

$$\Delta\Phi = 4\pi G\rho_0 a^2\delta = \frac{3}{2}\Omega_m\mathcal{H}^2\delta, \tag{4}$$

and $\Omega_m(\tau)$ is the time-dependent dark matter density fraction,

且 $\Omega_m(\tau)$ 是随时间变化的暗物质密度分数，

$$\Omega_m(\tau) = \Omega_m^{(0)}a^{-3}(\tau)\,/\left(\Omega_m^{(0)}a^{-3}(\tau) + \Omega_\Lambda^{(0)}\right),$$

while $\Omega_m^{(0)}, \Omega_\Lambda^{(0)}$ are density fractions at the current conformal time τ_0 .

而 $\Omega_m^{(0)}, \Omega_\Lambda^{(0)}$ 是当前共形时间 τ_0 下的密度分数。

The only sources of non-linearity in Eqs. 3 are convective derivatives, e.g., $v^j\partial_j v^i$. If we drop these terms for the time being, we will find the standard linear equations of motion that describe the cosmological growth of structure. Let us discuss this linear solution in detail.

式 (3) 中非线性的唯一来源是对流导数，例如 $v^j\partial_j v^i$ 。如果我们暂时舍去这些项，我们就会得到描述宇宙结构增长的标准线性运动方程。下面我们详细讨论这个线性解。

Linear Theory

线性理论

Looking at linearized Eq. (3), we notice that the source term in the r.h.s. is a gradient of the gravitational potential, which can only source the longitudinal part of v^i. Thus, we can neglect the curl part in what follows. Introducing the velocity divergence field

观察线性化的式 (3)，我们注意到方程右侧的源项是引力势的梯度，它仅能激发 v^i 的纵分量。因此，在下文中我们可以忽略旋度分量。引入速度散度场

$$\theta = -\frac{\partial_i v^i}{\mathcal{H}} \tag{5}$$

we can rewrite the Euler and continuity equations as

我们可将欧拉方程与连续性方程改写为

$$\mathcal{H}^{-1}\partial_\tau \delta - \theta = 0$$

$$\mathcal{H}^{-1}\partial_\tau \theta + \left(1 + \frac{\partial_\tau \mathcal{H}}{\mathcal{H}^2}\right)\theta - \frac{3}{2}\Omega_m(\tau)\,\delta = 0. \tag{6}$$

The solution to this equation depends on the background evolution. During matter domination, $\Omega_m(\tau) = 1, \mathcal{H} = \frac{2}{\tau}$, the cosmologically relevant solution is given by the growing mode,

该方程的解依赖于背景演化。在物质主导阶段，$\Omega_m(\tau) = 1, \mathcal{H} = \frac{2}{\tau}$，宇宙学相关的解由增长模式给出，

$$\theta = \delta = a(\tau)\,\delta_0(\mathbf{x}) = \delta^{(1)}(\tau, \mathbf{x}), \tag{7}$$

where $\delta_0(\mathbf{x})$ is the density initial fluctuation. In a more general situation, we have

其中 $\delta_0(\mathbf{x})$ 是初始密度涨落。在更一般的情况下，我们有

$$\delta^{(1)}(\tau, \mathbf{x}) = D_+(\tau)\,\delta_0(\mathbf{x}), \text{ where } D_+(\tau) = \frac{5}{2}\Omega_m^{(0)}\mathcal{H}_0^2\frac{\mathcal{H}}{a}\int_0^\tau d\tau' \frac{a(\tau')}{\mathcal{H}'^2(\tau')},$$

(8)

where $\mathcal{H}_0^2 = \mathcal{H}^2(\tau_0)$.

其中 $\mathcal{H}_0^2 = \mathcal{H}^2(\tau_0)$。

We will work in Fourier space (Our convention is $\delta(\mathbf{x}) = \int_{\mathbf{k}} f_{\mathbf{k}} e^{i\mathbf{k}\cdot\mathbf{x}}, \int_{\mathbf{k}} \equiv \int \frac{d^3k}{(2\pi)^3}$, and $\delta(\mathbf{k}) = \int d^3x \delta(\mathbf{x}) e^{-i\mathbf{k}\cdot\mathbf{x}}$.) where the initial conditions are defined by the field $\delta_0(\mathbf{k})$. This field is a stochastic variable. This reflects an important feature that the matter distribution is stochastic, i.e., the observed galaxy maps (tracing matter) can be thought of as drawn from a certain distribution. It is the statistical properties of this distribution that carry cosmological information and can be compared to model predictions. The simplest such statistic is the two-point function of the matter density,

我们将在傅里叶空间中计算 (我们的约定是 $\delta(\mathbf{x}) = \int_{\mathbf{k}} f_{\mathbf{k}} e^{i\mathbf{k}\cdot\mathbf{x}}, \int_{\mathbf{k}} \equiv \int \frac{d^3k}{(2\pi)^3}$，且 $\delta(\mathbf{k}) = \int d^3x \delta(\mathbf{x}) e^{-i\mathbf{k}\cdot\mathbf{x}}$ 。)，其中初始条件由场 $\delta_0(\mathbf{k})$ 定义。该场是一个随机变量，这反映了物质分布的一个重要性质: 物质分布是随机的，也就是说，追踪物质的观测星系图像可以认为是从某个分布中抽取得到的。正是该分布的统计性质携带了宇宙学信息，可与模型预言进行比较。其中最简单的统计量是物质密度的二点关联函数,

$$\langle \delta_0(\mathbf{k}) \delta_0(\mathbf{k}') \rangle = (2\pi)^3 \delta_D^{(3)}(\mathbf{k}+\mathbf{k}') P_{\rm lin}(k). \tag{9}$$

Hence, in linear theory, we have

因此，在线性理论框架下，我们得到

$$\left\langle \delta^{(1)}(\mathbf{k}) \delta^{(1)}(\mathbf{k}') \right\rangle = (2\pi)^3 \delta_D^{(3)}(\mathbf{k}+\mathbf{k}') P_{11}(k,\tau), \tag{10}$$

where $P_{11}(k,\tau) = D_+^2(\tau) P_{\rm lin}(k)$. As standard in cosmological perturbation theory, we choose the normalization such that $D_+(\tau=\tau_0)=1$, in which case $P_{\rm lin}(k)$ is a linear matter power spectrum at redshift zero. We show it as a function of wavenumber in Fig. 2 for the WMAP-like cosmology used in the simulations [44].

其中 $P_{11}(k,\tau) = D_+^2(\tau) P_{\rm lin}(k)$。正如宇宙学微扰论中的标准做法, 我们选择归一化使得 $D_+(\tau=\tau_0)=1$，此时 $P_{\rm lin}(k)$ 是红移零处的线性物质功率谱。我们在图 2 中给出了模拟 [44] 所用 WMAP 类宇宙学模型下，功率谱随波数的变化。

The linear matter power spectrum in the ΛCDM model has an intricate shape that reflects different stages in the cosmological evolution: it has asymptotics $P_{11} \propto k\,(k\to 0), P_{11} \propto k^{-3}\ln^2(k)\,(k\to\infty)$, and a peak at the wavenumber that corresponds to the comoving size of Hubble horizon at the time of the matter-radiation equality, $k_{\rm eq} \approx 0.015 h{\rm Mpc}^{-1}$. In a narrow range of scales, the matter power spectrum can be approximated as a power law [24, 50] ,

ΛCDM 模型的线性物质功率谱具有复杂的形状, 反映了宇宙演化的不同阶段: 它满足渐近行为 $P_{11} \propto k\,(k\to 0), P_{11} \propto k^{-3}\ln^2(k)\,(k\to\infty)$ ，在对应物质辐射相等时刻哈勃视界共动尺度的波数处存在一个峰 $k_{\rm eq} \approx 0.015 h{\rm Mpc}^{-1}$ 。在一个窄的尺度范围内，物质功率谱可以近似为幂律形式 [24, 50] ,

$$P_{\rm lin}(k) \approx \frac{1}{2\pi^2 k_{\rm NL}^3} \left(\frac{k}{k_{\rm NL}}\right)^n; \tag{11}$$

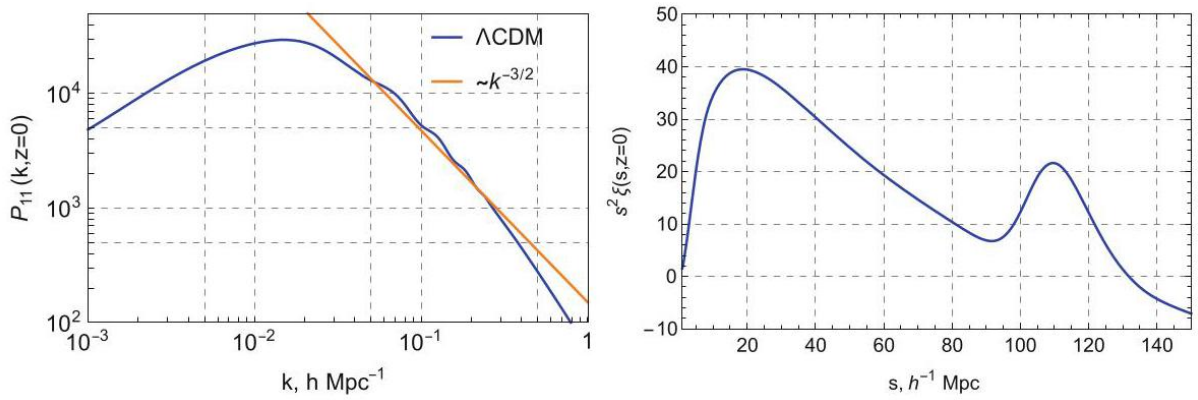

Fig. 2 Left panel: The linear matter power spectrum P_{11} at redshift $z = 0$ in the ΛCDM model (blue curve) vs. the power law approximation for $k \approx 0.1h\text{Mpc}^{-1}$. Right panel: The linear two-point correlation function

图 2 左图: ΛCDM 模型中红移 $z = 0$ 处的线性物质功率谱 P_{11} (蓝线) 与 $k \approx 0.1h\text{Mpc}^{-1}$ 的幂律近似。右图: 线性二点关联函数

see Fig. 2. From most observationally relevant wavenumbers are $k \sim 0.1h\text{Mpc}^{-1}$, where $n \approx -1.5$ provides a good approximation to the actual power spectrum. We stress that we will use this approximation only for rough estimates. All actual calculations will be based on the actual Λ CDM power spectrum.

参见图 2。对绝大多数观测相关波数而言，$k \sim 0.1h\text{Mpc}^{-1}$ 成立，此时 $n \approx -1.5$ 是对实际功率谱的良好近似。需要强调的是，我们仅将该近似用于粗略估计，所有实际计算都基于真实的 Λ CDM 功率谱。

Another important quantity is the position space correlation function, which is a Fourier image of the power spectrum,

另一个重要物理量是位置空间关联函数，它是功率谱的傅里叶变换,

$$\langle \delta(\mathbf{x})\,\delta(\mathbf{x}+\mathbf{s})\rangle \equiv \xi(s) = \frac{1}{2\pi^2}\int dk k^2 P_{\text{lin}}(k)\,\frac{\sin(ks)}{ks}. \tag{12}$$

The correlation function for the ΛCDM cosmology is shown in Fig.2. Note the bump at $s_{\text{BAO}} \sim 110h^{-1}\text{Mpc}$, which corresponds to the baryon acoustic oscillations in the matter power spectrum. We see that the correlation function is a smooth function of scales and it can be approximated as a power law in position space plus a Gaussian that roughly captures the BAO peak.

ΛCDM 宇宙学的关联函数如图 2 所示。可以看到在 $s_{\text{BAO}} \sim 110h^{-1}\text{Mpc}$ 处存在一个峰，对应物质功率谱中的重子声学振荡。可以看到关联函数是尺度的光滑函数，可以近似为位置空间中的幂律加上一个大致拟合 BAO 峰的高斯函数。

Let us estimate now what is the typical density variance at a given point $\mathbf{x}$. Quite surprisingly, we find that it is actually infinite for the ΛCDM power spectrum,

现在我们来估计给定点 $\mathbf{x}$ 处的典型密度涨落方差。出乎意料的是，我们发现对于 ΛCDM 功率谱，该值实际上是无穷大，

$$\left\langle \delta^2(\mathbf{x}) \right\rangle = \int \frac{d^3q}{(2\pi)^3} P_{\rm lin}(q) \to \infty. \tag{13}$$

This integral diverges in the UV, and hence, the assumption that δ is small is broken down by short-scale mass fluctuations that are formally infinite in the ΛCDM cosmology. It seems that our linear theory is not actually well defined at all.

该积分在紫外端发散，因此，δ 很小这一假设被小尺度质量涨落破坏，在 ΛCDM 宇宙学中该涨落形式上是无穷大。看来我们的线性理论实际上根本没有良好定义。

A more reasonable approach would be to remove the short-scale fluctuations first, i.e., introduce a low-pass filter, e.g., a spherical top hat in position space,

更合理的做法是先去除小尺度涨落，即引入低通滤波器，例如位置空间中的球形顶帽滤波器，

$$W_R(\mathbf{x}) = \frac{3}{4\pi} H(|\mathbf{x}| - R), \tag{14}$$

which effective removes all fluctuations from scales that are shorter than R^{-1} . Note that $H(x)$ above is the Heaviside step function. The filtered density field is given by $\delta^{(1)}(\mathbf{k})\widetilde{W}_R(kR)$, where $\widetilde{W}_R(kR) = 3j_1(kR)/(kR)$ is the Fourier transform of the top hat. The mass variance inside a sphere of the radius R is given by

它可以有效滤除所有尺度小于 R^{-1} 的涨落。注意上述 $H(x)$ 是赫维赛德阶跃函数。滤波后的密度场由 $\delta^{(1)}(\mathbf{k})\widetilde{W}_R(kR)$ 给出，其中 $\widetilde{W}_R(kR) = 3j_1(kR)/(kR)$ 是顶帽函数的傅里叶变换。半径为 R 的球内的质量方差为

$$\left\langle \delta_R^2(\mathbf{x}) \right\rangle = \int \frac{d^3k}{(2\pi)^3} P_{\rm lin}(k) \left|\widetilde{W}_R(kR)\right|^2. \tag{15}$$

By appropriately choosing the filtering scale R , we can make sure that the coarse-grained density fluctuations are under control. This observation suggests that natural variables in our perturbation theory should actually be smoothed density and velocity fields. Hence, we need, in fact, to smooth equations (3), which is not done in the PPMF. This is the first observation that signals the inconsistency of our toy model.

通过适当选择滤波尺度 R ，我们可以保证粗粒化密度涨落是受控的。这一观察说明我们微扰理论中的自然变量实际上应当是平滑后的密度场和速度场。因此，我们实际上需要对方程 (3) 做平滑处理，这在 PPMF 中并未完成。这是第一个表明我们这个玩具模型存在不自洽的观察结论。

Another quantity of interest is the displacement field, which measures how much does a fluid element positioned at $\mathbf{x}$ traveled over the structure formation history. Defining $\mathbf{x} = \mathbf{x}_{\rm ini} + \mathbf{s}(\mathbf{x}_{\rm ini})$, we find

另一个我们关注的物理量是位移场，它衡量结构形成历史中，位于 $\mathbf{x}$ 的流体元移动了多少距离。定义 $\mathbf{x} = \mathbf{x}_{\rm ini} + \mathbf{s}(\mathbf{x}_{\rm ini})$ 后，我们得到

$$\mathbf{s} = \int_{\tau_{\rm ini}}^{\tau_0} d\tau \mathbf{v}(\tau, \mathbf{x}). \tag{16}$$

The displacement field is also stochastic since it is sourced by $\mathbf{v}$, which is a random stochastic variable. Using the linear theory result $\partial_i v^i = -a\mathcal{H}\delta_0$, we find that variance of the displacement field is given by

位移场也是随机的，因为它由 $\mathbf{v}$ 源生发，而 $\mathbf{v}$ 是随机变量。利用线性理论结果 $\partial_i v^i = -a\mathcal{H}\delta_0$，我们得到位移场的方差为

$$\left\langle s_i(\mathbf{x}) s^i(\mathbf{x}) \right\rangle = \int_{\mathbf{q}} \frac{P_{11}(q)}{q^2}. \tag{17}$$

Unlike the mass fluctuation variance, the displacement variance in our universe is finite because the above integral actually converges for the ΛCDM power spectrum,

和质量涨落方差不同，我们宇宙中的位移方差是有限的，因为上述积分对于 ΛCDM 功率谱是收敛的，

$$\left\langle s_i(0) s^i(0) \right\rangle \approx \left[6h^{-1}\mathrm{Mpc}\right]^2. \tag{18}$$

However, if the power spectrum were a power law $P_{11} \propto k^n$, it would be divergent in the IR for $n \leq -1$ and in the UV for $n > -1$. Hence, the fact that the all-scale displacement variance is finite in our universe is simply a coincidence.

但如果功率谱是幂律形式 $P_{11} \propto k^n$，那么位移方差会在红外端对 $n \leq -1$ 发散，在紫外端对 $n > -1$ 发散。因此，我们宇宙中全尺度位移方差有限实际上只是一个巧合。

Non-linear Perturbation Theory

非线性微扰论

Let us now solve Eqs. (3) perturbatively. As before, we will replace the velocity field with its divergence. Let us first recast Eqs. (24) as second-order differential equations on δ and θ and in Fourier space,

现在我们对方程 (3) 进行微扰求解。和之前一样，我们会将速度场替换为其散度。首先我们将方程 (24) 改写为傅里叶空间中关于 δ 和 θ 的二阶微分方程，

$$\mathcal{H}^2\left[-a^2\partial_a^2 + \frac{3}{2}(\Omega_m - 2)\, a\partial_a + \frac{3}{2}\Omega_m\right]\delta_{\mathbf{k}} = \mathcal{H}^2\mathcal{I}_\beta + \mathcal{H}\partial_a(a\mathcal{H}\mathcal{I}_\alpha)$$

$$\mathcal{H}^2\left[a^2\partial_a^2 + \left(4 - \frac{3}{2}\Omega_m\right)a\partial_a + \left(2 + \frac{\partial_a^2\mathcal{H}}{\mathcal{H}} + \left(4 - \frac{3}{2}\Omega_m\right)\frac{\partial_a\mathcal{H}}{\mathcal{H}} - 3\Omega_m\right)\right]\theta_{\mathbf{k}}$$

$$= -\partial_a\left(a\mathcal{H}^2\mathcal{I}_\beta\right) - \frac{3}{2}\Omega_m\mathcal{H}^2\mathcal{I}_\alpha$$

(19)

where the sources are given by

其中源项由下式给出

$$\mathcal{S}_\alpha = -\int_{\mathbf{q}_1\mathbf{q}_2} \delta_D^{(3)}(\mathbf{k}-\mathbf{q}_{12})\,\alpha(\mathbf{q}_1,\mathbf{q}_2)\,\theta_{\mathbf{q}_1}\delta_{\mathbf{q}_2}, \tag{20}$$

$$\mathcal{S}_\beta = -\int_{\mathbf{q}_1\mathbf{q}_2} \delta_D^{(3)}(\mathbf{k}-\mathbf{q}_{12})\,\beta(\mathbf{q}_1,\mathbf{q}_2)\,\theta_{\mathbf{q}_1}\theta_{\mathbf{q}_2},$$

and we introduced the non-linear kernels

我们还引入了非线性核

$$\alpha(\mathbf{q}_1,\mathbf{q}_2) \equiv \frac{\mathbf{q}_{12}\cdot\mathbf{q}_1}{q_1^2},\ \beta(\mathbf{q}_1,\mathbf{q}_2) = \frac{\mathbf{q}_{12}^2(\mathbf{q}_1\cdot\mathbf{q}_2)}{2q_1^2q_2^2}. \tag{21}$$

The retarded Green's function of δ and θ, which can be obtained by solving the above equations with the source terms replaced by $\delta(a-a')$, is given by [6, 7]

δ 和 θ 的推迟格林函数可通过将源项替换为 $\delta(a-a')$ 求解上述方程得到，其表达式为 [6, 7]

$$G_\delta(a,a') = H(a-a')\,\frac{2}{5}\frac{1}{\mathcal{H}_0^2\Omega_m^{(0)}}\frac{D_+(a')}{a'}\left(\frac{D_-(a)}{D_-(a')} - \frac{D_+(a)}{D_+(a')}\right), \tag{22}$$

and $G_\theta = -\frac{d\ln D_+}{d\ln a}(a)\,G_\delta$, where $D_- = \mathcal{H}/(a\mathcal{H}_0)$ is the decaying mode and $H(x)$ is the Heaviside step function.

和 $G_\theta = -\frac{d\ln D_+}{d\ln a}(a)\,G_\delta$，其中 $D_- = \mathcal{H}/(a\mathcal{H}_0)$ 是衰减模，$H(x)$ 是赫维赛德阶跃函数。

It is convenient now to switch to a new time variable $\eta \equiv \ln D_+(\tau)$ and the rescaled velocity divergence field

现在我们可以方便地切换到新的时间变量 $\eta \equiv \ln D_+(\tau)$ 和标度变换后的速度散度场

$$\Theta = \frac{\theta}{f} = -\frac{\partial_i v^i}{f\mathcal{H}},\ \text{where}\ f \equiv \frac{d\ln D_+}{d\ln a}. \tag{23}$$

This choice allows us to minimize time dependence in the equations [14]. After these transformations, Eqs. (3) take the following form in Fourier space:

该选择可以最小化方程中的时间相关性 [14]。完成这些变换后，方程 (3) 在傅里叶空间中可写为如下形式:

$$\partial_\eta\delta_{\mathbf{k}} - \Theta_{\mathbf{k}} = \int_{\mathbf{q}_1\mathbf{q}_2} \delta_D^{(3)}(\mathbf{k}-\mathbf{q}_{12})\,\alpha(\mathbf{q}_1,\mathbf{q}_2)\,\Theta_{\mathbf{q}_1}\delta_{\mathbf{q}_2},$$

$$\partial_\eta\Theta_{\mathbf{k}} - \frac{3\Omega_m}{2f^2}\delta_{\mathbf{k}} + \left(\frac{3\Omega_m}{2f^2} - 1\right)\Theta_{\mathbf{k}} = \int_{\mathbf{q}_1\mathbf{q}_2} \delta_D^{(3)}(\mathbf{k}-\mathbf{q}_{12})\,\beta(\mathbf{q}_1,\mathbf{q}_2)\,\Theta_{\mathbf{q}_1}\Theta_{\mathbf{q}_2}. \tag{24}$$

In a matter-dominated universe, $\Omega_m = f = 1$, so the coefficients in the l.h.s. of the above equations are time-independent. In the actual ΛCDM cosmology, it turns out that $\Omega_m \approx f^2$ with a very good accuracy for all times. Therefore, it is customary to develop a perturbative scheme in which $\Omega_m/f^2 = 1$ at zeroth order. This approach is known as the "Einstein-de Sitter" (EdS) approximation [11,14,27]. In what follows, we will use this approximation and stick to the zeroth EdS order.

在物质主导的宇宙中，$\Omega_m = f = 1$ ，因此上述方程左侧的系数不随时间变化。在实际的 ΛCDM 宇宙学中，结果表明 $\Omega_m \approx f^2$ 在所有时刻都能达到极高的精度。因此，通常的做法是构建微扰框架，令 $\Omega_m/f^2 = 1$ 处于零阶。该方法被称为“爱因斯坦-德西特”(EdS) 近似 [11,14,27]。在下文中，我们将采用该近似并始终遵循零阶 EdS 假设。

To solve Eq. (24) perturbatively, we introduce the following series ansatz:

为了对式 (24) 进行微扰求解，我们引入如下级数拟设:

$$\delta(\mathbf{k},\tau) = D_+^n(\eta)\sum_{n=1}^{\infty}\delta^{(n)}(\mathbf{k}),\ \Theta(\mathbf{k},\tau) = D_+^n(\eta)\sum_{n=1}^{\infty}\Theta^{(n)}(\mathbf{k}), \tag{25}$$

where the n -th-order perturbative solution is given by

其中 n 阶微扰解由下式给出

$$\delta^{(n)}(\mathbf{k}) = \left[\prod_{i=1}^{n}\int_{\mathbf{q}_i}\right]\delta_D^{(3)}(\mathbf{k}-\mathbf{q}_{1\ldots n})\,F_n(\mathbf{q}_1,\ldots,\mathbf{q}_n)\left[\prod_{i=1}^{n}\delta_0(\mathbf{q}_n)\right],$$

(26)

$$\Theta^{(n)}(\mathbf{k}) = \left[\prod_{i=1}^{n}\int_{\mathbf{q}_i}\right]\delta_D^{(3)}(\mathbf{k}-\mathbf{q}_{1\ldots n})\,G_n(\mathbf{q}_1,\ldots,\mathbf{q}_n)\left[\prod_{i=1}^{n}\delta_0(\mathbf{q}_n)\right],$$

and F_n and G_n are some yet unspecified momentum-dependent kernels. Demanding that this ansatz solve Eqs. (24) at any given order in δ_0 , these equations then transform into recursion relations for the kernels F_n and G_n ,

且 F_n 和 G_n 是尚未确定的依赖动量的核。要求该拟设在 δ_0 的任意给定阶都满足方程 (24)，上述方程就会转化为核 F_n 和 G_n 的递推关系:

$$F_n(\mathbf{q}_1,\ldots\mathbf{q}_n) = \sum_{m-1}^{n-1}\frac{G_m(\mathbf{q}_1,\ldots,\mathbf{q}_m)}{(2n+3)(n-1)}\left[(2n+1)\,\alpha\left(\mathbf{q}_{1m},\mathbf{q}_{(m+1)\ldots n}\right)F_{n-m}(\mathbf{q}_{m+1},\ldots\mathbf{q}_n)\right.$$

$$\left.+2\beta\left(\mathbf{q}_{1m},\mathbf{q}_{(m+1)n}\right)G_{n-m}(\mathbf{q}_{m+1},\ldots\mathbf{q}_n)\right],$$

$$G_n(\mathbf{q}_1,\ldots\mathbf{q}_n) = \sum_{m-1}^{n-1}\frac{G_m(\mathbf{q}_1,\ldots,\mathbf{q}_m)}{(2n+3)(n-1)}\left[3\alpha\left(\mathbf{q}_{1m},\mathbf{q}_{(m+1)\ldots n}\right)F_{n-m}(\mathbf{q}_{m+1},\ldots,\mathbf{q}_n)\right.$$

$$\left.+2n\beta\left(\mathbf{q}_{1m},\mathbf{q}_{(m+1)\ldots n}\right)G_{n-m}(\mathbf{q}_{m+1},\ldots,\mathbf{q}_n)\right].$$

(27)In particular, we find $F_1 = G_1 = 1$ (recovering the linear growing mode), and

特别地，我们得到 $F_1 = G_1 = 1$ (恢复了线性增长模)，且

$$F_2(\mathbf{q}_1, \mathbf{q}_2) = \frac{5}{7} + \frac{(\mathbf{q}_1 \cdot \mathbf{q}_2)}{q_1 q_2}\left(\frac{q_1}{q_2} + \frac{q_2}{q_1}\right) + \frac{2}{7}\frac{(\mathbf{q}_1 \cdot \mathbf{q}_2)^2}{q_1^2 q_2^2}, \tag{28}$$

$$G_2(\mathbf{q}_1, \mathbf{q}_2) = \frac{3}{7} + \frac{(\mathbf{q}_1 \cdot \mathbf{q}_2)}{q_1 q_2}\left(\frac{q_1}{q_2} + \frac{q_2}{q_1}\right) + \frac{4}{7}\frac{(\mathbf{q}_1 \cdot \mathbf{q}_2)^2}{q_1^2 q_2^2}.$$

Note that the kernels F_n and G_n have IR singularities when some of its arguments are soft. If we keep l momenta fixed and send the remaining $n-l$ uniformly to zero, we will get

注意核 F_n 和 G_n 在部分自变量为软动量时存在红外奇点。如果我们保持 l 个动量固定，将剩余 $n-l$ 个动量统一趋近于零，我们会得到

$$\lim_{\varepsilon \to 0} F_n\left(\mathbf{k}_1, \ldots, \mathbf{k}_l, \varepsilon \mathbf{q}'_{l+1}, \ldots, \varepsilon \mathbf{q}'_n\right) = \mathcal{O}\left(\varepsilon^{l-n}\right) \tag{29}$$

and the same for G_n . We will return to these IR singularities later.

G_n 也有相同的结果。我们稍后会再讨论这些红外奇点。

Using Eq. (26), we can compute now various correlation functions in perturbation theory. The power spectrum at order $[\delta_0]^4$ is given by

利用式 (26)，我们现在可以在微扰论框架下计算各类关联函数。$[\delta_0]^4$ 阶的功率谱为

$$\begin{aligned}
\langle \delta_{\mathbf{k}} \delta_{\mathbf{k}'} \rangle &= \left\langle \left(\delta^{(1)}_{\mathbf{k}} + \delta^{(2)}_{\mathbf{k}} + \delta^{(3)}_{\mathbf{k}}\right)\left(\delta^{(1)}_{\mathbf{k}'} + \delta^{(2)}_{\mathbf{k}'} + \delta^{(3)}_{\mathbf{k}'}\right)\right\rangle \\
&= \left\langle \delta^{(1)}_{\mathbf{k}} \delta^{(1)}_{\mathbf{k}'} \right\rangle + \left\langle \delta^{(2)}_{\mathbf{k}} \delta^{(2)}_{\mathbf{k}'} \right\rangle + 2\left\langle \delta^{(3)}_{\mathbf{k}} \delta^{(1)}_{\mathbf{k}'} \right\rangle \\
&= (2\pi)^3 \delta^{(3)}_D(\mathbf{k} + \mathbf{k}')\left(P_{11} + P_{13} + P_{22}\right),
\end{aligned} \tag{30}$$

where we used the exchange symmetry $\mathbf{k} \leftrightarrow \mathbf{k}'$ of the P_{13} correction. In what follows, we will use primes to denote stripping off Dirac delta functions from statistical averages, e.g.,

此处我们利用了 $\mathbf{k} \leftrightarrow \mathbf{k}'$ 的交换对称性，它是 P_{13} 修正项的性质。在下文中，我们将用撇号表示统计平均中已经去掉狄拉克 δ 函数，例如:

$$\langle \delta_{\mathbf{k}} \delta_{\mathbf{k}'} \rangle' = P(k). \tag{31}$$

The combinations like $\left\langle \delta^{(2)}_{\mathbf{k}} \delta^{(1)}_{\mathbf{k}'} \right\rangle$ vanish for Gaussian initial conditions because they contain an odd number of the initial density fields, e.g., $\langle \delta_0(\mathbf{k}_1)\, \delta_0(\mathbf{k}_2)\, \delta_0(\mathbf{k}_3) \rangle = 0$. The statistical averages over δ_0 generate the following convolution integrals:

对于高斯初始条件，形如 $\left\langle \delta_{\mathbf{k}}^{(2)} \delta_{\mathbf{k}'}^{(1)} \right\rangle$ 的组合为零，因为这类组合包含奇数个初始密度场，例如 $\langle \delta_0(\mathbf{k}_1)\delta_0(\mathbf{k}_2)\delta_0(\mathbf{k}_3)\rangle = 0$。对 δ_0 的统计平均可得到如下卷积积分:

$$P_{22}(k) = \left\langle \delta_{\mathbf{k}}^{(2)} \delta_{\mathbf{k}'}^{(2)} \right\rangle' = 2\int_{\mathbf{q}} [F_2(\mathbf{q}-\mathbf{k},\mathbf{q})]^2 P_{11}(q) P_{11}(|\mathbf{k}-\mathbf{q}|), \tag{32}$$

$$P_{13}(k) = 2\left\langle \delta_{\mathbf{k}}^{(1)} \delta_{\mathbf{k}'}^{(2)} \right\rangle' = 6P_{11}(k)\int_{\mathbf{q}} F_3(\mathbf{k},\mathbf{q}-\mathbf{q}) P_{11}(q).$$

These integrals have some physical interpretation. When $q \gg k$, P_{22} describes how two short-scale modes with wavevectors $\mathbf{q}$ and $\mathbf{k}-\mathbf{q}$ produce a long-wavelength mode with wavevector $\mathbf{k}$. In contrast, the correction P_{13} captures the modulation of the existing mode $\mathbf{k}$ by a mode $\mathbf{q}$. We will discuss the physical effect of these corrections shortly when we consider IR and UV limits of these loop integrals.

这些积分具有明确的物理解释: 当 $q \gg k$, P_{22} 描述两个波矢为 $\mathbf{q}$ 和 $\mathbf{k}-\mathbf{q}$ 的小尺度模如何产生一个波矢为 $\mathbf{k}$ 的长波模；与之相反，修正项 P_{13} 描述的是既有模 $\mathbf{k}$ 受模 $\mathbf{q}$ 调制的效应。当我们讨论这些圈积分的红外极限与紫外极限时，我们很快会分析这些修正项的物理效应。

Another important aspect of non-linear structure formation is non-Gaussianity [7, 42, 58 − 61]. Indeed, we see that in perturbation theory the distribution of the overdensity field acquires higher-order correlations. The simplest one is the three-point correlation, captured by the bispectrum,

非线性结构形成的另一个重要方面是非高斯性 [7, 42, 58 − 61]。实际上我们可以看到，在微扰论中，overdensity 场的分布会产生高阶关联，最简单的就是三点关联，由双谱描述:

$$\langle \delta(\mathbf{k}_1)\delta(\mathbf{k}_2)\delta(\mathbf{k}_3)\rangle \equiv (2\pi)^3 \delta_D^{(3)}(\mathbf{k}_{123}) B(\mathbf{k}_1,\mathbf{k}_2,\mathbf{k}_3). \tag{33}$$

Using the perturbative expansion (25), we obtain, at order $\left[\delta_0^4\right]$:

利用微扰展开 (25)，我们得到 $\left[\delta_0^4\right]$ 阶的结果为:

$$B(\mathbf{k}_1,\mathbf{k}_2,\mathbf{k}_3) = \left\langle \delta_{\mathbf{k}_1}^{(2)} \delta_{\mathbf{k}_2}^{(1)} \delta_{\mathbf{k}_3}^{(1)} \right\rangle' + 2\,\text{cyc.} = 2F_2(\mathbf{k}_1,\mathbf{k}_2) P_{11}(k_1) P_{11}(k_2) + 2\,\text{cyc.}$$

(34)

Perturbation theory over $\delta^{(n)}$ and $\theta^{(n)}$ can be represented in terms of Feynman diagrams [6,7]. For example, the $\delta^{(n)}$ correction is shown in Fig. 3. The linear matter power spectrum, which results from a contraction of two linear density fields $\langle \delta_0(\mathbf{k})\delta_0(\mathbf{k}')\rangle$, can be represented with a filled circle. Then the total one-loop power spectrum will be a sum of tree diagrams shown in Fig. 3.

关于 $\delta^{(n)}$ 和 $\theta^{(n)}$ 的微扰论可以用费曼图表示 [6,7]，例如 $\delta^{(n)}$ 修正项如图 3 所示。线性物质功率谱由两个线性密度场 $\langle \delta_0(\mathbf{k})\delta_0(\mathbf{k}')\rangle$ 缩并得到，可以用实心圆表示，那么总单圈功率谱就是图 3 中所有树图的和。

IR and UV Singularities

红外与紫外奇点

Let us consider the IR limits of the one-loop power spectrum integrals. We find that the leading IR asymptotics of P_{13} and P_{22} exactly cancel [11],

我们来讨论单圈功率谱积分的红外极限。我们发现 P_{13} 和 P_{22} 的主导红外渐近项恰好抵消 [11],

$$P_{22}(k)|_{q\ll k,|\mathbf{k}-\mathbf{q}|\ll k} = \frac{k^2}{3}P_{11}(k)\int_{q\ll k}\frac{d^3q}{q^2}P_{11}(q) \tag{35}$$

$$P_{13}(k)|_{q\ll k} = -\frac{k^2}{3}P_{11}(k)\int_{q\ll k}\frac{d^3q}{q^2}P_{11}(q)\,.$$

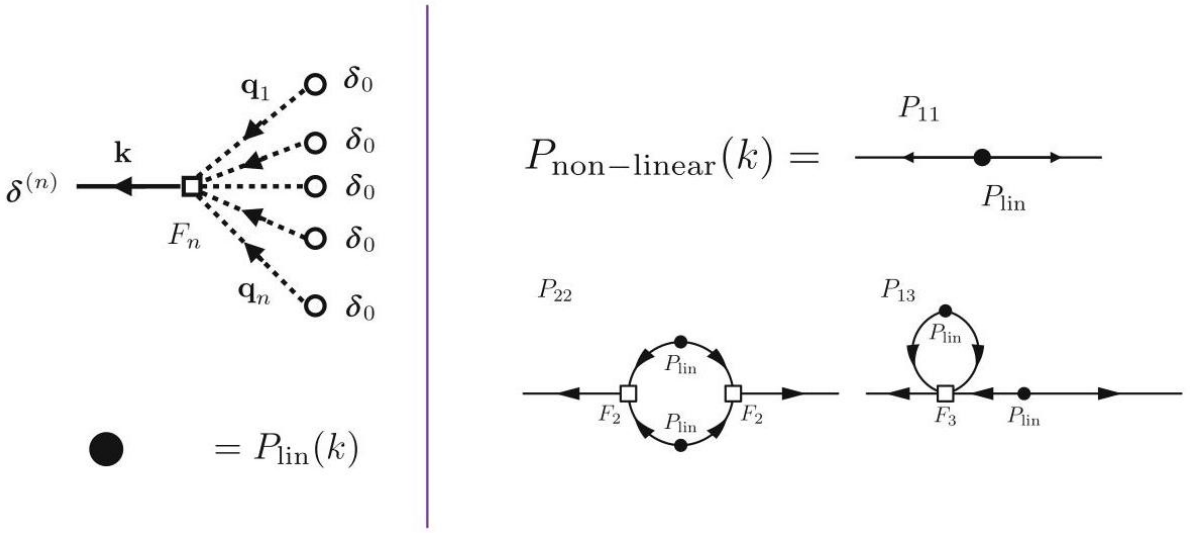

Fig. 3 Diagrammatic representation of the $\delta^{(n)}$ correction to the non-linear density field, linear matter power spectrum, and the non-linear matter power spectrum at the one-loop order

图 3 单圈阶下，$\delta^{(n)}$ 对非线性密度场、线性物质功率谱和非线性物质功率谱修正的图论表示

The integrals in the r.h.s. of the above equations contain the displacement variance in the IR domain (17). Thus, each of these terms describes how the matter power spectrum gets modulated by IR displacements. The individual corrections P_{13} and P_{22} , which are dominated by their IR limits, are quite large; see Fig. (5). The total one-loop matter power spectrum that remains after summing these terms together is five times smaller than each one-loop term individually.

上述方程右侧的积分包含红外区域 (17) 中的位移方差。因此，每一项都描述了物质功率谱被红外位移调制的机制。以红外极限为主导的单个修正项 P_{13} 和 P_{22} 数值都很大，参见图 (5)。这些项求和后得到的总单圈物质功率谱，比每个单圈项单独的数值小五倍。

The fact that individual integrals P_{13} and P_{22} do converge is a pure coincidence. In fact, the P_{13} and P_{22} integrals could be formally divergent for a power law spectrum with $P_{11} \propto q^{\upsilon}$ with $\upsilon < -1$. In this respect, the IR enhancements are often called "singularities." However, the IR singularities in P_{13} and P_{22} for any initial spectrum get exactly canceled once the integrals are summed together. Although the cancellation is straightforward at the one-loop power spectrum level, it becomes much more intricate at higher-loop order and for higher-order n-point functions, whose analysis is entangled by subleading IR divergences. IR singularities appear because the expansion of the final density field in terms of the initial field (26) violates the equivalence principle. The final physical observables, such as the n-point correlation functions, respect the equivalence principle, which explains the cancellations.

P_{13} 和 P_{22} 的单独积分都收敛纯粹是巧合。事实上，对于满足 $P_{11} \propto q^{\upsilon}$ 且 $\upsilon < -1$ 的幂律谱，P_{13} 和 P_{22} 积分在形式上可以是发散的。正因如此，红外增强通常被称为“奇点”。但对任意初始谱，积分求和后 P_{13} 和 P_{22} 中的红外奇点都会被恰好抵消。虽然这种抵消在单圈功率谱层面很直接，但在更高圈阶和高阶 n 点函数中会复杂得多，这类分析会被次领头阶红外发散纠缠。红外奇点的出现，是因为最终密度场按初始场展开的表达式 (26) 违反了等效原理。而 n 点关联函数这类最终物理可观测量满足等效原理，这就是抵消发生的原因。

The non-trivial IR limit obtained after the cancellation of the IR singularities is given by [11]:

红外奇点抵消后得到的非平凡红外极限由文献 [11] 给出:

$$P_{1-\text{loop}}\big|_{q\ll k,|\mathbf{k}-\mathbf{q}|\ll k} = \left(\frac{569}{735} - \frac{47}{105}kP_{11}'(k) + \frac{1}{10}k^2P_{11}''(k)\right)\sigma_l^2(k), \tag{36}$$

where $\sigma_l^2(k) \equiv \int_{q\ll k}\frac{d^3q}{(2\pi)^3}P(q)$ is the large-scale mass variance. We see that the IR modes actually couple the power spectrum through large-scale mass fluctuations and not the displacement. Note that we have formally assumed that $P_{11}(|\mathbf{k}-\mathbf{q}|)$ can be Taylor expanded around k and its derivatives w.r.t. k are small. This is certainly a good assumption if the linear power spectrum is a smooth function. This is certainly true for $q \ll k \sim 0.1h\text{Mpc}^{-1}$; see Fig. 2. However, P_{11} has a scale associated with the baryon acoustic oscillations, $k_{BAO} \sim 10^{-2}h\text{Mpc}^{-1}$. For modes with $q \sim k_{BAO} \ll k$, the Taylor expansion above breaks down, and therefore, the non-linear effects on the BAO need to be resummed [8, 15, 63] . To get some intuition on these effects, let us note that the full power spectrum can be presented as a sum of the smooth (power law) and wiggly components (see Fig. 4),

其中 $\sigma_l^2(k) \equiv \int_{q\ll k}\frac{d^3q}{(2\pi)^3}P(q)$ 是大尺度质量方差。我们可以看到，红外模式实际上是通过大尺度质量涨落与功率谱耦合，而非通过位移耦合。注意我们在此形式上假设 $P_{11}(|\mathbf{k}-\mathbf{q}|)$ 可以在 k 附近做泰勒展开，且它对 k 的导数很小。如果线性功率谱是光滑函数，这个假设显然成立。对 $q \ll k \sim 0.1h\text{Mpc}^{-1}$ 来说确实如此，参见图 2。但 P_{11} 存在与重子声学振荡相关的特征尺度 $k_{BAO} \sim 10^{-2}h\text{Mpc}^{-1}$ 。对于满足 $q \sim k_{BAO} \ll k$ 的模式，上述泰勒展开会失效，因此 BAO 的非线性效应需要重新求和 [8, 15, 63] 。为了直观理解这些效应，我们注意到完整功率谱可以表示为光滑 (幂律) 分量和振荡分量之和 (参见图 4),

$$P_{11}(k) = P_{\text{smooth}}(k) + P_w(k), \tag{37}$$

where the wiggly part can be approximated as $P_w(k) = f_s(k)\sin(k/k_{\text{BAO}})$ (f_s being a smooth envelop). Plugging this ansatz into (36), we obtain the total wiggly power spectrum at the one-loop order,

其中振荡分量可以近似为 $P_w(k) = f_s(k)\sin(k/k_{\rm BAO})$（$f_s$ 为光滑包络）。将这个拟设代入 (36)，我们得到单圈阶的总振荡功率谱，

$$P_w^{1-\rm loop}(k) = P_w(k) + \mathcal{O}(1)\times\sigma_l^2 P_w(k) - \frac{k}{k_{\rm BAO}}\left(\frac{47}{105} - \frac{kf_s'}{5f_s}\right) - \frac{k^2}{k_{\rm BAO}^2}\frac{\sigma_l^2}{10}P_w(k) \tag{k}$$

$$= \underbrace{f_s\left(1 - \frac{k^2}{k_{\rm BAO}^2}\frac{\sigma_l^2}{10}\right)}_{\text{BAO smoothing}}\sin\left(\frac{k}{k_{\rm BAO}}\left\{1 - \underbrace{\left[\frac{47}{105} - \frac{kf_s'}{5f_s}\right]}_{\text{Shift of the BAO phase}}\right\}\right) + \mathcal{O}(1)\times\sigma_l^2 P_w(k)\,. \tag{38}$$

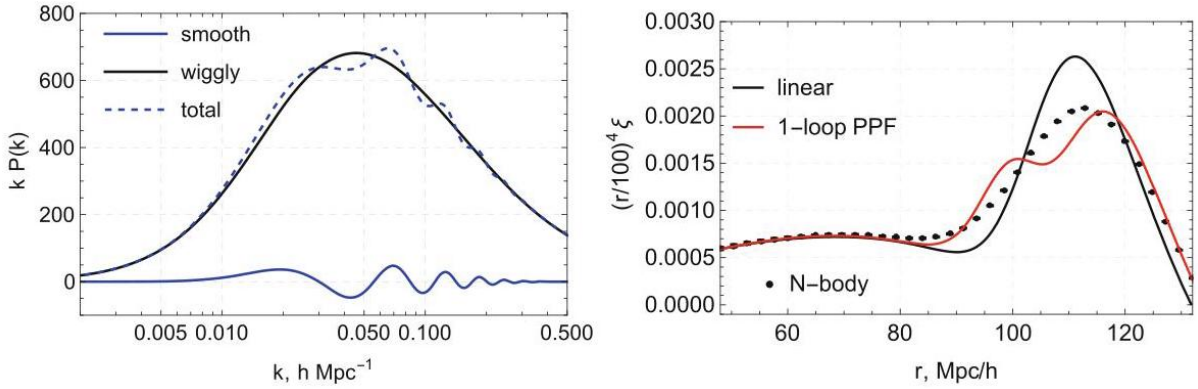

Fig. 4 Left panel: Wiggly-smooth decomposition of the linear matter power spectrum. Right panel: Rescaled $s^4\xi(s)$, where $\xi(s)$ is the position space two-point correlation function at $z = 0$. Dots are the data measurements from the Horizon Run N-body simulation. Both linear theory and one-loop PPF results fail to capture the shape of the BAO peak

图 4 左图: 线性物质功率谱的 wiggle 平滑分解。右图: 重标度后的 $s^4\xi(s)$，其中 $\xi(s)$ 是位置空间在 $z = 0$ 处的两点关联函数。点是 Horizon Run N 体模拟的测量数据。线性理论和单圈 PPF 结果都未能拟合出 BAO 峰的形状

We can see two effects here: (a) an overall suppression of the amplitude of the BAO (smoothing) and (b) the shift of their phase w.r.t. linear theory. The effective coupling constant $(k/k_{\rm BAO})^2\sigma_l^2$ can be parametrically enhanced for $k \gg k_{\rm BAO}$, which can potentially result in $(k/k_{\rm BAO})^2\sigma_l^2$ being an order one number. This is worrisome, as the two-loop correction to P_w, which scales like $(k/k_{\rm BAO})^4\sigma_l^4$, is not parametrically suppressed w.r.t. the one-loop result. Moreover, we did not take into account the fact that the Taylor expansion of $P_{11}(|\mathbf{k}-\mathbf{q}|)$ inside the P_{22} integral actually breaks down for $q \sim k_{\rm BAO}$, and thus, we have a breakdown of naive perturbation theory in two places here. This fact is manifest when we compare the predictions of linear theory and one-loop PPF models to the data (see Fig.4), which clearly fail to capture the behavior observed in N-body simulations. However, we will see later that there is a way to resum these kinds of corrections from the perturbative series. This procedure is called IR resummation.

我们在此可以看到两个效应:(a) BAO 振幅整体压低 (平滑化); (b) 其相位相对线性理论发生偏移。有效耦合常数 $(k/k_{\rm BAO})^2\sigma_l^2$ 对于 $k \gg k_{\rm BAO}$ 可以出现参数层面的增强，这可能导致 $(k/k_{\rm BAO})^2\sigma_l^2$ 达到 O(1) 量级。这一问题值得担忧，因为对 P_w 的两圈修正标度为 $(k/k_{\rm BAO})^4\sigma_l^4$，相对单圈结果并没有参数层面的压低。此外，我们尚未考虑到，对于 $q \sim k_{\rm BAO}$，P_{22} 积分中 $P_{11}(|\mathbf{k}-\mathbf{q}|)$ 的泰勒展开实际上已经失效，因此我们的 naive 微扰论在这里有两处失效。当我们将线性理论和单圈 PPF 模型的预言与数据 (见图 4) 对比时，这一事实十分明显: 二者都显然无法拟合 N 体模拟中观测到的行为。不过我们后续会看到，存在一种对微扰级数中的这类修正进行重求和的方法，这个过程叫做 IR 重求和。

Now let us focus on the UV limit of loop integrals, $q \gg k$. We have [7]

现在我们将目光聚焦于圈积分的紫外极限 $q \gg k$，我们有文献 [7] 给出的结果

$$P_{22}(k)|_{k\ll q} = \frac{9}{196\pi^2}k^4\int_{k\ll q}\frac{q^2dq}{q^4}P_{11}^2(q) \tag{39}$$

$$P_{13}(k)|_{k\ll q} = -\frac{61}{630\pi^2}k^2P_{11}(k)\int_{k\ll q}\frac{q^2dq}{q^2}P_{11}(q)\,.$$

We see that the UV limit of P_{22} does not involve $P_{11}(k)$ and moreover it scales like k^4 on large scales. In agreement with Peebles' arguments, it describes how two short modes generate power on large scales. We will discuss this effect in detail shorty. In contrast, the UV limit of P_{13} describes how $P_{11}(k)$ gets modulated by the short-scale displacements. Importantly, the $P_{22}(P_{13})$ integrals are divergent in the UV for a power law spectrum with $\upsilon \geq 1/2\,(\upsilon \geq -1)$. However, for the actual Λ CDM power spectrum, they turned out to converge. This does not mean that they have converged to the right answer though: the modes in the domain $q \gg k$ cannot be described by a perfect fluid at all. In particular, we do not expect to capture the effects of halo virialization.

我们可以看到，P_{22} 的紫外极限不包含 $P_{11}(k)$，此外它在大尺度上的标度行为为 k^4。这与 Peebles 的论证一致，描述了两个短波模如何在大尺度上产生功率。我们很快会详细讨论这一效应。反之，P_{13} 的紫外极限描述了 $P_{11}(k)$ 如何被短尺度位移调制。重要的是，对于满足 $\upsilon \geq 1/2\,(\upsilon \geq -1)$ 的幂律谱，$P_{22}(P_{13})$ 积分在紫外是发散的。不过对于实际的 Λ CDM 功率谱，这些积分最终是收敛的。但这并不意味着它们收敛到了正确结果: 在 $q \gg k$ 区域的波模根本无法用理想流体描述。我们尤其无法预期该方法能拟合晕坍缩的效应。

At the one-loop level, the mistake introduced by doing the loop integrals all the way up to infinity turned out to be small for the ΛCDM power spectrum. However, at higher-loop orders, it becomes very significant [11,12]. In Fig. 5, we show the one-, two-, and three-loop corrections to the matter power spectrum in PPFM. We see that the two-loop correction is as big as the one loop and the three-loop term is larger than the first two loops combined. This apparent breakdown of perturbation theory is produced by the uncontrolled UV corrections that become more and more sizable at higher-loop orders. Note that the leading UV corrections in the low- k limit are negative and proportional to k^2P_{11} . Just like in the one-loop case, they correspond to UV displacements. The appearance of these UV enhancements signals that perturbation theory misses the halo virialization physics, which would confine the DM particles inside the halo and reduce their actual displacement in comparison with the perturbation theory prediction. Indeed, in perturbation theory, the two DM particles would continue to move to ever-increasing distances from one another instead of sticking together and forming a halo as shown in cartoon 1.

在单圈阶，将圈积分一直计算到无穷远引入的误差对 ΛCDM 功率谱而言很小。但在更高圈阶，误差会变得非常显著 [11,12]。在图 5 中，我们展示了 PPFM 框架下物质功率谱的一、二、三圈修正。可以看到，两圈修正的大小和单圈修正相当，而三圈项的大小比前两圈修正之和还要大。这种微扰论的明显失效是由不受控的紫外修正导致的，这些修正在更高圈阶会变得越来越大。注意，低 k 极限下的领头阶紫外修正为负，且与 k^2P_{11} 成正比。和单圈情况一样，这些修正对应紫外位移。这类紫外增强的出现说明微扰论遗漏了晕的维里化物理——维里化会将暗物质粒子束缚在晕内部，相比微扰论的预言降低了它们的实际位移。实际上在微扰论中，两个暗物质粒子会不断相互远离，而不会像示意图 1 展示的那样结合在一起形成暗物质晕。

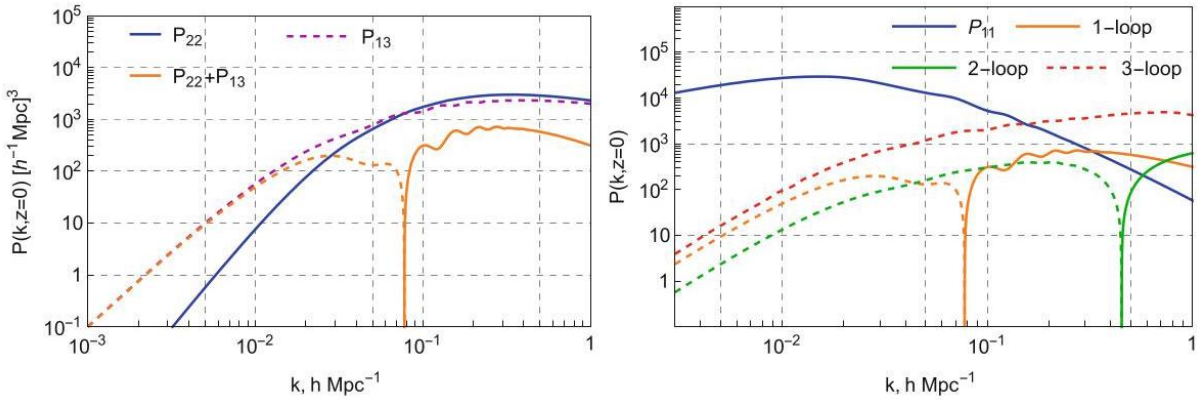

Fig. 5 Left panel: Individual loop corrections P_{22} and P_{13} and their sum. Right panel: Tree-level (linear theory) and various loop corrections to the matter power spectrum computed within the pressureless perfect fluid (PPF) hydrodynamics. Dashed curves show negative contributions. PPF predictions are dominated by displacements that receive uncontrolled contributions from the UV modes. This produces a large spurious suppression of the matter power spectrum on large scales and leads to a breakdown of the PPF perturbation theory

图 5 左图: 单独的圈修正 P_{22} 和 P_{13} 以及它们的和。右图: 无压强理想流体 (PPF) 流体力学框架下计算得到的树级 (线性理论) 物质功率谱和各阶圈修正。虚线表示负贡献。PPF 预言被来自紫外模式的不受控贡献主导的位移项支配，这会导致大尺度上物质功率谱出现虚假的大幅压低，最终造成 PPF 微扰论失效

A more meaningful approach to the UV problem would be to introduce a UV cutoff $\Lambda \sim O\left(R_{\rm vir}^{-1}\right)$ in the integrals. But then the answer would necessarily depend on that cutoff. The naive pressureless perfect fluid theory does not have any means to systematically remove the cutoff dependence from the answer. This problem will be resolved in the EFTofLSS by means of a non-trivial stress tensor.

解决紫外问题更合理的方法是在积分中引入紫外截断 $\Lambda \sim O\left(R_{\rm vir}^{-1}\right)$，但这样得到的结果必然会依赖于该截断，朴素的无压强理想流体理论没有办法系统性地从结果中消除截断依赖性。这个问题会在大尺度结构有效场论 (EFTofLSS) 中通过非平凡的应力张量解决。

Physical IR Effects

物理红外效应

Let us discuss the physical IR and UV effects that our perturbation theory is missing. As far as IR effects are concerned, the problem is that these effects happened to be large and need to be treated non-perturbatively. Let us get more insight into their dynamics. Imagine two dark matter particles in a homogeneous flow. This flow represents an IR limit of the loop integrals. The flow can displace each particle by as much as $\sim 6h^{-1}\text{Mpc}$; see Eq. (18). However, the correlation between the two DM particles will not be affected, as both of them are displaced by the flow equally. This result can be traced back to the equivalence principle. One can think of these two DM particles as being placed in an "Einstein elevator." All physical observables, such as the two-point correlation function, should be insensitive to the large-scale acceleration. Cancellation of the effect due to an IR flow, thanks to the equivalence principle, precisely translates into the cancellation between the P_{13} and P_{22} integrals: each term separately describes how the power spectrum is modulated by the large-scale displacements, but the net effect of such displacements should be zero.

下面我们讨论微扰理论未涵盖的物理红外 (IR) 和紫外 (UV) 效应。就红外效应而言，问题在于这类效应恰好幅度很大，需要用非微扰方法处理。我们来更深入地理解其动力学: 想象均匀流中有两个暗物质粒子，这个流代表圈积分的红外极限。流可以将每个粒子最多移动 $\sim 6h^{-1}\text{Mpc}$ ，参见式 (18)。但两个暗物质 (DM) 粒子之间的关联不会受到影响，因为二者被流同等位移。这个结果可以追溯到等效原理: 我们可以把这两个 DM 粒子看作处在“爱因斯坦电梯”中，所有物理可观测量 (例如两点关联函数) 都应当对大尺度加速度不敏感。得益于等效原理，红外流效应的抵消恰好等价于 P_{13} 积分与 P_{22} 积分之间的抵消: 每一项单独描述大尺度位移如何调制功率谱，但这类位移的总效应应当为零。

To get a rough picture of the effect, let us assume that the large-scale (IR) displacement is constant. When the two DM particles are displaced by a homogeneous displacement field $\mathbf{s}_{\parallel}$ (see the left panel of Fig. 6), their correlation function will not change,

为了对该效应建立大致图像，我们假设大尺度 (红外) 位移是常数。当两个 DM 粒子被均匀位移场 $\mathbf{s}_{\parallel}$ 位移时 (参见图 6 左图)，它们的关联函数不会发生改变，

$$\left\langle \delta\left(0+\mathbf{s}_{\parallel}\right) \delta\left(\mathbf{x}+\mathbf{s}_{\parallel}\right)\right\rangle=\langle \delta(0) \delta(\mathbf{x})\rangle. \tag{40}$$

The above result is a simple consequence of the fact that the correlation function depends only on the absolute separation between the points (statistical homogeneity).

上述结果是关联函数仅依赖于两点绝对间距 (统计均匀性) 的直接推论。

Now let us imagine that the flow is not exactly homogeneous, i.e., the gravitational acceleration has a gradient. This situation is illustrated in the right panel of Fig. 6. Physically, this would mean that the two DM particles (or density clumps) would be displaced from one another. Once we average over different patches of space, this should result in a loss of correlation between the two particles and hence the suppression of the correlation function. Indeed, this gradient can be described by an additional displacement $\mathbf{s}_{\perp}$,

现在我们假设流并非完全均匀，即引力加速度存在梯度。图 6 右图展示了这种情况。从物理上看，这意味着两个 DM 粒子 (或密度团块) 会发生相对位移。当我们对不同空间区域取平均后，这会导致两个粒子之间的关联减弱，进而压低关联函数。实际上，这种梯度可以用额外位移 $\mathbf{s}_\perp$ 描述，

$$\langle \delta(0)\,\delta(\mathbf{x}+\mathbf{s}_\perp)\rangle = \int_{\mathbf{k}} e^{i\mathbf{k}\cdot\mathbf{x}} \left\langle e^{i\mathbf{k}\mathbf{s}_\perp}\right\rangle P(k) = \left\langle e^{(\mathbf{s}_\perp\cdot\nabla)}\right\rangle \int_{\mathbf{k}} e^{i\mathbf{k}\cdot\mathbf{x}} P(k)\,, \tag{41}$$

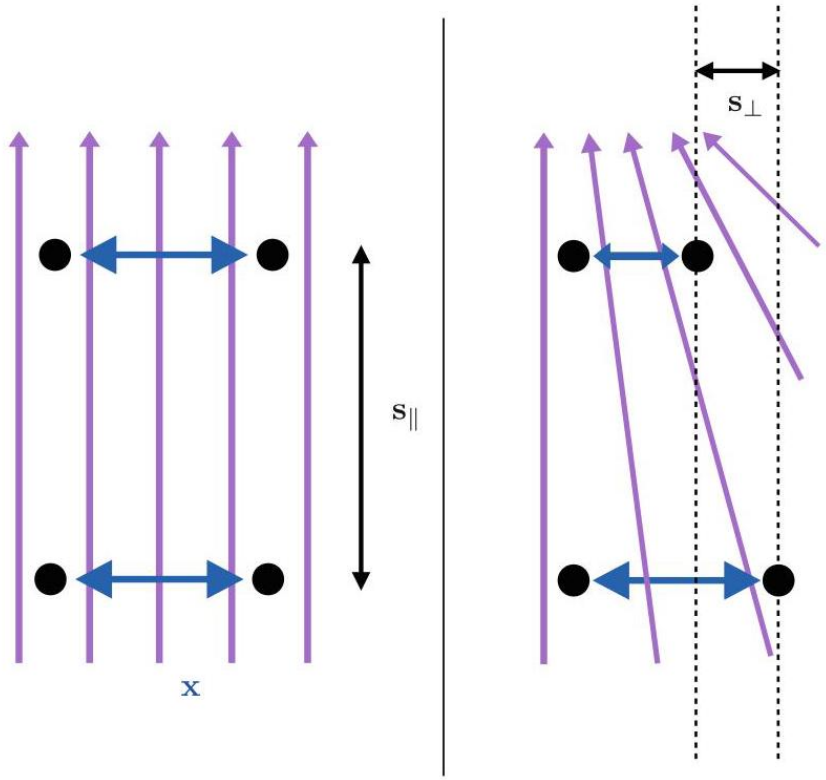

Fig. 6 Cartoon picture of non-linear IR effects. Left panel: The homogeneous flow (produced by infinitely soft modes) does not affect correlation properties of DM particles. Right panel: If the flow converges (or diverges), DM particles would be moved closer (or further). Thus, the two-point correlation function of the DM density will waken when averaged over many flows

图 6 非线红外效应的示意图。左图: 均匀流 (由无穷软模产生) 不会影响 DM 粒子的关联性质。右图: 如果流汇聚 (或发散)，DM 粒子会被移动得更近 (或更远)。因此对多个流取平均后，DM 密度的两点关联函数会减弱。

where we assumed for simplicity that the displacement gradient is not correlated with the original density field. Using the cumulant expansion theorem, we obtain

为简单起见，我们这里假设位移梯度与原密度场不相关。利用累积量展开定理，我们得到

$$\langle \delta(0)\,\delta(\mathbf{x}+\mathbf{s}_\perp)\rangle = e^{\sum\limits_{n=1} \frac{1}{n!}\left\langle (\mathbf{s}_\perp\cdot\nabla)^n_c\right\rangle} \langle \delta(0)\,\delta(\mathbf{x})\rangle = e^{\frac{1}{2}\left\langle s^i_\perp s^j_\perp\right\rangle \partial_i\partial_j} \langle \delta(0)\,\delta(\mathbf{x})\rangle, \tag{42}$$

where in the second equality above we made use that the bulk flows are described by linear theory, i.e., only the second-order cumulant of $\mathbf{s}_\perp$ survives. We see that the relevant expansion parameter here is the gradient of the correlation function times the displacement. If the correlation function were exact power law, $\xi(r) \propto (r/r_{\rm NL})^\gamma$, the bulk flow effects would be perturbative, $\langle s^i s_i \rangle / r^2 \ll 1$. Indeed, we could Taylor expand the exponent in (42), and this expansion would be controlled by a small parameter $(r_{NL}/r)^2$ (we used that in this example $\langle s^i s_i \rangle \sim r_{\rm NL}^2$).

在上文第二个等式中，我们利用了整体流由线性理论描述的性质，即仅 $\mathbf{s}_\perp$ 的二阶累积量保留。我们可以看到，此处相关的展开参数是关联函数的梯度乘以位移。如果关联函数是严格的幂律形式 $\xi(r) \propto (r/r_{\rm NL})^\gamma$，则整体流效应是微扰的 $\langle s^i s_i \rangle / r^2 \ll 1$。实际上我们可以对 (42) 式的指数做泰勒展开，该展开由小参数 $(r_{NL}/r)^2$ 控制 (本例中我们用到了 $\langle s^i s_i \rangle \sim r_{\rm NL}^2$)。

However, the effect of bulk flows is non-perturbative for the BAO part of the correlation functions, $\xi_{\rm BAO}(r) \propto \exp\left\{-\left(2\sigma_{\rm BAO}^2\right)^{-1}(r - r_{\rm BAO})^2\right\}$, where σ is the linear width of the BAO peak in position space $\sim 5h^{-1}$Mpc. Indeed,

然而，对于关联函数中的重子声学振荡 (BAO) 部分，整体流的效应是非微扰的，即 $\xi_{\rm BAO}(r) \propto \exp\left\{-\left(2\sigma_{\rm BAO}^2\right)^{-1}(r - r_{\rm BAO})^2\right\}$，其中 σ 是位置空间中 BAO 峰的线性宽度 $\sim 5h^{-1}$Mpc。实际上，

$$\left\langle s_\perp^2 \right\rangle \partial_r^2 \xi_{\rm BAO} \sim \frac{\langle s^i s_i \rangle}{\sigma_{\rm BAO}^2} \xi_{\rm BAO} \sim \mathcal{O}(1) \times \xi_{\rm BAO}, \tag{43}$$

i.e., we cannot Taylor expand the exponent in (42). In actual perturbation theory however, $\mathbf{s}_\perp \propto \frac{\nabla}{\Delta}\delta^{(1)}$, and thus, this exponent would only show up order by order in the perturbative expansion. Note that in this picture, the non-perturbative nature of the non-linear evolution of the BAO results from a similarity between the width of the BAO peak and the RMS displacement. As a result of these large displacements, the BAO correlation degrades, i.e., the amplitude of the BAO peak diminishes [29]. This coincides with the qualitative prediction of the one-loop correction that we have seen earlier. This behavior is also confirmed in N-body simulations; see Fig. 4.

也就是说，我们无法对 (42) 式中的指数进行泰勒展开。然而在实际微扰论中，$\mathbf{s}_\perp \propto \frac{\nabla}{\Delta}\delta^{(1)}$，因此该指数只会在微扰展开中逐阶出现。请注意，在该图像中，重子声学振荡 (BAO) 非线性演化的非微扰性质源于 BAO 峰宽与均方位移之间的相似性。这些大位移会导致 BAO 关联退化，即 BAO 峰的振幅减小 [29]。这与我们之前看到的单圈修正的定性预测一致。该行为也在 N 体模拟中得到了证实，参见图 4。

Physical UV Effects

物理紫外效应

Let us now discuss typical corrections due to physics that we are missing in our perfect fluid toy model. Let us estimate typical corrections due to virialized motions [51]. Our discussion will be based on the famous Peebles' argument for the estimation of the large-scale power spectrum due to virial motions. Imagine a distribution of N dark matter particles. Their density in Fourier space is given by

现在我们讨论我们的理想流体 toy 模型中未包含的物理导致的典型修正。我们来估计维里化运动带来的典型修正 [51]。我们的讨论基于著名的皮布尔斯论证，该论证用于估计维里运动引起的大尺度功率谱。设想有一个 N 暗物质粒子分布。它们在傅里叶空间的密度为

$$\rho_{\mathbf{k}} = \sum_n m_n e^{i\mathbf{k}\mathbf{x}_n}. \tag{44}$$

Now imagine that there is a short-scale process that moves each particle by a small displacement $\Delta\mathbf{x}_n$. This generates the following correction to the density field:

现在设想存在一个小尺度过程，使每个粒子产生小位移 $\Delta\mathbf{x}_n$ 。这对密度场产生了如下修正:

$$\rho_{\mathbf{k}} = \sum_n m_n e^{i\mathbf{k}(\mathbf{x}_n+\Delta\mathbf{x}_n)} = \sum_n m_n e^{i\mathbf{k}\mathbf{x}_n}\left(1 + i\mathbf{k}\Delta\mathbf{x}_n - \frac{k_i k_j}{2}\Delta x_n^i \Delta x_n^j + \mathcal{O}\left(k^3\Delta x^3\right)\right). \tag{45}$$

The first term in the l.h.s. is the usual background density, the second term vanishes due to momentum conservation $\left(\sum_n m_n \Delta\mathbf{x}_n = 0\right)$, so the first non-trivial correction due to particles' reshuffling is given by

左侧第一项是常规背景密度，第二项因动量守恒 $\left(\sum_n m_n \Delta\mathbf{x}_n = 0\right)$ 消失，因此粒子重排带来的首个非平凡修正为

$$\Delta\rho_{\mathbf{k}} = -\frac{k_i k_j}{2}\sum_n m_n e^{i\mathbf{k}\mathbf{x}_n}\Delta x_n^i \Delta x_n^j. \tag{46}$$

We see that the mass and momentum conservation dictate the k^2 dependence of the perturbed density field. The typical displacements inside the halo are of the order of the halo virial radius, $\Delta x_n \sim R_{\rm vir}$, and hence the typical corrections to the density field due to the halo virial scale as $(R_{\rm vir}k)^2$. If the short-scale displacements are completely uncorrelated with large-scale modes, the total correction to the matter power spectrum can be estimated as

我们看到质量与动量守恒决定了扰动密度场对 k^2 的依赖关系。暗物质晕内部的典型位移量级为晕维里半径 $\Delta x_n \sim R_{\rm vir}$ ，因此晕维里效应对密度场的典型修正标度为 $(R_{\rm vir}k)^2$ 。如果小尺度位移与大尺度模式完全不相关，那么对物质功率谱的总修正可以估计为

$$P_{\rm vir}(k) \sim (kR_{\rm vir})^4 R_{\rm vir}^3. \tag{47}$$

This is the famous Peebles' result on the leading behavior of the matter power spectrum generated by virialized structures. Since this contribution is uncorrelated with long-wavelength modes, it is purely stochastic. However, it is also possible that the short-scale displacements Δx_n are actually correlated with the long-wavelength density field $\delta_{\mathbf{k}}$, i.e., $\delta_{\rm vir}(\mathbf{k}) \propto k^2 R_{\rm vir}^2 \delta_{\mathbf{k}}$. In practice, this correlation can be generated by tidal forces [9]. Then the short-scale motions would modulate the matter power spectrum on large scales,

这就是关于维里化结构产生的物质功率谱领头行为的著名皮布尔斯结果。由于该贡献与长波长模式不相关，它完全是随机的。但小尺度位移 Δx_n 也有可能实际上与长波长密度场 $\delta_{\mathbf{k}}$ 相关，即 $\delta_{\rm vir}(\mathbf{k}) \propto k^2 R_{\rm vir}^2 \delta_{\mathbf{k}}$ 。实际上这种相关性可以由潮汐力产生 [9]。此时小尺度运动将会调制大尺度上的物质功率谱，

$$\left\langle \delta_{\rm vir}(\mathbf{k}')\, \delta_{\mathbf{k}}^{(1)} \right\rangle' = -k^2 R_{\rm vir}^2 P_{11}(k). \tag{48}$$

This is the leading deterministic effect of halo virialization on the large-scale matter power spectrum. A similar effect can be generated by pressure. Indeed, adding the usual pressure term $c_s^2 \nabla\delta\rho/\rho$ to the r.h.s. of the Euler equation (3), we get

这是暗晕维里化对大尺度物质功率谱的领头确定性效应。压强也可以产生类似效应。实际上，向欧拉方程 (3) 的右侧添加常规压强项 $c_s^2 \nabla\delta\rho/\rho$ ，我们得到

$$\frac{\partial}{\partial t} v^i + H v^i + v^j \partial_j v^i = -\partial_i \Phi - c_s^2 \partial_i \delta, \tag{49}$$

which gives us the following Euler equation in Fourier space:

它给出了傅里叶空间中如下形式的欧拉方程:

$$\dot{\Theta}_{\mathbf{k}} - \frac{3}{2}\delta_{\mathbf{k}} + \frac{1}{2}\Theta_{\mathbf{k}} = \int_{\mathbf{q}_1 \mathbf{q}_2} \delta_D^{(3)}(\mathbf{k} - \mathbf{q}_{12}) \frac{\mathbf{q}_{12}^2 (\mathbf{q}_1 \cdot \mathbf{q}_2)}{2 q_1^2 q_2^2} \Theta_{\mathbf{q}_1} \Theta_{\mathbf{q}_2} - \frac{k^2 c_s^2}{\mathcal{H}^2} \delta_{\mathbf{k}}. \tag{50}$$

Treating the sound speed term as a perturbation and using the density Green's function (22), we find

将声速项当作微扰处理，并利用密度格林函数 (22)，我们得到

$$\delta_{\mathbf{k}}^{(c_s^2)} = \int da' G_\delta(a, a') \left(-k^2 c_s^2 \delta_{\mathbf{k}}^{(1)} \right) \equiv -k^2 \gamma \delta_{\mathbf{k}}^{(1)}. \tag{51}$$

This produces to the following correction to the matter power spectrum:

它对物质功率谱产生了如下修正:

$$P_{1\text{-loop}}(k) = P_{11}(k) + P_{22}(k) + P_{13}(k) - 2k^2 \gamma P_{11}. \tag{52}$$

The upshot is that the virialization effects actually act like an effective pressure in the fluid equations!

结论就是: 维里化效应实际上在流体方程中等效于有效压强!

On dimensional grounds, the size of the pressure parameter γ should be of the order of $R_{\rm vir}^2$. The effective sound speed can be estimated as $c_s^2 \sim (R_{\rm vir}\mathcal{H})^2 \sim 10^{-6} c^2$, where c is the speed of light. This is similar to the speed of sound of ordinary water. We stress however that this effective pressure is different from the microscopic pressure of ordinary fluids. The hydrodynamical description of normal fluids is adequate down to scales of order the molecules' mean free path. Thus, the hydrodynamic description is valid, e.g., for the dynamics of sound waves. In contrast, the description of the dark matter fluid with the effective pressure is

valid only for $k \ll k_c = 2\pi R_{\rm vir}^{-1}$. Since $k_c \sim \mathcal{H}/c_s$ here is the analog of the Jeans length, the dark matter effective fluid description (51) breaks down before it could describe sound waves.

量纲分析可得, 压强参数 γ 的大小应为 $R_{\rm vir}^2$ 量级。有效声速可以估计为 $c_s^2 \sim (R_{\rm vir}\,\mathcal{H})^2 \sim 10^{-6}c^2$, 其中 c 是光速。这和普通水的声速相近。但我们需要强调, 这种有效压强不同于普通流体的微观压强。普通流体的流体力学描述在向下直到分子平均自由程量级的尺度上都是适用的, 因此流体动力学描述对声波动力学这类过程是有效的。与之相反, 带有效压强的暗物质流体描述仅对 $k \ll k_c = 2\pi R_{\rm vir}^{-1}$ 适用。由于此处 $k_c \sim \mathcal{H}/c_s$ 是金斯长度的对应量, 暗物质有效流体描述 (51) 在能够描述声波之前就已经失效了。

Lessons

结论总结

Let us summarize the lessons that we have taken from the pressureless perfect fluid hydrodynamics. First, one needs to work with coarse-grained fields, as only these fields have small fluctuations. Otherwise, the fluid description does not have a small parameter.

我们来总结从无压理想流体动力学中得到的结论。首先, 我们需要使用粗粒化场, 因为只有这类场的涨落很小; 否则流体描述不存在小参数。

The second lesson is that the UV behavior of the theory needs to be properly renormalized. In most of physical systems, the dynamics of the long-wavelength fluctuations must be insensitive to the details of the short-scale physics. This property is called ”decoupling.” This fact should be reflected in the correct equations for structure formation. We have seen that in the PPF formalism, this is not the case. The loop integrals there receive large corrections from the short scales where the fluid description does not apply. And there are no technical tools within the PPF to fix this issue and remove these large enhancements (”singularities”). This clearly indicates the inconsistency of the PPF approach from the mathematical viewpoint. In addition, there are physical effects of halo virialization and backreaction on large scales that are missing in the PPF hydrodynamics.

第二个结论是, 该理论的紫外行为需要适当重整化。在大多数物理系统中, 长波长涨落的动力学必定不依赖短尺度物理的细节, 这一性质称为“退耦”, 该性质应当体现在描述结构形成的正确方程中。我们已经看到, 在 PPF 形式中情况并非如此: 此处圈积分会从流体描述不适用的短尺度获得大修正, 而且 PPF 框架内没有技术手段可以解决这个问题, 消除这些大增强 (即“奇点”)。这从数学角度清晰表明 PPF 方法不自洽。此外, PPF 动力学还缺失了晕 virial 化的物理效应以及大尺度上的反作用效应。

The third important lesson is that there are also IR singularities, which plague individual loop contributions. These singularities cancel when all corrections are summed together at a given loop order. The origin of these singularities is in the fact that the perturbative expansion in terms of the density field does not respect the equivalence principle. Although this looks like a technical inconvenience, the presence of IR singularities obscures the analysis of physical IR effects that alter the BAO feature in the matter distribution. These effects turned out to be large in our universe and hence require a non-perturbative treatment.

第三个重要结论是，单个圈贡献中还存在红外奇点，这些奇点会困扰计算。当对给定圈阶的所有修正求和时，这些奇点会相互抵消。这类奇点的起源在于，密度场的微扰展开不满足等效原理。尽管这看起来只是技术上的不便，但红外奇点的存在会干扰对改变物质分布中重子声学振荡特征的物理红外效应的分析。我们已经知道这些效应在我们的宇宙中幅度很大，因此需要非微扰处理。

The first two drawbacks of the PPF approach are straightforward to fix. The analysis presented above suggests that this can be done by means of using a nonzero stress tensor and smoothing the resulting equations of motion. This is the core idea of the EFTofLSS. The IR issue, however, is less straightforward. The EFT principles itself do not help in this situation because the IR singularities are artifacts of the standard Eulerian description. There is no good solution to this problem in terms of Eulerian hydrodynamics. We will show later how this issue is resolved with another formulation of the EFTofLSS called time-sliced perturbation theory.

PPF 方法的前两个缺陷很容易修正: 上述分析表明，可以通过引入非零应力张量、对运动方程做平滑处理来解决问题，这正是大尺度结构有效场论 (EFTofLSS) 的核心思想。但红外问题就没这么简单了，有效场论原理本身对此并无帮助，因为红外奇点是标准欧拉描述的人造产物，在欧拉流体动力学框架下不存在好的解决方案。我们后续会说明，这个问题如何通过 EFTofLSS 的另一种表述——时间切片微扰论——解决。

Large-Scale Structure as an Effective Fluid

大尺度结构作为有效流体

There are several ways to obtain equations of motions for the coarse-grained matter density and velocity fields [9, 23]. In the ”top-down” approach, we start with a UV model, e.g., the Newtonian dynamics of N particles. This ensemble of particles is described by the Boltzmann-Vlasov equation. Coarse graining this equation and taking moments of the distribution function, we would arrive at equations for a general vicious fluid. The process of coarse graining has a meaning of ”integrating out” short-scale degrees of freedom.

我们可以通过多种方法得到粗粒化物质密度场和速度场的运动方程 [9, 23]。在“自上而下”方法中，我们从一个紫外模型出发，例如 N 个粒子的牛顿动力学。这一粒子系综由玻尔兹曼-弗拉索夫方程描述。对该方程进行粗粒化并取分布函数的矩，我们就能得到一般黏性流体的运动方程。粗粒化过程的含义是“积分掉”小尺度自由度。

In the ”bottom-up” approach, we start with the most general equations of motion for large-scale degrees of freedom, which are the DM density and velocity fields. In this case, the situation is equivalent to that of ordinary fluids, with the most general description being that of an imperfect fluid interacting through gravity. Then we coarse grain these equations by applying a low-pass filter with a momentum cutoff Λ . The resulting equations will be, again, general equations of motion for a viscous fluid. Thus, from the technical point of view, we have to solve now the following system:

在“自下而上”方法中，我们从描述大尺度自由度的最普遍运动方程出发，这里的大尺度自由度就是暗物质密度场和速度场。这种情况和普通流体等价，最普遍的描述就是通过引力相互作用的非理想流体。随后我们通过动量截断为 Λ 的低通滤波器对这些方程做粗粒化处理。得到的方程仍然是黏性流体的普遍运动方程。因此，从技术层面来看，我们现在需要求解下述方程组:

$$\frac{\partial}{\partial\tau}\delta_\ell + \partial_i\left[(1+\delta_\ell)\,v^i_\ell\right] = 0$$

$$\frac{\partial}{\partial\tau}v^i_\ell + \mathcal{H}v^i_\ell + v^j_\ell\partial_j v^i_\ell + \partial_i\Phi_\ell = -\frac{1}{\rho_\ell}\left[\partial_j\sigma^{ij}\right]_\Lambda, \tag{53}$$

supplemented with the coarse-grained Poisson equation,

并补充粗粒化泊松方程,

$$\Delta\Phi_\ell = \frac{3}{2}\mathcal{H}^2\Omega_m(\tau)\,\delta_\ell. \tag{54}$$

These equations look almost the same as the equation for PPF, but however, there are several important differences. First, our variables here are long-wavelength overden-sity and velocity fields [23,48] (Note that the actual physical variable in our system is the coarse-grained momentum field, while the velocity field in Eq. (53) is formally built out of the smoothed momentum and density fields. This velocity field is ”bare,” i.e., it should be distinguished from the physical, finite velocity field, which differs from v^j_ℓ by a counterterm.). Even though these coarse-grained variables explicitly depend on the smoothing scale Λ , the physical observables do not. Technically, this is realized by means of counterterms embedded in the stress tensor.

这些方程看起来和 PPF(完美流体) 的方程几乎一致，但存在几个重要区别。首先，我们这里的变量是长波长密度扰动场和速度场 [23,48](注意我们体系中实际的物理变量是粗粒化动量场，式 (53) 中的速度场是形式上由平滑后的动量场和密度场构造而来的。该速度场是“裸”量，也就是说它需要和物理的有限速度场区分开，后者与 v^j_ℓ 相差一个抵消项。)。尽管这些粗粒化变量显式依赖于平滑尺度 Λ，但物理可观测量并不依赖它。从技术上来说，这一点是通过嵌入应力张量中的抵消项实现的。

Second, there is a non-trivial stress tensor σ^{ij} , which encapsulates the effects of short-scale backreaction. In the EFT approach, this backreaction is captured by means of effective operators that involve only long-distance degrees of freedom, such as δ_ℓ , and their gradients. In the context of fluid dynamics, the most general expression for σ_{ij} in a derivative expansion is

其次，存在非平凡的应力张量 σ^{ij} ，它概括了小尺度反作用的效应。在有效场论方法中，这种反作用由仅包含长距离自由度的有效算符 (例如 δ_ℓ 及其梯度) 来描述。在流体动力学框架下，导数展开中 σ_{ij} 的最普遍表达式为

$$\sigma_{ij} = p\delta_{ij} - \zeta\delta_{ij}\left(\partial_k v^k\right) - \eta\left(\partial_i v_j + \partial_j v_i - \frac{2}{3}\delta_{ij}\left(\partial_k v^k\right)\right), \tag{55}$$

where η and ζ are shear and bulk viscosities, respectively. Unfortunately, it turns out that the fluid ansatz (55) is not general enough for our purposes. In particular, we should also add terms involving various con-

tractions of the tidal tensor $t_{ij} \propto \partial_i\partial_j\Phi - \delta_{ij}\Delta\Phi/3$. In addition, we have to go beyond the lowest order in the derivative expansion.

其中 η 和 ζ 分别是剪切黏度和体黏度。遗憾的是，流体假设 (55) 对我们的研究目标来说不够普遍。具体来说，我们还需要添加包含潮汐张量 $t_{ij} \propto \partial_i\partial_j\Phi - \delta_{ij}\Delta\Phi/3$ 各类缩并的项。此外，我们还需要拓展到导数展开最低阶之外的项。

Working consistently within EFT approach, we should write down all possible operators involving long-distance degrees of freedom that are consistent with the symmetries of the problem. At a given order in perturbation theory, there will be only a finite number of operators that we need to keep in the theory model. These operators will appear with free coefficients, which should be treated just like Wilson coefficients in other EFTs. The values of these Wilson coefficients should be determined experimentally. We stress that they are physical parameters describing our cosmological fluid and neglecting them (or setting them to zero) is incorrect, just like it is incorrect to neglect bulk and shear viscosities when describing a fluid. Now we discuss properties of the effective stress tensor in detail.

在 EFT 方法内一致地进行研究，我们应当写下所有满足问题对称性的、包含长距离自由度的可能算符。在微扰论的给定阶数下，理论模型中只需要保留有限个算符。这些算符带有自由系数，我们应当将这些系数和其他 EFT 中的威尔逊系数一样处理。这些威尔逊系数的取值应当由实验确定。我们要强调的是，它们是描述我们宇宙学流体的物理参数，忽略它们 (或将它们设为零) 是不正确的，就像描述流体时忽略体黏度和剪切黏度同样不正确。下面我们详细讨论有效应力张量的性质。

The Stress Tensor and Time (Non)-locality

应力张量与时间 (非) 局域性

The quantity that appears in the r.h.s. of the effective Euler equation is the smoothed divergence of the effective stress tensor, $\frac{1}{\rho_\ell}\left[\partial_j\sigma^{ij}\right]_\Lambda$. This term incorporates the effects of the short-scale physics and its backreaction on large scales. As we discussed earlier, it contains response of short-scale (virialized) modes to large-scale tidal forces. In the EFT approach, we need to expand the stress tensor in derivatives of the long-wavelength field while being consistent with rotation symmetry and the equivalence principle. At leading order in the number of density fields and its gradients, we get (In principle, one should also add here shear and bulk viscosity terms analogous to (55), but their contribution is completely degenerate with $\partial^i\delta$ at the level of the one-loop power spectrum, so we ignore these terms for simplicity.)

有效欧拉方程右侧出现的量是有效应力张量的平滑散度，$\frac{1}{\rho_\ell}\left[\partial_j\sigma^{ij}\right]_\Lambda$ 。该项包含小尺度物理及其对大尺度的反作用效应。正如我们此前讨论的，它包含小尺度 (已维里化) 模式对大尺度潮汐力的响应。在有效场论方法中，我们需要将应力张量按长波场导数展开，同时满足旋转对称性和等效原理。在密度场及其梯度数量的领头阶，我们得到 (原则上，我们还应在此处添加类似 (55) 的剪切与体粘滞项，但它们的贡献在单圈功率谱层面与 $\partial^i\delta$ 完全简并，因此为简化起见我们忽略这些项。)

$$\frac{1}{\rho_\ell}\left[\partial_j\sigma^{ij}\right]_\Lambda = c_s^2(\tau)\,\partial^i\delta(\mathbf{x},\tau)\,, \tag{56}$$

where $c_s^2(\tau)$ is a time-dependent Wilson coefficient. Note that the stress tensor cannot depend on the gravitational potential Φ or its gradient $\partial_i\Phi$ - this would contradict the equivalence principle, which states that these quantities can be removed by a gauge choice and hence cannot affect dynamics.

其中 $c_s^2(\tau)$ 是含时威尔逊系数。注意，应力张量不能依赖引力势 Φ 或其梯度 $\partial_i\Phi$ ——这会违反等效原理: 等效原理指出这些量可通过规范选择消去，因此不会影响动力学。

The expression (56) has a nice property that it is local in time and space. However, there is no reason why it should be the case. The problem is that short-wavelength modes, which we integrate out in (56), evolve on the same time scale $\mathcal{H}^{-1}$ as the long-wavelength modes. Before virialization, the short modes evolve with the same growth factor as the long modes. This means that we cannot really time-average the evolution of short modes. Thus, we need to take into account the fact that the short modes affect the entire evolution of long-wavelength perturbations along the fluid trajectory. We should generalize (56) to [7]

表达式 (56) 有一个很好的性质，它在时间和空间上都是局域的。然而，并没有理由要求它必须满足局域性。问题在于，我们在 (56) 中积掉的短波模式，与长波模式在相同的时间尺度 $\mathcal{H}^{-1}$ 上演化。在维里化之前，短模式与长模式遵循相同的增长因子演化。这意味着我们无法真正对短模式的演化做时间平均。因此，我们需要考虑短模式会影响流体轨迹上长波扰动的整个演化过程。我们应当将 (56) 推广为文献 [7] 中的形式:

$$\frac{1}{\rho_\ell}\left[\partial_j\sigma^{ij}\right]_\Lambda = \int_{\tau_{\text{ini}}}^{\tau} d\tau' K(\tau,\tau')\,\partial^i\delta\left(\mathbf{x}_{fl}[\mathbf{x},\tau;\tau'],\tau'\right), \tag{57}$$

where $\mathbf{x}_{fl}[\mathbf{x},\tau;\tau']$ is the trajectory of the fluid element with Eulerian coordinate $\mathbf{x}$ at time $\tau.\tau'$ parameterizes this trajectory. $K(\tau,\tau')$ is some (unknown) time-dependent kernel. This expression is hard to work with. However, we can Taylor expand $\delta\left(\mathbf{x}_{fl}[\mathbf{x},\tau;\tau'],\tau'\right)$ around the fluid trajectory,

其中，欧拉坐标为 $\mathbf{x}$ 的流体元在时刻 $\tau.\tau'$ 的轨迹为 $\mathbf{x}_{fl}[\mathbf{x},\tau;\tau']$，该轨迹参数化了运动过程。$K(\tau,\tau')$ 是某个 (未知的) 含时核。这个表达式很难处理，但我们可以对流体轨迹附近的 $\delta\left(\mathbf{x}_{fl}[\mathbf{x},\tau;\tau'],\tau'\right)$ 做泰勒展开，

$$\delta\left(\mathbf{x}_{fl}[\mathbf{x},\tau;\tau'],\tau'\right) = \delta(\mathbf{x},\tau) + (\tau'-\tau)\frac{D}{D\tau}\delta + \frac{(\tau'-\tau)^2}{2}\frac{D^2}{D\tau^2}\delta + \ldots \tag{58}$$

where we introduced the convective derivative $D/D\tau \equiv \partial_\tau + v^i\partial_i$ and the peculiar velocity along the flow $v^i(\mathbf{x},\tau) \equiv \left.\frac{d\mathbf{x}_{fl}}{d\tau}\right|_{(\mathbf{x},\tau)}$. The integral along the flow can be written in terms of Eulerian quantities,

此处我们引入了对流导数 $D/D\tau \equiv \partial_\tau + v^i\partial_i$ 和沿流场的本动速度 $v^i(\mathbf{x},\tau) \equiv \left.\frac{d\mathbf{x}_{fl}}{d\tau}\right|_{(\mathbf{x},\tau)}$。沿流场的积分可以用欧拉量表示为:

$$\begin{aligned}&\int_{\tau_{\text{ini}}}^{\tau} d\tau' K(\tau,\tau')\,\partial^i\delta\left(\mathbf{x}_{fl}[\mathbf{x},\tau;\tau'],\tau'\right)\\ &= \left[\int_{\tau_{\text{ini}}}^{\tau} d\tau' K(\tau,\tau')\right]\partial^i\delta(\mathbf{x},\tau) + \left[\int_{\tau_{\text{ini}}}^{\tau} d\tau' K(\tau,\tau')(\tau'-\tau)\right]\frac{D}{D\tau}\partial^i\delta(\mathbf{x},\tau) + \ldots\end{aligned} \tag{59}$$

Naively, this expansion still contains an infinite number of terms, so it does not look very useful. However, it simplifies in perturbation theory, where we should only keep a finite number of fields in convective derivatives. Indeed, the terms with convective derivatives can be simplified by using equations of motion (assuming EdS for simplicity here),

单纯看这个展开式仍然包含无穷多项，因此看起来没什么用。但它在微扰论中会简化: 我们只需要保留对流导数中有限个场项。实际上，含对流导数的项可以利用运动方程化简 (此处为简化假设为爱因斯坦德西特宇宙),

$$\frac{D}{D\tau}\delta = \mathcal{H}\Theta\left(1+\delta\right)$$

(60)

$$\frac{D}{D\tau}\Theta = \mathcal{H}^{-1}\left(-\frac{1}{2}\mathcal{H}^2\Theta + \frac{3}{2}\mathcal{H}^2\delta + \partial_i v^j \partial_j v^i - \partial^i\left[\rho_\ell^{-1}\partial^j\sigma_{ij}\right]\right).$$

The stress tensor in the equations above should be computed iteratively. From the structure of these equations, we see that at a given order in perturbation theory, one has to keep track of a finite number of terms in (58). For instance, at one-loop order, it is sufficient to use the linear theory solution (8) in the r.h.s. of (58), in which case there will be only one linearly independent term proportional to $\partial^i\delta^{(1)}$. Now we can formally sum all the infinite series, which can be packaged into an overall coefficient in front of the linear density field:

上述方程中的应力张量需要迭代计算。从这些方程的结构可以看出，在微扰论的给定阶数下，我们只需要跟踪 (58) 中有限数量的项。例如，在单圈阶，只需在线性理论中求解 (58) 右侧的 (8) 式，此时只会得到一个与 $\partial^i\delta^{(1)}$ 成正比的线性独立项。现在我们可以对整个无穷级数做形式求和，最终可以整理为线性密度场前的一个整体系数:

$$\frac{1}{\rho_\ell}\left[\partial_j\sigma^{ij}\right]_\Lambda = \left[\int_{\tau_{\rm ini}}^{\tau} d\tau' K\left(\tau,\tau'\right)\left(\prod_{n=0}^{\infty}\frac{\left(\tau'-\tau\right)^n}{n!}\partial_\tau^n\right)\right] D\left(\tau\right)\partial^i\delta_0\left(\mathbf{x}\right) \tag{61}$$

$$= c_s^2\left(\tau\right)\partial^i\delta^{(1)}\left(\mathbf{x},\tau\right).$$

This is the same result as (56). However, this simplicity does not hold at higher orders in perturbation theory, where convective derivatives induce operators nonlocal in space.

这与 (56) 的结果一致。但这种简洁性在微扰论的更高阶不成立，高阶下对流导数会产生空间非局域算符。

All in all, non-locality in time is an important property of the EFTofLSS. However, it can be removed perturbatively, so the resulting expression for the stress tensor takes a manifestly local in time expression. The time non-locality, however, does not disappear completely: we trade it for non-locality in space, which is produced by convective derivatives as in Eq. (58).

总而言之，时间非定域性是大尺度结构有效场论 (EFTofLSS) 的一个重要性质。但它可以通过微扰论消除，因此最终得到的应力张量表达式是明显时间定域的。不过时间非定域性并没有完全消失: 我们只是将其转化为空间非定域性，这种空间非定域性由式 (58) 中的对流导数产生。

Stochasticity

随机性

Small-scale perturbations may not be statistically correlated over long distances. Non-linear collapse of matter and virialization processes can erase memory of the initial conditions, so that the short-scale density field becomes partly uncorrelated with the long-wavelength modes. In other words, the actual realization of the effective stress tensor is expected to be different from its expectation value. The density field thus develops a stochastic (noise) component. In order to incorporate this in the EFT, we need to include a stochastic term in the effective stress-energy tensor,

小尺度扰动在长距离上可能不存在统计关联。物质的非线性坍缩和位力化过程会抹除初始条件的记忆，因此短尺度密度场会在一定程度上与长波长模式退关联。换言之，有效应力张量的实际实现会偏离其期望均值，因此密度场会产生一个随机 (噪声) 分量。为了在有效场论 (EFT) 中纳入该效应，我们需要在有效能动张量中加入一个随机项，

$$\frac{1}{\rho_\ell}\left[\partial_j \sigma^{ij}\right]_\Lambda \supset J^i, \quad \text{where} \quad \left\langle J^i \delta_\ell \right\rangle = 0. \tag{62}$$

This term propagates a stochastic component to the density field,

该项会为密度场引入一个随机分量，

$$\delta^{\text{stoch.}} \propto \partial_i J^i. \tag{63}$$

Symmetry arguments constrain the scale dependence of $\delta^{\text{stoch.}}$. As we have seen above, mass and momentum conservation dictate that in the $k \to 0$ limit, it goes as $\delta^{\text{stoch.}} \propto k^2$, which implies

对称性论证约束了 $\delta^{\text{stoch.}}$ 的标度依赖关系。正如我们上文所见，质量与动量守恒要求，在 $k \to 0$ 极限下，它满足 $\delta^{\text{stoch.}} \propto k^2$，这意味着

$$\left\langle \delta^{\text{stoch.}}(\mathbf{k}') \delta^{\text{stoch.}}(\mathbf{k}) \right\rangle' = P_J(k) = R^7_{\text{stoch.}} k^4 + \dots, \tag{64}$$

where $R_{\text{stoch.}}$ is some parameter with dimensionality of length.

其中 $R_{\text{stoch.}}$ 是一个量纲为长度的参数。

One-Loop Power Spectrum in the EFTofLSS

大尺度结构有效场论 (EFTofLSS) 中的单圈功率谱

Knowing the stress tensor at leading order in the EFT, we can now compute the full one-loop prediction. Focusing on the scalar part of the EFT Euler equation, we get

已知 EFT 中领先阶的应力张量，我们现在可以计算完整的单圈预言。聚焦于 EFT 欧拉方程的标量部分，我们得到

$$\dot{\delta}_{\mathbf{k}} - \Theta_{\mathbf{k}} = \int_{\mathbf{q}_1\mathbf{q}_2}^{\Lambda} \delta_D^{(3)}(\mathbf{k}-\mathbf{q}_{12}) \frac{\mathbf{q}_{12}\cdot\mathbf{q}_1}{q_1^2} \Theta_{\mathbf{q}_1}\delta_{\mathbf{q}_2},$$

$$\dot{\Theta}_{\mathbf{k}} - \frac{3}{2}\delta_{\mathbf{k}} + \frac{1}{2}\Theta_{\mathbf{k}} = \int_{\mathbf{q}_1\mathbf{q}_2}^{\Lambda} \delta_D^{(3)}(\mathbf{k}-\mathbf{q}_{12}) \frac{\mathbf{q}_{12}^2(\mathbf{q}_1\cdot\mathbf{q}_2)}{2q_1^2q_2^2} \Theta_{\mathbf{q}_1}\Theta_{\mathbf{q}_2} - \frac{k^2c_s^2(\tau)}{\mathcal{H}^2}\delta_{\mathbf{k}} + \frac{\partial_i J^i}{\mathcal{H}^2},$$

(65)

where we have assumed that smoothing out the fields with a low-pass filter is equivalent to cutting off the integral at Λ. An alternative form of this equation is given by Eq. (24) with a slightly modified source,

其中我们假设，用低通滤波器平滑场等价于将积分在 Λ 处截断。该方程的另一种形式由式 (24) 给出，仅源项有小幅修改，

$$\mathcal{H}^2\mathcal{H}_\beta \to \mathcal{H}^2\mathcal{S}_\beta + \tau_\theta,\ \tau_\theta \equiv \partial^i\left[\frac{1}{\rho_\ell}\partial^j\sigma_{ij}\right] = \left(c_s^2\partial^2\delta + \partial^i J_i\right). \tag{66}$$

This representation is useful because it allows us to easily evaluate the corrections to the density field produced by the effective stress tensor,

这种表示很有用，因为它允许我们轻松计算有效应力张量对密度场的修正，

$$\delta_{\mathbf{k}}^{(\sigma)} = \int da' G_\delta(a,a')\,\tau_\theta(a'), \tag{67}$$

where $G_\delta(a,a')$ is Green’s function of Eq. (24). It is convenient to present the total density field as

其中 $G_\delta(a,a')$ 是式 (24) 的格林函数。将总密度场写为如下形式会更方便:

$$\delta_{\mathbf{k}}^{\rm NL} = \delta_{\mathbf{k}}^{(1)} + \delta_{\mathbf{k}}^{(2)} + \delta_{\mathbf{k}}^{(3)} + \delta_{\mathbf{k}}^{\text{stress.}} + \delta_{\mathbf{k}}^{\text{stoch.}}, \tag{68}$$

where $\delta_{\mathbf{k}}^{(n)}$ are the corrections coming from the PPF part of the EFT equations (in the absence of the stress tensor), while $\delta_{\mathbf{k}}^{\text{stress.}}$ and $\delta_{\mathbf{k}}^{\text{stoch.}}$ are contributions coming from the deterministic and stochastic components of the stress tensor, respectively. The $\delta_{\mathbf{k}}^{(n)}$ terms are the same as the ones that we computed before. The only difference now is that all fields now have support only for $k \le \Lambda$.

其中 $\delta_{\mathbf{k}}^{(n)}$ 是 EFT 方程 PPF 部分 (无应力张量时) 带来的修正，而 $\delta_{\mathbf{k}}^{\text{stress.}}$ 和 $\delta_{\mathbf{k}}^{\text{stoch.}}$ 分别是应力张量确定性分量和随机分量的贡献。$\delta_{\mathbf{k}}^{(n)}$ 项和我们之前计算的一致, 唯一的区别在于现在所有场仅在 $k \le \Lambda$ 处有支撑。

The field $\delta_{\mathbf{k}}^{\text{stoch.}}$ only correlates with itself. Its power spectrum is given in (64). Hence, the only new piece that we have to compute is $\delta_{\mathbf{k}}^{\text{stress.}}$. Its calculation is identical to the computation of the effective pressure correction in Eqs. (49) and (51). In perturbation theory, we can replace $\delta_{\mathbf{k}}$ in the effective pressure term with $\delta_{\mathbf{k}}^{(1)}$ and, using Green’s function (22), get

场 $\delta_{\mathbf{k}}^{\text{stoch.}}$ 仅和自身关联，它的功率谱由式 (64) 给出。因此，我们只需要计算新的部分 $\delta_{\mathbf{k}}^{\text{stress.}}$ ，其计算过程和式 (49) 与 (51) 中有效压强修正的计算完全相同。在微扰论中，我们可以将有效压强项中的 $\delta_{\mathbf{k}}$ 替换为 $\delta_{\mathbf{k}}^{(1)}$ ，再利用格林函数 (22) 得到

$$\delta_{\mathbf{k}}^{\text{stress.}} = -\gamma_\Lambda k^2 \delta_{\mathbf{k}}^{(1)} \equiv -\int da' G_\delta(a,a') k^2 c_s^2(a') \delta_{\mathbf{k}}^{(1)}(a') . \tag{69}$$

The total matter power spectrum at the one-loop order is given by

单圈阶的总物质功率谱由下式给出:

$$P_{\text{non-linear}}(k) = P_{11}(k,\eta) + P_{22}^\Lambda(k,\eta) + P_{13}^\Lambda(k,\eta) - 2\gamma_\Lambda k^2 P_{11}(k,\eta) + P_J(k) . \tag{70}$$

Let us see how the EFT corrections help renormalize the one-loop power spectrum. For this reason, it is important to stress that γ_Λ and R_{stoch} that we had so far are "bare" parameters, i.e., they contain both "infinite," or Λ -dependent, pieces and the finite ones, which capture the physical UV effects. We split the loop integral into the Λ -dependent piece we do not trust and a calculable piece that we trust because it's evaluated over the modes where we know that the EFT is correct. The corresponding regions are defined by a wavenumber q_{trust} . Let us consider first the P_{13} contribution,

我们来看 EFT 修正如何帮助单圈功率谱重整化。因此需要强调: 我们目前得到的 γ_Λ 和 R_{stoch} 都是“裸”参数，即它们同时包含依赖于 Λ 的“无穷”部分和捕捉物理紫外效应的有限部分。我们将圈积分拆分为两部分: 我们不可信的 Λ 依赖部分，以及我们可信的可计算部分——因为后者是在我们已知 EFT 有效的模式上积分的。对应区域由波数 q_{trust} 定义。我们首先考虑 P_{13} 贡献,

$$P_{13}^\Lambda = 6P_{11}(k) \int_{\mathbf{q}, q\le q_{\text{trust}}} F_3(\mathbf{k},\mathbf{q},-\mathbf{q}) P_{11}(q) \tag{71}$$

$$+6P_{11}(k) \int_{\mathbf{q}, q_{\text{trust}}\le q\le\Lambda} F_3(\mathbf{k},\mathbf{q},-\mathbf{q}) P_{11}(q) .$$

For simplicity, we assume that $\Lambda > q_{\text{trust}} \gg k$, in which case the second term above can be simplified as (we use the UV limit (39))

为简化起见，我们假设 $\Lambda > q_{\text{trust}} \gg k$ ，此时上述第二项可以化简为 (我们使用紫外极限 (39)):

$$6P_{11}(k) \int_{\mathbf{q}, q_{\text{trust}}\le q\le\Lambda} F_3(\mathbf{k},\mathbf{q},-\mathbf{q}) P_{11}(q) = -\frac{61}{630\pi^2} k^2 P_{11}(k) \int_{q_{\text{trust}}}^\Lambda dq P_{11}(q) . \tag{72}$$

This term potentially diverges in the limit $\Lambda \to \infty$. This divergence, however, can be explicitly canceled by an appropriate choice of γ_Λ :

该项在 $\Lambda \to \infty$ 极限下可能发散。不过，这种发散可以通过恰当选择 γ_Λ 显式抵消:

$$\gamma_{\Lambda}=\gamma_{\text{finite}}-\frac{61}{1260\pi^{2}}\int_{q_{\text{trust}}}^{\Lambda}dqP_{11}(q)\,. \tag{73}$$

Thus, the physical P_{13} -like contribution is independent of Λ :

因此，物理的类 P_{13} 贡献与 Λ 无关:

$$P_{13}^{\Lambda}-2\gamma_{\Lambda}k^{2}P_{11}=-2\gamma_{\text{finite}}\,k^{2}P_{11}+6P_{11}(k)\int_{\mathbf{q},q\leq q_{\text{trust}}}F_{3}(\mathbf{k},\mathbf{q},-\mathbf{q})\,P_{11}(q)\,, \tag{74}$$

which means that the effective sound speed renormalizes the P_{13} loop. In practice, this means that we can choose any Λ in our calculations, even $\Lambda=\infty$. Note that the finite counterterm γ_{finite} is not determined by theory - it should be fit from the data.

这意味着有效声速对 P_{13} 圈做了重整化。实际计算中，我们可以在计算中选择任意 Λ，甚至 $\Lambda=\infty$ 。注意有限抵消项 γ_{finite} 无法由理论确定——它需要从数据中拟合得到。

A similar calculation shows that the P_{22} correction is successfully renormalized by the noise term P_{J} :

类似的计算表明，P_{22} 修正可以被噪声项 P_{J} 成功重整化:

$$\begin{aligned}
P_{22}^{A}+P_{J}&=2\int_{\mathbf{q},q\leq q_{\text{trust}}}\left[F_{2}(\mathbf{k}-\mathbf{q},\mathbf{q})\right]^{2}P_{11}(q)\,P_{11}(\mathbf{k}-\mathbf{q})\\
&\quad+2\int_{\mathbf{q},q_{\text{trust}}<q\leq A}\left[F_{2}(\mathbf{k}-\mathbf{q},\mathbf{q})\right]^{2}P_{11}(q)\,P_{11}(\mathbf{k}-\mathbf{q})+P_{J}\\
&=2\int_{\mathbf{q},q\leq q_{\text{trust}}}\left[F_{2}(\mathbf{k}-\mathbf{q},\mathbf{q})\right]^{2}P_{11}(q)\,P_{11}(\mathbf{k}-\mathbf{q})\\
&\quad+k^{4}\left[\frac{9}{196\pi^{2}}\int_{q_{\text{trust}}}^{\Lambda}\frac{dq}{q^{2}}P_{11}^{2}(q)+R_{\text{stoch}}^{7}\right]\\
&=2\int_{\mathbf{q},q\leq q_{\text{trust}}}\left[F_{2}(\mathbf{k}-\mathbf{q},\mathbf{q})\right]^{2}P_{11}(q)\,P_{11}(\mathbf{k}-\mathbf{q})+\left(R_{\text{stoch}}^{\text{finite}}\right)^{7}k^{4},
\end{aligned} \tag{75}$$

where we formally defined

这里我们形式化定义:

$$R_{\text{stoch}}^{7}=\left(R_{\text{stoch}}^{\text{finite}}\right)^{7}-\frac{9}{196\pi^{2}}\int_{q_{\text{trust}}}^{\Lambda}\frac{dq}{q^{2}}P_{11}^{2}(q)\,. \tag{76}$$

The final, renormalized EFT power spectrum at one-loop order is given by

最终，重整化后的单圈阶 EFT 功率谱由下式给出:

$$P_{\text{non-linear}}(k)=P_{11}(k,\eta)+2\int_{\mathbf{q},q\leq q_{\text{trust}}}\left[F_{2}(\mathbf{k}-\mathbf{q},\mathbf{q})\right]^{2}P_{11}(q)\,P_{11}(\mathbf{k}-\mathbf{q})$$

$$+6P_{11}(k)\int_{\mathbf{q},q\le q_{\text{trust}}} F_3(\mathbf{k},\mathbf{q},-\mathbf{q})P_{11}(q) - 2\gamma_{\text{finite}}k^2P_{11}(k,\eta) + \left(R_{\text{stoch}}^{\text{finite}}\right)^7 k^4. \tag{77}$$

This expression depends on two Wilson coefficients γ_{finite} and $R_{\text{stoch}}^{\text{finite}}$. The physical value of q_{trust} should be around $0.3h\text{Mpc}^{-1}$ for redshifts $z \sim 0.5$. In practice, it turned out that the one-loop integrals are saturated around k_{eq} for the ΛCDM spectrum. Hence, the one-loop result essentially does not depend on $q_{\text{trust}} > k_{\text{eq}}$, so we can even choose $q_{\text{trust}} = \infty$.

该表达式依赖两个威尔逊系数 γ_{finite} 和 $R_{\text{stoch}}^{\text{finite}}$。对于红移 $z \sim 0.5$，q_{trust} 的物理值应在 $0.3h\text{Mpc}^{-1}$ 左右。实际计算中发现，对于 ΛCDM 谱，单圈积分在 k_{eq} 附近达到饱和，因此单圈结果本质上不依赖 $q_{\text{trust}} > k_{\text{eq}}$，我们甚至可以选取 $q_{\text{trust}} = \infty$。

Power Counting and the Scaling Universe

幂次计数与标度宇宙

The key aspect of effective field theory is power counting, which allows one to estimate the importance of various operators. In the EFTofLSS, we have two important parameters: the overdensity field and its gradients. In this section, we show that in fact, both of them effectively depend on just one small parameter, which is the ratio of the wavenumber of interest to the physical non-linear wavenumber, k/k_{NL}. This dependence is akin to the E/M dependence in other EFTs, e.g., in the EFT of quantum gravity $M = M_{\text{P}}$ or $M = \Lambda_{\text{QCD}}$ in ChPT [32].

有效场论的核心要点是幂次计数，它可以用来估计不同算符的重要程度。在大尺度结构有效场论 (EFTofLSS) 中，我们有两个重要参数: 密度涨落场及其梯度。在本节中我们将说明，实际上二者都仅依赖于同一个小参数，即感兴趣波数与物理非线性波数的比值 k/k_{NL}。这种依赖关系与其他有效场论中的 E/M 依赖类似，例如量子引力有效场论中的 $M = M_{\text{P}}$，或是手征微扰论 (ChPT) 中的 $M = \Lambda_{\text{QCD}}$ [32]。

Let us assume that the initial power spectrum is a power law as in Eq. (11). Then the dimensionless power spectrum, which is related to position space density variance, is given by

我们假设初始功率谱满足式 (11) 的幂律形式。那么与位置空间密度方差相关的无量纲功率谱为

$$\Delta(k) = \frac{k^3}{2\pi^2}P_{\text{lin}}(k) = \left(\frac{k}{k_{\text{NL}}}\right)^{n+3}. \tag{78}$$

Since $\Delta \sim \delta^2$, we see that each density field scales like

由 $\Delta \sim \delta^2$ 可知，每个密度场的标度行为如下

$$\delta \sim \left(\frac{k}{k_{\text{NL}}}\right)^{\frac{n+3}{2}} \ll 1 \text{ if } k \ll k_{\text{NL}}. \tag{79}$$

In a scaling universe, one can easily estimate the finite part of the loop integrals,

在标度宇宙中，我们可以很容易地估计圈积分的有限部分，

$$\Delta^2_{\mathrm{L-\ loop}}(k) = \left(\frac{k}{k_{\mathrm{NL}}}\right)^{(L+1)(n+3)}. \tag{80}$$

The sound speed terms and the stochastic contributions can also be easily estimated,

声速项和随机贡献也可以很容易地估计，

$$\Delta^2_{c_s^2}(k) = \left(\frac{k}{k_{\mathrm{NL}}}\right)^{n+5},\ \Delta^2_{\dot{J}}(k) = \left(\frac{k}{k_{\mathrm{NL}}}\right)^{7}. \tag{81}$$

Then the total power spectrum is given by

总功率谱则为

$$\Delta^2_{\text{non-linear}} = \underbrace{\left(\frac{k}{k_{\mathrm{NL}}}\right)^{n+3}}_{\text{linear}} + \underbrace{\left(\frac{k}{k_{\mathrm{NL}}}\right)^{2(n+3)}}_{1-\text{ loop}} + \underbrace{\left(\frac{k}{k_{\mathrm{NL}}}\right)^{5+n}}_{\text{counterterm}} + \underbrace{\left(\frac{k}{k_{\mathrm{NL}}}\right)^{7}}_{\text{stochastic}}. \tag{82}$$

For our universe, the matter power spectrum in the quasi-linear regime can be approximated as a power law with $n = -1.5$ and $k_{\mathrm{NL}} \sim 0.3h\mathrm{Mpc}^{-1}$ (at $z = 0$). Then we find for $k \sim 0.1$:

对于我们的宇宙，准线性区域的物质功率谱可以近似为幂律，满足 $n = -1.5$ 和 $k_{\mathrm{NL}} \sim 0.3h\mathrm{Mpc}^{-1}$ (在 $z = 0$ 处)。由此我们得到 $k \sim 0.1$ 的结果:

$$\Delta^2_{\text{linear}} < \Delta^2_{\text{one-loop}} < \Delta^2_{\text{counterterm}} \ll \Delta^2_{\text{two-loop}} < \Delta^2_{\text{stochastic}}. \tag{83}$$

Thus, the stochastic term can be neglected at the one-loop order. The actual ΛCDM universe is, of course, not a scaling universe. But the scaling universe estimates happen to be quite accurate, which makes them useful to get an idea of the size of higher-order corrections in the EFT.

因此，随机项在单圈阶可以忽略。当然，真实的 ΛCDM 宇宙并不是标度宇宙，但标度宇宙给出的估计恰好相当准确，因此它对我们了解有效场论中高阶修正的量级很有帮助。

Path Integral Methods: Time-Sliced Perturbation Theory

路径积分方法: 时间分片微扰论

Large-scale structure theory has two key ingredients: initial conditions and time evolution. The typical physical observables are n -point correlation functions of random stochastic weakly non-Gaussian fields at a given time of the observation. This problem can be naturally formulated in the language of generating functionals. In particular, correlation functions in the EFTofLSS can be calculated using the following generating functional:

大尺度结构理论有两个关键组成部分: 初始条件和时间演化。典型物理可观测量是观测给定时刻随机弱非高斯随机场的 n 点关联函数。该问题可以自然地用生成泛函语言表述，具体而言，大尺度结构有效场论 (EFTofLSS) 中的关联函数可通过以下生成泛函计算:

$$Z[J_\delta] = \int \mathcal{D}\delta_0 \mathcal{P}_0[\delta_0]\, e^{\int_{\mathbf{k}} J_\delta(-\mathbf{k})\delta_{\mathbf{k}}[\delta_0]}, \text{ where } \mathcal{P}_0[\delta_0] = \mathcal{N}^{-1} \exp\left\{\int_{\mathbf{k}} \frac{|\delta_0(\mathbf{k})|^2}{2P_{\text{lin}}(k)}\right\},$$

(84)

$\mathcal{N}^{-1}$ is a normalization constant, and the functional $\delta[\delta_0]$ is obtained through a perturbative solution of the fluid equations, $\delta[\delta_0] = D_+\delta_0 + D_+^2[F_2\delta_0]^2 + \cdots$. This relationship encodes the dynamics of the system. The path integral above is over all possible configurations of the initial density field. This field is assumed to have a Gaussian probability density functional (PDF) $\mathcal{P}_0$. The n-point correlator can be obtained by taking n derivatives of the generating functional w.r.t. the source J_δ ,

$\mathcal{N}^{-1}$ 是归一化常数，泛函 $\delta[\delta_0]$ 通过流体方程 $\delta[\delta_0] = D_+\delta_0 + D_+^2[F_2\delta_0]^2 + \cdots$ 的微扰解得到，该关系编码了系统的动力学。上述路径积分对初始密度场的所有可能构型积分，该场被认为服从高斯概率密度泛函 (PDF) $\mathcal{P}_0$ 。n 点关联子可以通过对源 J_δ 取 n 次生成泛函的导数得到,

$$\langle \delta_{\mathbf{k}_1} \ldots \delta_{\mathbf{k}_n} \rangle = \left.\frac{\delta^n Z[J_\delta]}{\delta J_\delta(-\mathbf{k}_1)\ldots\delta J_\delta(-\mathbf{k}_n)}\right|_{J_\delta=0} = \int \mathcal{D}\delta_0 \left(\prod_{i=1}^n \delta(\mathbf{k}_i)\right) \mathcal{P}_0[\delta_0].$$

(85)

The initial field, however, is not a directly observable physical quantity. If we want to work in terms of actual observables at a final time, it is natural to equivalently rewrite the generating functional (84) as

然而初始场并非可直接观测的物理量。如果我们要基于末态的实际可观测量进行研究，自然可以将生成泛函 (84) 等价改写为

$$Z[J_\delta] = \int \mathcal{D}\delta \mathcal{P}[\delta;\tau]\, e^{\int_{\mathbf{k}} J_\delta(-\mathbf{k})\delta_{\mathbf{k}}}, \tag{86}$$

where the integration runs over configurations of the final density field δ . Its probability distribution function, however, $\mathcal{P}[\delta;\tau]$, is not Gaussian anymore. Note that we also do not need to know the functional $\delta[\delta_0]$. Indeed, in the expression (86), we have traded the time evolution of fields for the time evolution of their PDF. And it is the cumulants of this PDF that we are ultimately interested in.

其中积分对末态密度场 δ 的构型进行。但它的概率分布函数 $\mathcal{P}[\delta;\tau]$ 不再是高斯分布。注意我们也不需要知道泛函 $\delta[\delta_0]$ 。实际上，在式 (86) 中，我们已经用场的概率密度泛函的时间演化替换了场本身的时间演化，而我们最终关心的正是该概率密度泛函的累积量。

The approach in which one studies the PDF of large-scale structure at a finite time instead of cosmological random fields is called time-sliced perturbation theory (TSPT) [14, 15, 36, 39, 68]. TSPT is a tool for efficient calculations of cosmological equal-time correlation functions. In this section, we give a brief overview of this method and emphasize its advantages over the standard EFTofLSS formulation for IR resummation and UV renormalization.

这种研究有限时刻大尺度结构概率密度泛函而非宇宙随机场的方法称为时间分片微扰论(TSPT)[14, 15, 36, 39, 68]。TSPT 是高效计算宇宙等时关联函数的工具。在本节中，我们简要概述该方法，并强调相比标准 EFTofLSS 形式，它在红外重求和与紫外重整化方面的优势。

Generating Functional for Large-Scale Structure

大尺度结构生成泛函

In cosmological perturbation theory, we are interested in overdensity and velocity divergence fields. For adiabatic initial conditions, these two fields are fully correlated; see (8). It is convenient to choose the velocity divergence field as a statistically independent variable in the generating functional. We will denote its PDF as $\mathcal{P}[\Theta, \eta]$. For simplicity, let us assume that the dynamics is described by the PPF equations. This will be sufficient for the purposes of this section. Then, at any moment of time, the overdensity field can be expressed through Θ as

在宇宙学微扰论中，我们研究的对象是 overdensity 场和速度散度场。对于绝热初始条件，这两个场完全关联；参见 (8)。在生成泛函中将速度散度场选作统计独立变量是很方便的，我们将其概率密度函数记为 $\mathcal{P}[\Theta, \eta]$ 。为简化起见，我们假设动力学由 PPF 方程描述，这满足本节的研究需求。那么，任意时刻的 overdensity 场都可以通过 Θ 表示为

$$\delta(\mathbf{k}) \equiv \delta[\Theta; \eta, \mathbf{k}] = \sum_{n=1}^{\infty} \frac{1}{n!} \int_{\mathbf{q}_1} \dots \int_{\mathbf{q}_n} K_n(\eta; \mathbf{q}_1, \dots, \mathbf{q}_n) (2\pi)^3 \delta_D^{(3)}(\mathbf{k} - \mathbf{q}_{1\dots n}) \prod_{j=1}^{n} \Theta_{\mathbf{q}_j}.$$

(87)

Note that in contrast to the PPF ansatz (26), the r.h.s. of this equation features the fully non-linear field Θ . The expansion (87) can be inserted into the Euler equation (24) to obtain the following equation of motion for the velocity field:

请注意，与 PPF 假设 (26) 不同，该方程的等号右侧出现了完全非线性场 Θ 。将展开式 (87) 代入欧拉方程 (24)，即可得到速度场的下述运动方程:

$$\partial_\eta \Theta(\mathbf{k}) \equiv \mathcal{I}[\Theta; \eta] = \sum_{n=1}^{\infty} \int_{\mathbf{q}_1} \dots \int_{\mathbf{q}_n} \frac{1}{n!} I_n(\eta; \mathbf{q}_1, \dots, \mathbf{q}_n) \delta_D^{(3)}(\mathbf{k} - \mathbf{q}_{1\dots n}) \prod_{j=1}^{n} \Theta_{\mathbf{q}_j}.$$

(88)

Note that in the EdS approximation, the kernels K_n and I_n are time-independent. $I_1 = K_1 = 1$ corresponds to the standard adiabatic growing mode.

请注意，在 EdS 近似下，核 K_n 和 I_n 不随时间变化。$I_1 = K_1 = 1$ 对应标准绝热增长模式。

The generating functional for correlation functions of δ and Θ is given by

δ 和 Θ 的关联函数生成泛函由下式给出

$$Z\left[J_\delta, J; \eta\right] = \int \left[\mathcal{D}\Theta\right] \mathcal{P}\left[\Theta; \eta\right] \exp\left\{\int_{\mathbf{k}} \Theta\left(\mathbf{k}\right) J\left(-\mathbf{k}\right) + \int_{\mathbf{k}} \delta\left[\Theta; \eta, \mathbf{k}\right] J_\delta\left(-\mathbf{k}\right)\right\}.$$

(89)

Equal-time correlation functions of δ and Θ are obtained by taking functional derivatives w.r.t. sources J_δ and J , e.g., the matter power spectrum is given by

δ 和 Θ 的等时关联函数可通过对源 J_δ 和 J 取泛函导数得到，例如，物质功率谱为

$$\left(2\pi\right)^3 \delta_D^{(3)}\left(\mathbf{k} + \mathbf{k}'\right) P\left(\eta; k\right) = \left.\frac{\delta^2 Z}{\delta J_\delta\left(-\mathbf{k}\right) \delta J_\delta\left(-\mathbf{k}'\right)}\right|_{J_\delta = J = 0}. \tag{90}$$

The conservation of probability implies the Liouville equation for the PDF:

概率守恒给出概率密度函数满足的刘维尔方程:

$$\partial_\eta \mathcal{P}\left[\Theta, \tau\right] + \int_{\mathbf{k}} \frac{\delta}{\delta\Theta\left(\mathbf{k}\right)} \left(\mathcal{P}\left[\Theta, \tau\right] \mathcal{I}\left[\Theta; \eta\right]\right) = 0. \tag{91}$$

By analogy with QFT, we can rewrite the PDF perturbatively in Θ ,

类比量子场论，我们可以将概率密度函数按 Θ 做微扰改写，

$$\mathcal{P}\left[\Theta, \tau\right] = \mathcal{N}^{-1} \exp\left\{-\sum_{n=1}^{\infty} \frac{1}{n!} \int_{\mathbf{k}_1} \dots \int_{\mathbf{k}_n} \Gamma_n^{\mathrm{tot}}\left(\eta; \mathbf{k}_1, \dots, \mathbf{k}_n\right) \prod_{j=1}^{n} \Theta\left(\mathbf{k}_j\right)\right\},$$

(92)

where $\mathcal{N}$ is a normalization constant. The expression above is reminiscent of the 1PI QFT effective action. Plugging this into the Liouville equation, we obtain the hierarchy of equations for vertices Γ_n^{tot} ,

其中 $\mathcal{N}$ 是归一化常数。上述表达式类似于量子场论中的 1PI 有效作用量。将其代入刘维尔方程，我们得到顶点 Γ_n^{tot} 满足的方程组层级，

$$\begin{aligned}
&\dot{\Gamma}_n^{\mathrm{tot}}\left(\eta; \mathbf{k}_1, \dots, \mathbf{k}_n\right) \\
&+ \sum_{m=1}^{n} \sum_{\sigma} \frac{I_m\left(\eta; \mathbf{k}_{\sigma(1)}, \dots, \mathbf{k}_{\sigma(m)}\right)}{m!\left(n-m\right)!} \Gamma_{n-m+1}^{\mathrm{tot}}\left(\eta; \sum_{i=1}^{m} \mathbf{k}_{\sigma(i)}, \mathbf{k}_{\sigma(m+1)}, \dots, \mathbf{k}_{\sigma(n)}\right) \\
&= \left(2\pi\right)^3 \delta_D^{(3)}\left(\mathbf{k}_{1\dots n}\right) \int_{\mathbf{q}} I_{n+1}\left(\eta; \mathbf{q}, \mathbf{k}_1, \dots, \mathbf{k}_n\right),
\end{aligned}$$

(93)

where the sum in the second term on the l.h.s. is done over all permutations σ of n indices. It is useful to decompose the solution of this equation as

其中左侧第二项对 n 指标的所有排列 σ 求和。将该方程的解做如下分解是十分有用的:

$$\Gamma_n^{\text{tot}} = \Gamma_n + C_n \tag{94}$$

where Γ_n is the solution of the homogeneous equation with the initial conditions matching the initial statistical distribution, while C_n is the solution of the nonhomogeneous equation with vanishing initial conditions. Then Γ_n have the meaning of the one-particle irreducible (1PI) contributions to the tree-level equal-time n-point functions with "amputated" external propagators. In contrast, C_n have the meaning of counterterms that cancel ultraviolet divergences in loop integrals.

其中 Γ_n 是齐次方程满足初始统计分布初始条件的解，而 C_n 是非齐次方程满足零初始条件的解。此时 Γ_n 的物理意义是“截肢”外传播子树级等时 n 点函数的单粒子不可约 (1PI) 贡献。与之相对，C_n 的物理意义是抵消圈积分中紫外发散的抵消项。

In order to solve Eq. (93), we adopt the EdS approximation for kernels I_n , in which case we can use an ansatz that separates time and momentum dependence,

为求解方程 (93)，我们对核 I_n 采用 EdS 近似，该情况下我们可以使用分离时间依赖和动量依赖的假设,

$$\Gamma_n(\eta;\mathbf{k}_1,\dots,\mathbf{k}_n) = \sum_{l=2}^{n} e^{-l\eta}\Gamma_n^{(l)}(\mathbf{k}_1,\dots,\mathbf{k}_n),\ n \geq 2. \tag{95}$$

Note that $\Gamma_1 = 0$ as a result of statistical homogeneity, $\langle\Theta\rangle = 0$. This implies the following recursion relation for $\Gamma_n^{(l)}$ with $l < n$:

请注意，由统计齐次性可得 $\Gamma_1 = 0$ ，即 $\langle\Theta\rangle = 0$ 。这给出 $\Gamma_n^{(l)}$ 在满足 $l < n$ 时的递推关系:

$$\Gamma_n^{(l)}(\mathbf{k}_1,\dots,\mathbf{k}_n) =$$

$$-\frac{1}{n-l}\sum_{m=2}^{n-l+1}\sum_{\sigma}\frac{I_m\left(\mathbf{k}_{\sigma(1)},\dots,\mathbf{k}_{\sigma(m)}\right)}{m!\,(n-m)!}\Gamma_{n-m+1}\left(\eta;\sum_{i=1}^{m}\mathbf{k}_{\sigma(i)},\mathbf{k}_{\sigma(m+1)},\dots,\mathbf{k}_{\sigma(n)}\right). \tag{96}$$

Note that all $\Gamma_n^{(l)}$ with $l < n$ are uniquely determined by vertices of lower orders. The vertex $\Gamma_n^{(n)}$ should be fixed by initial conditions. Without loss of generality, we assume that they are set at $\eta \to -\infty$ and

请注意，所有满足 $l < n$ 的 $\Gamma_n^{(l)}$ 都可由低阶顶点唯一确定。顶点 $\Gamma_n^{(n)}$ 需要由初始条件确定。不失一般性，我们假设它们在 $\eta \to -\infty$ 处设定，且

$$\lim_{\eta\to-\infty} e^{n\eta}\Gamma(\eta;\mathbf{k}_1,\dots,\mathbf{k}_n) = \Gamma_n^{(n)}(\mathbf{k}_1,\dots,\mathbf{k}_n). \tag{97}$$

One can derive similar equations for the counterterms C_n and find that they are time-independent and completely fixed by the kernels I_n .

我们可以为抵消项 C_n 推导出类似方程，发现它们不随时间变化，且完全由核 I_n 确定。

For the Gaussian initial conditions, the solution to Eq. (93) simplifies greatly. In this case, the initial distribution is given by

对于高斯初始条件，方程 (93) 的解会大幅简化。该情况下初始分布为

$$\lim_{\eta\to-\infty}\mathcal{P}\left[\Theta;\eta\right]=\mathcal{N}^{-1}\exp\left\{-\int_{\mathbf{k}}\frac{\left|\Theta_{\mathbf{k}}\right|^{2}}{2D_{+}^{2}\left(\eta\right)P_{\mathrm{lin}}\left(k\right)}\right\}, \tag{98}$$

where we introduced

此处我们引入

$$g\left(\eta\right)\equiv D_{+}\left(\eta\right)=e^{\eta}. \tag{99}$$

This implies

由此可得

$$\Gamma_{2}^{(2)}=\frac{\left(2\pi\right)^{3}\delta_{D}^{(3)}\left(\mathbf{k}_{1}+\mathbf{k}_{2}\right)}{P_{\mathrm{lin}}\left(k_{1}\right)},\ \Gamma_{n}^{(n)}\left(\mathbf{k}_{1},\ldots,\mathbf{k}_{n}\right)=0\ \text{ for } n>2. \tag{100}$$

This means that all $\Gamma_{n}^{(l)}$ with $l>2$ vanish and the solution is simply

这意味着所有满足 $l>2$ 的 $\Gamma_{n}^{(l)}$ 均为零，解可简单写为

$$\begin{aligned}\Gamma_{n}\left(\mathbf{k}_{1},\ldots,\mathbf{k}_{n}\right)&=\frac{1}{g^{2}\left(\eta\right)}\overline{\Gamma}_{n}\left(\mathbf{k}_{1},\ldots,\mathbf{k}_{n}\right)\\ \overline{\Gamma}_{n}\left(\mathbf{k}_{1},\ldots,\mathbf{k}_{n}\right)&=-\frac{1}{n-2}\sum_{m=2}^{n-l+1}\sum_{\sigma}\frac{I_{m}\left(\mathbf{k}_{\sigma(1)},\ldots,\mathbf{k}_{\sigma(m)}\right)}{m!\left(n-m\right)!}\overline{\Gamma}_{n-m+1}\\ &\times\left(\sum_{i=1}^{m}\mathbf{k}_{\sigma(i)},\mathbf{k}_{\sigma(m+1)},\ldots,\mathbf{k}_{\sigma(n)}\right).\end{aligned} \tag{101}$$

Remarkably, in the case of Gaussian initial conditions and in the EdS approximation, all vertices have a universal time dependence $\propto g^{-2}$, and all of them are sourced by the Gaussian initial weight and hence $P_{\mathrm{lin}}\left(k\right)$. The parameter g^{2} plays a role of the expansion parameter (coupling constant). Due to momentum conservation, the vertices are proportional to the Dirac δ -functions so it is convenient to introduce primed vertices where such δ -functions are stripped off,

值得注意的是，在高斯初始条件和 EdS 近似下，所有顶点都具有普适时间依赖关系 $\propto g^{-2}$ ，且所有顶点均由高斯初始权重产生，因此满足 $P_{\mathrm{lin}}\left(k\right)$ 。参数 g^{2} 充当膨胀参数 (耦合常数)。由于动量守恒，顶点与狄拉克 δ 函数成正比，因此引入剥离这类 δ 函数后的带撇顶点会更方便，

$$\overline{\Gamma}_{n}\left(\mathbf{k}_{1},\ldots,\mathbf{k}_{n}\right)=\left(2\pi\right)^{3}\delta_{D}^{(3)}\left(\mathbf{k}_{1\ldots n}\right)\overline{\Gamma}_{n}^{\prime}\left(\mathbf{k}_{1},\ldots,\mathbf{k}_{n}\right). \tag{102}$$

Once the tree-level 1PI n-point functions are fixed, the calculation of equal-time correlation functions proceeds by a perturbative expansion of the generating functional (92) around the Gaussian weight. This is identical to the perturbative calculations of n-point functions in QFT. Just like in the usual QFT, this computation can be represented in terms of Feynman diagrams. These diagrams are built of vertices $\Gamma_n, n \geq 3$, and lines correspond to propagators $g^2 P_{\rm lin}$; see Fig. 7. One should also include vertices corresponding to counterterms $C_n, n \geq 1$ in order to subtract certain UV divergences in loop diagrams. In this sense, counterterms appear in TSPT quite naturally.

确定树图级 1PI n 点函数后，等时关联函数的计算可通过对生成泛函 (92) 在高斯权重附近做微扰展开完成。这与量子场论中 n 点函数的微扰计算完全一致。和常规量子场论一样，该计算可以用费曼图表示。这些图由顶点 $\Gamma_n, n \geq 3$ 构成，线对应传播子 $g^2 P_{\rm lin}$ ；参见图 7。为了扣除圈图中的部分紫外发散，还需要引入对应抵消项 $C_n, n \geq 1$ 的顶点。从这个意义上说，抵消项自然出现在 TSPT 中。

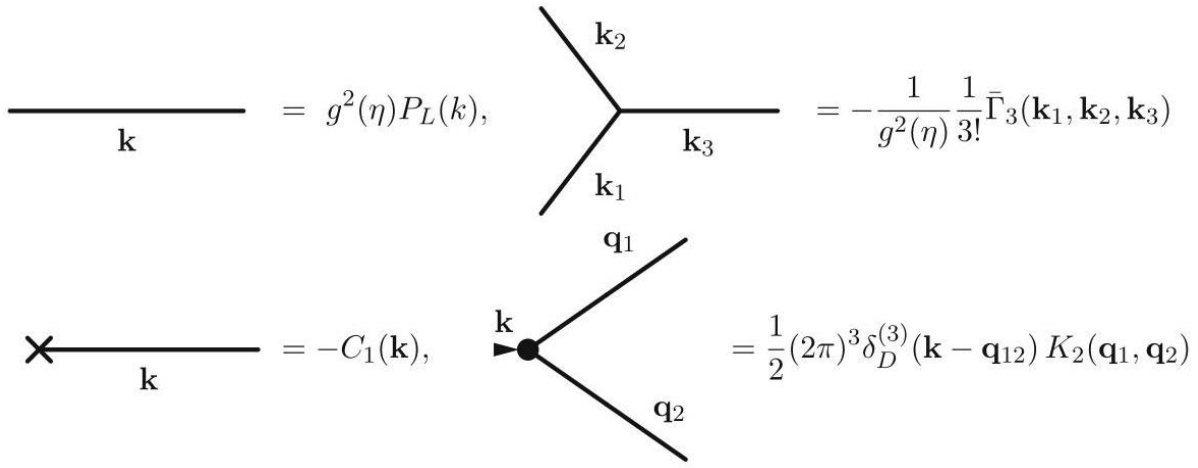

Fig. 7 Examples of TSPT Feynman rules

图 7 TSPT 费曼规则示例

To compute an n -point correlation function of the velocity divergence, one has to draw all diagrams with n external legs. It is easy to see that diagrams with larger number of loops are proportional to higher powers of $g(\eta)$. Hence, $g(\eta)$ plays the same role as a coupling constant in QFT. For the correlators of the density field δ , one should use the expression (87) which is akin to an expression for composite operators in QFT. It gives rise to additional vertices proportional to the kernels K_n ; these are denoted by an external arrow; see Fig. 7.

要计算速度散度的 n 点关联函数，需要画出所有带 n 个外腿的图。不难看出，圈数越多的图正比于 $g(\eta)$ 越高次幂。因此 $g(\eta)$ 在量子场论中起到和耦合常数相同的作用。对于密度场关联函数 δ ，应当使用表达式 (87)，该式类似量子场论中复合算符的表达式。它会产生正比于核 K_n 的额外顶点；这些顶点用外箭头标记；参见图 7。

Soft Limits and IR Safety

软极限与红外安全性

Since we have used the PPF equations as sources in the TSPT PDF calculations, our resulting expressions for the equal-time correlation functions must be identical to that of the PPF hydrodynamics that we discussed before. This is indeed the case. However, the intermediate calculations required to obtain n-point functions are completely different. The PPF loop diagrams contain unphysical IR divergences that cancel only when all diagrams of a given order are summed together. In contrast, this problem is absent in TSPT, where all loop diagrams are manifestly IR safe. This is to be expected as the individual building blocks of TSPT are all IR safe since they correspond to the physical 1PI equal-time correlators.

由于我们在时间分片微扰论 PDF 计算中将 PPF 方程用作源，我们得到的等时关联函数结果表达式必然与我们之前讨论的 PPF 流体力学结果完全一致，事实也确实如此。但得到 n 点函数所需的中间计算过程却完全不同。PPF 圈图包含非物理红外发散，这类发散仅在对给定阶的所有图求和后才会抵消。与之相比，时间分片微扰论不存在该问题，其所有圈图都具有明显的红外安全性。这一点符合预期: 时间分片微扰论的各基础单元都满足红外安全性，因为它们对应物理的单粒子不可约等时关联函数。

One can prove that the vertices $\overline{\Gamma}_n, C_n$, and K_n appearing in the TSPT Feynman graphs are bounded at finite values of their arguments. If we split the arguments of a n -point kernel $\overline{\Gamma}_n$ into "hard" momenta $k_1, \ldots, \mathbf{k}_l$ that we keep fixed and "soft" momenta $\mathbf{q}_1, \ldots \mathbf{q}_{n-l}$ that we send to zero uniformly as $\mathbf{q}_i = \varepsilon \mathbf{q}_i', \varepsilon \to 0$, we find that it does not have any poles

我们可以证明，时间分片微扰论费曼图中出现的顶点 $\overline{\Gamma}_n, C_n$ 和 K_n 在其自变量取有限值时都是有界的。若我们将 n 点核 $\overline{\Gamma}_n$ 的自变量拆分为保持固定的“硬”动量 $k_1, \ldots, \mathbf{k}_l$ ，以及按 $\mathbf{q}_i = \varepsilon \mathbf{q}_i', \varepsilon \to 0$ 方式一致趋近于零的“软”动量 $\mathbf{q}_1, \ldots \mathbf{q}_{n-l}$ ，可以发现该核不存在任何极点

$$\lim_{\varepsilon \to 0} \overline{\Gamma}_n \left(\mathbf{k}_1, \ldots, \mathbf{k}_l, \varepsilon \mathbf{q}_1', \ldots, \varepsilon \mathbf{q}_{n-l}' \right) = \mathcal{O}\left(\varepsilon^0 \right). \tag{103}$$

The same is true for C_n and K_n . The IR safety of TSPT vertices (103) can be contrasted with the PPF kernels F_n and G_n , which have poles at soft momenta; see (29). The absence of IR singularities of TSPT can be shown to be a direct consequence of the equivalence principle.

对于 C_n 和 K_n 结论同样成立。时间分片微扰论顶点 (103) 的红外安全性与 PPF 核 F_n 和 G_n 形成对比，后两者在软动量处存在极点，参见 (29)。可以证明，时间分片微扰论不存在红外奇点是等效原理的直接结果。

IR Resummation

红外重求和

The transparent IR structure of the TSPT perturbative expansion allows us to identify and resum physical IR contributions that are responsible for the non-linear evolution of the BAO. In order to identify these

contributions in the perturbative series, it is customary to split the initial power spectrum into the smooth component $P_{\rm smooth}$ and an oscillatory ("wiggly") contribution P_w (37). This decomposition induces a similar split of the TSPT vertices as they are sourced by the linear matter power spectrum,

时间切片微扰论 (TSPT) 微扰展开清晰的红外结构使我们能够识别并重求和导致重子声学振荡 (BAO) 非线性演化的物理红外贡献。为了在微扰级数中识别这些贡献，通常将初始功率谱分解为光滑分量 $P_{\rm smooth}$ 和振荡 ("wigly") 贡献 P_w (37)。由于 TSPT 顶点由线性物质功率谱源生，该分解会诱导 TSPT 顶点发生同样的分裂，

$$\overline{\Gamma}_n = \overline{\Gamma}_n^s + \overline{\Gamma}_n^w . \tag{104}$$

Then, one finds that the wiggly vertices are enhanced in the soft limit. For instance, the three-point vertex expanded for $q \ll k$ and to linear order in P_w is given by

随后可以发现，wigly 顶点在软极限下会被增强。例如，对 $q \ll k$ 展开、对 P_w 做一阶展开得到的三点顶点为

$$\overline{\Gamma}_3 \to \frac{\mathbf{k}\cdot\mathbf{q}}{q^2}\left(\frac{P_w(|\mathbf{k}+\mathbf{q}|) - P_w(q)}{P^2_{\rm smooth}(k)}\right). \tag{105}$$

In the formal limit $q \to 0$, the difference between the two power spectra in the numerators vanishes as q and hence cancels the $1/q$ enhancement in agreement with the equivalence principle. However, the Taylor expansion of $P_w(|\mathbf{k}+\mathbf{q}|)$ blows up for $k_{\rm BAO} \lesssim q \ll k$. Non-linear correlation functions receive large corrections from modes in this range. Fortunately, using TSPT, one can identify the enhanced contributions and systematically resum them to any desired accuracy order. The key point is that one can derive an analog of (105) for any n-point function and any number of soft momenta. This yields the following factorization formula:

在形式极限 $q \to 0$ 下，分子中两个功率谱的差按 q 趋于零，因此抵消了 $1/q$ 增强，这与等效原理一致。然而，$P_w(|\mathbf{k}+\mathbf{q}|)$ 的泰勒展开在 $k_{\rm BAO} \lesssim q \ll k$ 处发散。非线性关联函数会从该范围的模式得到大修正。幸运的是，借助 TSPT 可以识别这些增强贡献，并将它们系统地重求和到任意期望的精度阶。关键在于，我们可以对任意 n 点函数、任意数量的软动量推导出类似 (105) 的结果，由此得到如下因子化公式:

$$\overline{\Gamma}_n'^w\left(\mathbf{k}_1,\dots,\mathbf{k}_m - \sum_{j=1}^{n-m}\mathbf{q}_j,\mathbf{q}_1,\dots,\mathbf{q}_{n-m}\right) = (-1)^{n-m}\left(\prod_{j=1}^{n-m} D_{\mathbf{q}_j}\right)\Gamma_m'^w(\mathbf{k}_1,\dots,\mathbf{k}_m), \tag{106}$$

where $D_{\mathbf{q}}$ is a differential operator with the following action on the wiggly power spectrum:

其中 $D_{\mathbf{q}}$ 是对 wigly 功率谱作用如下的微分算符:

$$D_{\mathbf{q}}P_w(k) = \frac{\mathbf{k}\cdot\mathbf{q}}{q^2}\left(e^{\mathbf{q}\cdot\nabla_{\mathbf{k}'}} - 1\right)P_w(k')\Big|_{k'=k}. \tag{107}$$

One sees that for $q/k = \varepsilon \ll 1$ each $D_{\mathbf{q}} \sim \varepsilon^{-1}$, i.e.,

不难看出，对 $q/k = \varepsilon \ll 1$ 的每个 $D_{\mathbf{q}} \sim \varepsilon^{-1}$ ，即

$$\overline{\Gamma}_n'^{w}\left(\mathbf{k}_1, \ldots, \mathbf{k}_m - \sum_{j=1}^{n-m} \mathbf{q}_j, \mathbf{q}_1, \ldots, \mathbf{q}_{n-m}\right) = \mathcal{O}\left(\varepsilon^{m-n}\right). \tag{108}$$

This property allows us to formulate power counting rules that determine the order of enhancement ("degree of IR divergence") of each TSPT diagram. For that, one has to split each loop momentum into hard and soft regions, separated by a scale k_S . Then we just have to count the number of soft legs attached to a wiggly vertex $\overline{\Gamma}_n^w$ of a given TSPT diagram. Equation (108) tells us that a diagram with the largest number of soft legs will be most enhanced in the IR. At leading order in the degree of infrared enhancement and zeroth order in hard loops, this corresponds to the "daisy" diagrams; see Fig. 8. The daisy diagrams nicely exponentiate,

该性质允许我们建立幂计数规则，确定每个 TSPT 图的增强阶（“红外发散度”）。为此需要将每个圈动量分为硬区和软区，由标度 k_S 分隔。随后我们只需统计给定 TSPT 图中连接到 wigly 顶点 $\overline{\Gamma}_n^w$ 的软外线数量。式 (108) 表明，软外线数量最多的图在红外下增强程度最高。在红外增强的领头阶、硬圈的零阶下，这对应“雏菊图”；参见图 8。雏菊图可以很好地指数化，

$$P_w^{\text{IR res, LO}} = e^{-\sum^2 k^2} P_w(\eta; k) \quad \text{where}$$

$$\sum^2 = \frac{4\pi}{3} \int_0^{k_S} dq P_{\text{smooth}}(q) \left[1 - j_0(q r_{\text{BAO}}) + 2 j_2(q r_{\text{BAO}})\right]. \tag{109}$$

Note that the expansion in terms of the wiggly-smooth spectra is simply a bookkeeping tool that allows one to keep track of the enhanced contributions. Since the smooth contributions are never enhanced in the IR, one can combine the wiggly and smooth parts after resummation without changing the perturbative order of the resummed corrections. This amounts to promoting the factorization formula Eq. (106) to the total TSPT vertex Γ_n . This procedure allows one to circumvent any ambiguity in the wiggly-smooth split. In practice, however, this ambiguity appears only in higher orders of the perturbative expansion and therefore is negligible for practical applications.

请注意，按 wigly 谱和光滑谱展开仅仅是跟踪增强贡献的记账工具。由于光滑贡献在红外下永远不会被增强，我们可以在重求和后合并 wigly 部分和光滑部分，不会改变重求和修正的微扰阶。这相当于将式 (106) 的因子化公式推广到总 TSPT 顶点 Γ_n 。该过程可以规避 wigly-光滑分解中的所有歧义。但实际上，这种歧义仅出现在微扰展开的高阶，因此在实际应用中可以忽略。

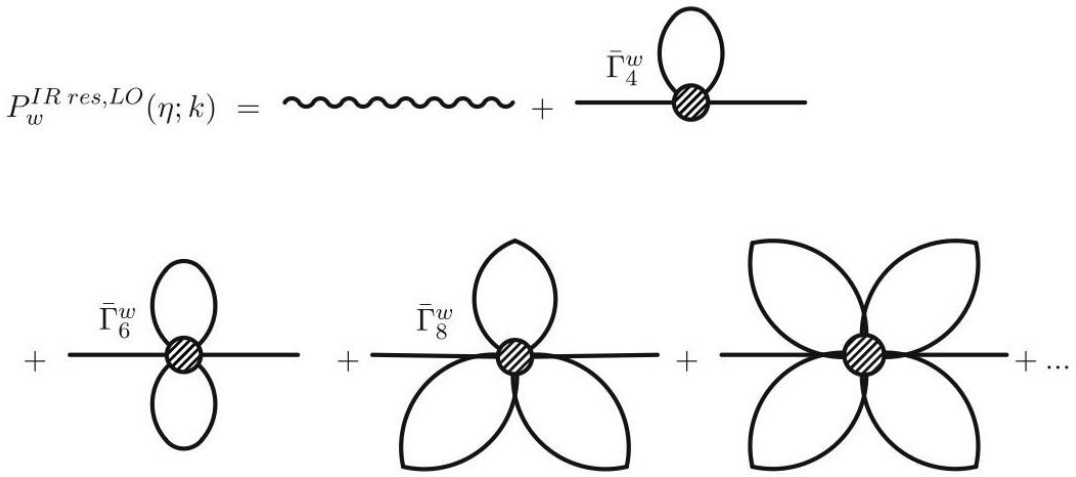

Fig. 8 Feynman diagram representation of IR resummation at leading order in the IR enhancement

图 8 红外增强领头阶下红外重求和的费曼图表示

The key advantage of the TSPT approach for IR resummation is that it provides us with a systematic program of resumming enhanced IR contributions that can be carried out to any required accuracy. Thus, it allows one to go beyond the leading order in a controlled fashion. For instance, one can include hard loops and obtain an expression for the IR-resummed matter power spectrum at one-loop order,

TSPT 方法用于红外重求和的核心优势在于，它为我们提供了一个系统的方案，可以对增强红外贡献进行重求和，并且能达到任意所需精度。因此，它可以在可控的框架下超出领头阶计算。例如，我们可以包含硬圈，得到单圈阶红外重求和的物质功率谱表达式，

$$P^{\text{IRres, NLO}}(\eta;k) = P_s(\eta;k) + e^{-\Sigma^2 k^2} P_w(\eta;k)\left(1+\sum^2 k^2\right)$$

(110)

$$P_{1-\text{loop}}\left[P_s + e^{-\Sigma^2 k^2} P_w\right],$$

where $P_{1-\text{loop}}[P_{\text{lin}}]$ is the one-loop integral treated as a functional of the linear matter power spectrum. The expression (110) is operationally very simple: at one-loop order, one just has to compute the one-loop integrals using the tree-level IR-resummed power spectrum as an input instead of the usual linear power spectrum. This simple prescription is reminiscent of the Schwinger-Dyson resummation approach in non-perturbative QFT. Note however that Eq. (110) is not a simple ad hoc prescription; it is a result of the rigorous and systematic resummation of Feynman diagrams.

其中 $P_{1-\text{loop}}[P_{\text{lin}}]$ 是视为线性物质功率谱泛函的单圈积分。表达式 (110) 在操作上非常简单: 在单圈阶，我们只需使用树级红外重求和功率谱 (而非通常的线性功率谱) 作为输入来计算单圈积分。这个简单的规则让人联想到非微扰量子场论中的施温格-戴森重求和方法。但需要注意，式 (110) 并不是一个简单的特设规则，它是对费曼图进行严格系统重求和得到的结果。

Importantly, within TSPT, IR resummation can be easily expended to higher-order n-point functions at an arbitrary order in hard loops and for any (subleading) degree of infrared enhancement.

重要的是，在时间切片微扰论 (TSPT) 中，红外重求和可以很容易地推广到硬圈任意阶、任意 (次 Leading) 红外增强程度的高阶 n 点函数。

UV Renormalization

紫外重整化

Another advantage of TSPT is that it allows for a formulation of the EFTofLSS in the language of Wilsonian renormalization group within the three-dimensional Euclidean QFT. Let us show how these ideas work in practice.

时间切片微扰论 (TSPT) 的另一个优势在于，它允许我们在三维欧几里得量子场论框架内，用威尔逊重整化群语言表述大尺度结构有效场论 (EFTofLSS)。下面我们演示这套思路的实际应用。

Let us derive the Wilson-Polchinski renormalization group equation [52,71] for large-scale structure. Imagine that we start with a full action for matter clustering and integrate out short-scale modes of the velocity divergence field Θ up to momentum scale Λ . This procedure should not affect physical n-point functions: integrating out the short scales should change the effective vertices in a way that would keep the low-energy physics intact. This gives rise to the renormalization group (RG) flow of the effective action. To derive the flow, we cut off the free propagator with a sharp momentum cutoff (Any other reasonable choice of the cutoff function leads to the same result.),

我们来推导适用于大尺度结构的威尔逊-波尔钦斯基重整化群方程 [52,71]。假设我们从物质成团的完整作用量出发，将速度散度场 Θ 动量高于截断尺度 Λ 的短尺度模式积掉。这一过程不应当改变物理 n 点函数: 积掉短尺度模式只会修正有效顶点，低能物理保持不变，由此引出有效作用量的重整化群 (RG) 流。为推导该流，我们对自由传播子引入尖锐动量截断 (选择任何其他合理的截断函数都会得到相同结果),

$$P^{\Lambda}(\eta;k) \equiv P_L(\eta;k)\,H(\Lambda-k) = \begin{cases} P_L(\eta;k), & k<\Lambda \\ 0, & k>\Lambda \end{cases}.$$

(111)

Our partition function for large-scale structure then takes the form

我们大尺度结构的配分函数可写为如下形式

$$Z[J] = \int [\mathcal{D}\Theta] \exp\left\{ -\int_{\mathbf{p}} \left(\frac{\Theta(\mathbf{p})\,\Theta(-\mathbf{p})}{2P^{\Lambda}(\eta;p)} + J(-\mathbf{p})\,\Theta(\mathbf{p}) \right) + L_{\text{int}}(\Theta,\Lambda) \right\}.$$

(112)

Requiring that $Z[J]$ do not depend on the cutoff Λ , we obtain the standard Polchinski RG equation [52],

要求 $Z[J]$ 不依赖于截断 Λ ，我们就得到了标准的波尔钦斯基 RG 方程 [52],

$$\Lambda\frac{\partial L_{\text{int}}}{\partial\Lambda}=-\frac{1}{2}\int_{\mathbf{p}}\Lambda\frac{\partial P^{\Lambda}(\eta;p)}{\partial\Lambda}\left(\frac{\partial L_{\text{int}}}{\partial\Theta(-\mathbf{p})}\frac{\partial L_{\text{int}}}{\partial\Theta(\mathbf{p})}+\frac{\partial^{2}L_{\text{int}}}{\partial\Theta(-\mathbf{p})\partial\Theta(\mathbf{p})}\right). \tag{113}$$

Note that we chose the current to have support only at low momenta; thus, it vanishes when multiplied by the term $dP^{\Lambda}/d\Lambda$ which has support only near the cutoff Λ . In the spirit of TSPT, we use the effective action ansatz

注意我们选择源仅在低动量区有支撑；因此它和仅在截断 Λ 附近有支撑的项 $dP^{\Lambda}/d\Lambda$ 相乘后结果为零。遵循 TSPT 的思路，我们采用如下有效作用量假设

$$L_{\text{int}}=-\sum_{n=1}^{\infty}\frac{1}{n!}\int_{\mathbf{q}_1}\ldots\int_{\mathbf{q}_n}\Gamma_n^{\Lambda}(\mathbf{q}_1,\ldots,\mathbf{q}_n)\,\Theta(\mathbf{q}_1)\ldots\Theta(\mathbf{q}_n). \tag{114}$$

Plugging this into the renormalization group equation (113) yields

将其代入重整化群方程 (113) 可得

$$\Lambda\frac{\partial\Gamma_n^{\Lambda}}{\partial\Lambda}=\frac{1}{2}\int_{\mathbf{p}}\Lambda\frac{\partial P^{\Lambda}(\eta;p)}{\partial\Lambda}\left(-\Gamma_{n+2}^{\Lambda}(\mathbf{q}_1,\ldots,\mathbf{q}_n,\mathbf{p},-\mathbf{p})\right.$$
$$\left.+\sum_{m=1}^{n+1}\sum_{i_1<i_2<\ldots<i_{m-1}}\Gamma_m^{\Lambda}(\mathbf{q}_{i_1},\ldots,\mathbf{q}_{i_{m-1}},\mathbf{p})\,\Gamma_{n+2-m}^{\Lambda}(\mathbf{q}_{i_m},\ldots,\mathbf{q}_{i_{n+m-2}},-\mathbf{p})\right). \tag{115}$$

These equations cannot be solved exactly as the equation for the n -th vertex involves $n+1$ ' s and $n+2$ ' s vertices. One can, however, find solutions to the RG equations perturbatively by expanding over the growth factor g^2 , which corresponds to the TSPT loop expansion,

这些方程无法精确求解，因为 n 阶顶点的方程会包含 $n+1$ 和 $n+2$ 阶顶点。不过我们可以通过对增长因子 g^2 做展开，微扰地求解 RG 方程，这对应 TSPT 的圈展开，

$$\Gamma_n^{\Lambda}=\sum_{l=0}^{\infty}g^{2(l-1)}\Gamma_n^{(l),\Lambda} \tag{116}$$

where l denotes the loop order. The power spectrum is simply given by $P_L(\eta;k)=\ g^2\bar{P}(k)$. Plugging this decomposition into Eq. (115), and striping off the delta functions, one arrives at the final form for the RG - equations,

其中 l 表示圈阶。功率谱可简单表示为 $P_L(\eta;k)=\ g^2\bar{P}(k)$ 。将该分解代入式 (115)，去掉德尔塔函数后，我们得到 RG 方程的最终形式，

$$\frac{\partial\Gamma_n'^{(l),\Lambda}}{\partial\Lambda}=\frac{1}{2}\int_{\mathbf{p}}\frac{\partial\bar{P}^{\Lambda}(p)}{\partial\Lambda}\left(-\Gamma_{n+2}'^{(l-1),\Lambda}(\mathbf{q}_1,\ldots,\mathbf{q}_n,\mathbf{p},-\mathbf{p})\right)$$
$$+\frac{1}{4}\sum_{m=1}^{n+1}\sum_{i_1<i_2<\ldots<i_{m-1}}\sum_{l'=0}^{l}\Lambda\frac{\partial\bar{P}^{\Lambda}\left(\left|\sum_{A=1}^{m-1}\mathbf{q}_{i_A}\right|\right)}{\partial\Lambda}\times$$

$$\left[\Gamma_m^{\prime(l^{\prime}),\Lambda}\left(\mathbf{q}_{i_1},\dots,\mathbf{q}_{i_{m-1}},-\sum_{A=1}^{m-1}\mathbf{q}_{i_A}\right)\Gamma_{n+2-m}^{\prime(l-l^{\prime}),\Lambda}\left(\mathbf{q}_{i_m},\dots,\mathbf{q}_{i_{n+m-2}},-\sum_{A=m}^{n+m-2}\mathbf{q}_{i_A}\right)\right.$$
$$\left.+\Gamma_m^{\prime(l-l^{\prime}),\Lambda}\left(\mathbf{q}_{i_1},\dots,\mathbf{q}_{i_{m-1}},-\sum_{A=1}^{m-1}\mathbf{q}_{i_A}\right)\Gamma_{n+2-m}^{\prime(l^{\prime}),\Lambda}\left(\mathbf{q}_{i_m},\dots,\mathbf{q}_{i_{n+m-2}},-\sum_{A=m}^{n+m-2}\mathbf{q}_{i_A}\right)\right].$$

(117)

Renormalization of the composite operator $\delta[\Theta;\eta]$ is straightforward. We just need to add it to the effective action ansatz (114)

复合算符 $\delta[\Theta;\eta]$ 的重整化十分直接。我们只需将其加入有效作用量假设 (114)

$$L_{\text{int}} \to L_{\text{int}} + \sum_{n=1}^{\infty}\frac{1}{n!}\int_{\mathbf{k}} J_\delta(-\mathbf{k})\int_{\mathbf{q}_1}\dots\int_{\mathbf{q}_n} K_n^\Lambda(\mathbf{q}_1,\dots,\mathbf{q}_n;\mathbf{k})\,\Theta(\mathbf{q}_1)\dots\Theta(\mathbf{q}_n),$$

(118)

plug it into Eq. (113), and take a derivative w.r.t. J_δ . This will generate an RG flow for kernels K_n^Λ similar to the RG flow of Γ_n . Just like in the case of Γ_n , this RG flow can be solved perturbatively.

再代入式 (113)，对 J_δ 求导。这将得到核函数 K_n^Λ 的 RG 流，与 Γ_n 的 RG 流形式类似。和 Γ_n 的情况一样，该 RG 流也可以微扰求解。

Several comments are in order.

接下来做几点说明。

1. The equations (117) fix the Λ dependence of the vertices in the Wilsonian effective action so that all physical observables do not depend on the cutoff. This, however, does not specify the vertices completely. For that, we need to set up initial conditions for the RG equations at any given order in g^2 . To that end, we need to match the low-energy TSPT correlation functions to n-point functions of the EFTofLSS. We will discuss this matching in detail shortly.

1. 方程 (117) 固定了威尔逊有效作用量中顶点对 Λ 的依赖关系，从而保证所有物理观测量都不依赖于截断。但这并不能完全确定顶点，为此我们需要为 RG 方程在 g^2 的任意阶设定初始条件。具体来说，我们需要将低能 TSPT 关联函数与 EFTofLSS 的 n 点函数做匹配，我们很快会详细讨论这个匹配过程。

2. From Eq. (116), we observe that all the counterterms are manifestly local in time. This can be contrasted with the usual EFT of LSS where locality in time of the final correlation functions emerges only a posteriori.

2. 从式 (116) 可以看到，所有抵消项都明显是时间局域的。这和通常的大尺度结构 EFT 不同，后者最终关联函数的时间局域性是事后才得到的。

3. Renormalization of the connected correlation functions Γ_n has an important technical advantage: it guarantees that our renormalization procedure is consistent in the Bogoliubov-Parasiuk-Hepp-Zimmermann sense. That means the counterterm that cancels a divergence from a certain one-particle irreducible (1PI)

diagram will also cancel similar divergences that appear in more complicated diagrams embedding this 1PI graph. Therefore, once a particular 1PI diagram is renormalized, one should not worry about divergences which may appear in more complex graphs involving this diagram - they must be canceled by the same

3. 连通关联函数 Γ_n 的重整化有一个重要的技术优势: 它保证了我们的重整化过程在博戈留波夫-帕西亚克-赫普-齐默尔曼意义下自洽。这意味着，抵消某个单粒子不可约 (1PI) 图发散的抵消项，同样可以抵消包含该 1PI 图的更复杂图中出现的同类发散。因此，一旦某个特定 1PI 图完成重整化，就无需担心包含该图的更复杂图中出现新的发散——这些发散必然会被同一个

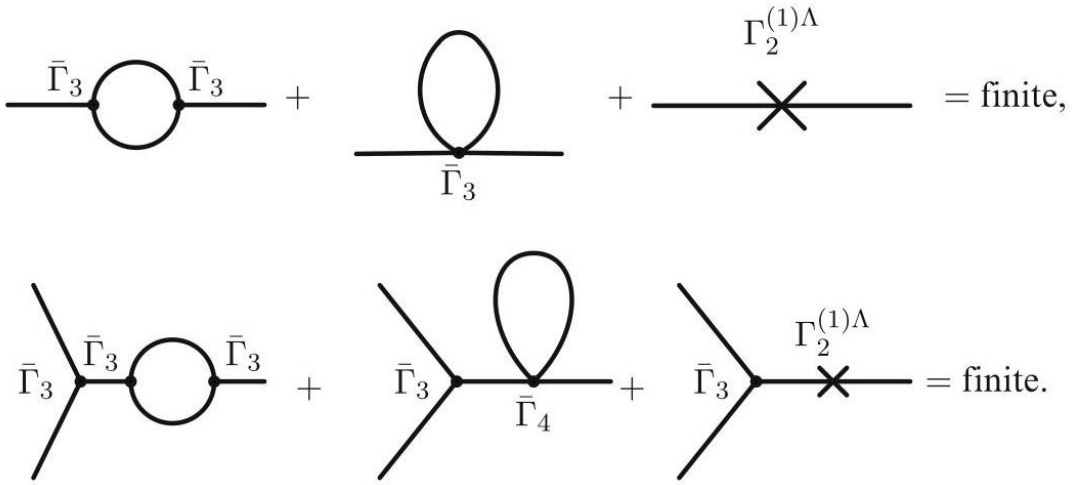

Fig. 9 Diagrammatic representation of the systematic UV renormalization in TSPT: lower-loop order diagrams embedded in higher-order ones (nested divergences) do not require new counterterms. They are removed by the same counterterms that renormalize lower-order 1PI correlation functions

图 9 TSPT 中系统性紫外重整化的图表示: 低圈阶图嵌入高圈阶图 (嵌套发散) 不需要新的抵消项，这些发散可以用重整化低阶 1PI 关联函数的同一组抵消项消除

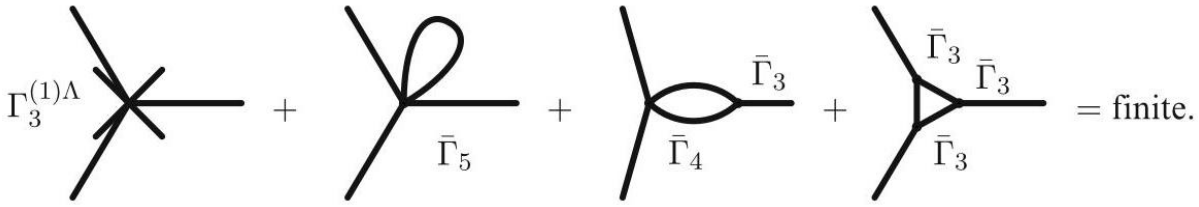

Fig. 10 Diagrammatic representation of the systematic UV renormalization in TSPT: new counterterms are required only for the one-particle irreducible correlation functions

图 10 时间切片微扰论 (TSPT) 中系统性紫外重整化的图表示: 仅单粒子不可约关联函数需要新 counterterms(抵消项)

1PI counterterm inserted in an analogous graph. This procedure is illustrated in Fig. 9.

插入在类似图中的 1PI 抵消项。该过程如图 9 所示。

As a consequence of the systematic renormalization, new counterterms are required only for the connected correlation functions; see Fig. 10. Note that this is not the case in the usual Eulerian EFTofLSS [1].

作为系统性重整化的结果，仅连通关联函数需要新的抵消项，参见图 10。请注意，常规欧拉格式 LSS 有效场论 (EFTofLSS)[1] 并非如此。

Tree-Level RG Matching

树层级重整化群匹配

It is reasonable to assume that the tree-level vertices $\left(\sim g^{-2}\right)$ for momenta $k < \Lambda$ coincide with those derived from PPF. This is natural as the difference between PPF and real dynamics should only appear in loop calculations. Thus, we can demand that the tree-level vertices reproduce the ones from PPF TSPT in the limit $\Lambda \to \infty$. An explicit calculation shows that $\Gamma_3^{\prime(0),\Lambda}\left(\mathbf{k}_1, \mathbf{k}_2, \mathbf{k}_3\right) = \overline{\Gamma}_3^{\prime}\left(\mathbf{k}_1, \mathbf{k}_2, \mathbf{k}_3\right)$ and

可以合理假设，动量为 $k < \Lambda$ 的树层级顶点 $\left(\sim g^{-2}\right)$ 与从优先势函数 (PPF) 导出的顶点一致。这很合理，因为优先势函数和真实动力学之间的差异只会出现在圈计算中。因此我们可以要求，在极限 $\Lambda \to \infty$ 下，树层级顶点还原出优先势函数三体可微传播理论 (TSPT) 中的顶点。显式计算表明 $\Gamma_3^{\prime(0),\Lambda}\left(\mathbf{k}_1, \mathbf{k}_2, \mathbf{k}_3\right) = \overline{\Gamma}_3^{\prime}\left(\mathbf{k}_1, \mathbf{k}_2, \mathbf{k}_3\right)$ 且

$$\Gamma_4^{\prime(0),\Lambda}\left(\mathbf{k}_1, \mathbf{k}_2, \mathbf{k}_3, \mathbf{k}_4\right) = \overline{\Gamma}_4^{\prime}\left(\mathbf{k}_1, \mathbf{k}_2, \mathbf{k}_3, \mathbf{k}_4\right) \tag{119}$$

$$-\left(H\left(k_{12}-\Lambda\right)\overline{\Gamma}_3^{\prime}\left(\mathbf{k}_1, \mathbf{k}_2, -\mathbf{k}_{12}\right)\bar{P}\left(k_{12}\right)\overline{\Gamma}_3^{\prime}\left(\mathbf{k}_3, \mathbf{k}_4, -\mathbf{k}_{34}\right) + \text{ cyc .}\right).$$

Note that the Λ dependence appears for the first time in the tree-level four-point vertex.

注意，Λ 依赖项首次出现在树层级四顶点中。

One-Loop RG Matching

单圈重整化群匹配

The one-loop vertices $\left(\sim g^0\right)$ must cancel the Λ dependence appearing from the loop integrals; hence, we call them "counterterms." In order to account for physical effects of short modes, these counterterms should also have finite, Λ -independent contributions, specified by the RG initial conditions. One way to fix them is to match the one-loop renormalized vertices to the TSPT vertices obtained when the dynamical kernels I_n from PPF are replaced by those of the EFTofLSS. The first non-trivial counterterm that we find is the one-point function that cancels the tadpole. This counterterm can be identified with C_1 in the TSPT for the PPF equations. Solving the RG equations for the power spectrum, we find the following one-loop counterterm:

单圈顶点 $(\sim g^0)$ 必须抵消圈积分中出现的 Λ 依赖，因此我们将其称为“抵消项”。为了体现短模式的物理效应，这些抵消项还应包含由重整化群初始条件指定的有限、与 Λ 无关的贡献。确定这些抵消项的一种方法是，将单圈重整化顶点与将 PPF 的动力学核 I_n 替换为 LSS 有效场论 (EFTofLSS) 的动力学核后得到的 TSPT 顶点进行匹配。我们找到的第一个非平凡抵消项是消除蝌蚪图的单点函数。该抵消项可以对应到 PPF 方程 TSPT 中的 C_1。求解功率谱的重整化群方程，我们得到如下单圈抵消项:

$$\Gamma_2'^{(1),\Lambda}(\mathbf{k},-\mathbf{k}) = \Gamma_2'^{(1),\,\text{infinite}}(\mathbf{k},-\mathbf{k};\Lambda) + \Gamma_2'^{(1),\,\text{finite}}(\mathbf{k},-\mathbf{k})$$

$$= \frac{1}{2}\int_{\mathbf{q}} \bar{P}(q)\,\bar{\Gamma}_4'(\mathbf{q},-\mathbf{q},\mathbf{k},-\mathbf{k})\,H(q-\Lambda)$$

$$-\frac{1}{2}\int_{\mathbf{q}} \bar{P}(q)\,\bar{P}(|\mathbf{k}-\mathbf{q}|)\,\bar{\Gamma}_3'(\mathbf{q},-\mathbf{q}+\mathbf{k},-\mathbf{k})\,\bar{\Gamma}_3'(-\mathbf{q},\mathbf{q}-\mathbf{k},\mathbf{k})\,H(q-\Lambda)$$

$$+C_2^{(1)}(\mathbf{k},-\mathbf{k}) + \Gamma_2'^{(1),\,\text{finite}}(\mathbf{k},-\mathbf{k}).$$

(120)

The first two terms in the r.h.s. above are simply minus the UV limits of the one-loop integrals. Their presence guarantees that the UV divergences of the loop expansion would be canceled for any initial power spectrum. The third term in the r.h.s. is the TSPT PPF counterterm C_n , which we included in order to reproduce the PPF result in the $\Lambda \to \infty$ limit (Inclusion of this term in $\Gamma_2'^{(1),\Lambda}(\mathbf{k},-\mathbf{k})$ is optional. It can be considered as a particular renormalization scheme.). The last term $\Gamma_2'^{(1),\,\text{finite}}(\mathbf{k},-\mathbf{k})$ is the finite counterterm that captures the physical backreaction of short-scale modes. The simplest way to reproduce the one-loop EFT corrections is to use the UV-inspired approach that assumes that the k dependence of the finite counterterm matches that of the infinite counterterm part,

上述等式右侧的前两项恰好是单圈积分紫外极限的负值。它们的存在保证了对于任意初始功率谱，圈展开的紫外发散都能被抵消。等式右侧第三项是 TSPT PPF 抵消项 C_n ，我们加入它是为了在 $\Lambda \to \infty$ 极限下重现 PPF 结果 (该项是否包含在 $\Gamma_2'^{(1),\Lambda}(\mathbf{k},-\mathbf{k})$ 中是可选的，可将其视为一种特殊的重整化方案)。最后一项 $\Gamma_2'^{(1),\,\text{finite}}(\mathbf{k},-\mathbf{k})$ 是有限抵消项，描述短尺度模式的物理反作用。重现单圈 EFT 修正最简单的方法是采用紫外启发的方法，该方法假设有限抵消项的 k 依赖与无穷大抵消项部分的依赖一致，

$$\Gamma_2'^{(1),\,\text{infinite}}(\mathbf{k},-\mathbf{k};\Lambda) = \mathcal{O}(1)\times\frac{k^2}{P_L(k)}\int_{\mathbf{q},q\geq\Lambda}\frac{P(q)}{q^2}$$

(121)

$$\Rightarrow \Gamma_2'^{(1),\,\text{finite}}(\mathbf{k},-\mathbf{k}) = \frac{\alpha(\eta)\,k^2}{P_L(k)\,k_{\text{NL}}^2},$$

where the coefficient α needs to be fixed by observations. Formally, the above equation reproduces the power spectrum correction due to the effective stress tensor $\sim k^2 P_{11}$. As mentioned above, however, a more systematic procedure would be to match the finite counterterms to the EFTofLSS n-point functions. This way, it is guaranteed that all physical EFT corrections are taken into account.

其中系数 α 需要由观测确定。形式上，上述方程重现了有效应力张量 $\sim k^2 P_{11}$ 带来的功率谱修正。但正如上文所述，更系统的处理方式是将有限抵消项与 EFTofLSS 的 n 点函数匹配。通过这种方法，可以保证所有物理的 EFT 修正都被纳入考虑。

Comparison with Data

与数据对比

As we have discussed earlier, IR resummation and UV counterterms are necessary in order to describe the actual data. In the context of dark matter, we show here that the one- and two-loop EFT model allows to noticeably increase the range of validity of the analytic description and fit the N-body simulation data down to scales where naive phenomenological models, like SPT, break down.

正如我们此前讨论的，要描述实际数据，红外重求和和紫外抵消项是必不可少的。本文针对暗物质情况证明，单圈和两圈 EFT 模型可以显著拓宽解析描述的有效范围，能够将 N 体模拟数据拟合到朴素唯象模型 (如 SPT) 失效的尺度。

In Fig. 11, we show the results for the matter power spectrum of the Horizon Run N-body simulations at $z = 0$. We see that linear theory breaks down at $k \approx 0.03 h\text{Mpc}^{-1}$, while the one- and two-loop IR-resummed EFT models fit the data up to $k \approx 0.12 h\text{Mpc}^{-1}$ and $k \approx 0.27 h\text{Mpc}^{-1}$, respectively. We see that both the overall slope and the shape of the BAO wiggles are well captured by the EFT. In order to emphasize the success of IR resummation, we show in the right panel of Fig. 11 the results for the position space two-point correlation function. We see that the shape of the BAO peak is now accurately captured, which can be contrasted with the linear theory and PPF approximation results 4.

图 11 给出了 $z = 0$ 处 Horizon Run N 体模拟的物质功率谱结果。我们可以看到，线性理论在 $k \approx 0.03 h\text{Mpc}^{-1}$ 处就已失效，而经过红外重求和的单圈和两圈 EFT 模型分别可以在直至 $k \approx 0.12 h\text{Mpc}^{-1}$ 和 $k \approx 0.27 h\text{Mpc}^{-1}$ 的范围内拟合数据。可以看到，EFT 很好地捕捉了 BAO 振荡的整体斜率和形状。为了突出红外重求和的效果，我们在图 11 的右 panel 给出位置空间两点关联函数的结果。我们可以看到，BAO 峰的形状现在被准确捕捉，这和线性理论以及 PPF 近似的结果 4 形成了鲜明对比。

Galaxy Bias and Redshift Space Distortions

星系偏差与红移空间畸变

So far, our discussion has been limited to the case of dark matter in physical coordinate space. What we observe in spectroscopic galaxy surveys are actually galaxies, which trace matter in a non-linear fashion. The coordinates of these galaxies are reconstructed using their observed redshifts, which are contaminated by peculiar velocities. Both effects represent extra sources of non-linearity, which can be systematically incorporated in the EFTofLSS theory model. In this section, we will discuss these effects very briefly. An interested reader can find more details in comprehensive reviews [6, 31] and original works [3, 45, 46, 49, 62, 64] .

迄今为止，我们的讨论仅限于物理坐标空间中的暗物质情形。我们在星系巡天光谱观测中实际探测到的是星系，星系以非线性方式追踪物质分布。这些星系的坐标是通过观测红移重构得到的，而本动速度会污染红移观测结果。上述两种效应都是非线性的额外来源，都可以系统地纳入 EFTofLSS 理论模型中。本节我们将非常简要地讨论这些效应，感兴趣的读者可以在综述 [6, 31] 和原始研究 [3, 45, 46, 49, 62, 64] 中找到更多细节。

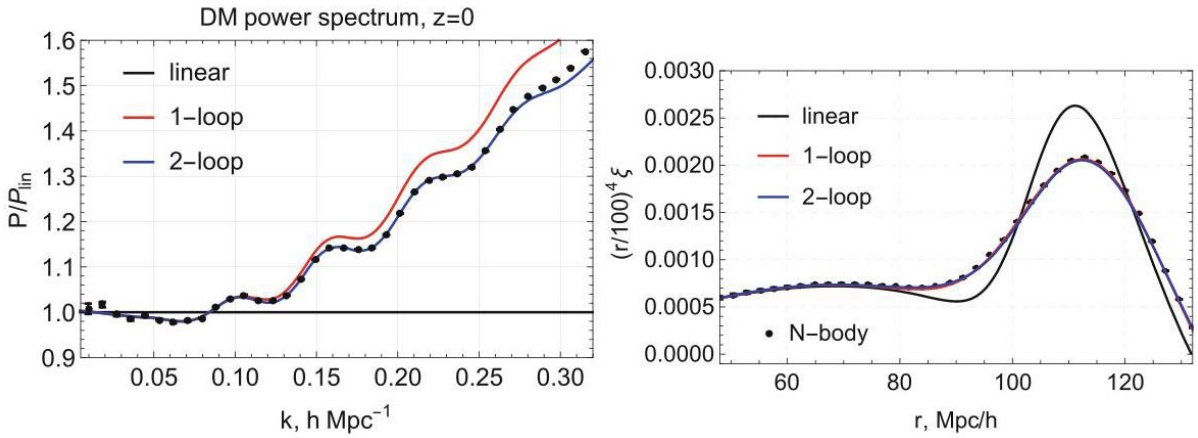

Fig. 11 Left panel: Matter power spectra normalized to the linear theory prediction $P_{\rm lin}$. We show the fully non-linear spectrum extracted from the Horizon Run (HR) N-body simulation (dots) at $z = 0$, the linear theory curve (straight black line), and the IR-resummed EFT model at one-and two-loop orders (in red and blue, respectively). Right panel: The position space two-point correlation function for the same models against the HR data

图 11 左图: 归一化到线性理论预测的物质功率谱 $P_{\rm lin}$ 。我们展示了 $z = 0$ 处从 Horizon Run(HR)N 体模拟提取的全非线性谱 (点)、线性理论曲线 (黑色直线)，以及一阶和两阶圈阶的红外重整 EFT 模型 (分别为红色和蓝色)。右图: 相同模型对应位置空间的两点关联函数与 HR 数据的对比

Galaxies in the EFT

有效场论中的星系

The relationship between the galaxy density and the underlying matter field is called ”galaxy bias.” In the EFT framework, one can describe this relationship entirely based on the symmetries and the decoupling argument. On general grounds, the observed galaxy density on large scale can only be a function of the long-wavelength density and the tidal field $t^{ij} \propto \partial_i\partial_j\Phi - (1/3)\,\delta_{ij}\Delta\Phi$. Since the time evolution of small scales is slow, we need to include memory effects. To that end, one should write down a time integral that involves all possible operators consistent with symmetries and built from the long-wavelength degrees of freedom, taken along the fluid trajectory,

星系密度与 underlying 物质场之间的关系被称为“星系偏置”。在 EFT 框架下，我们可以完全基于对称性和退耦论证描述该关系。一般而言，大尺度上观测到的星系密度只能是长波密度与潮汐场 $t^{ij} \propto \partial_i \partial_j \Phi - (1/3)\,\delta_{ij} \Delta \Phi$ 的函数。由于小尺度的时间演化较慢，我们需要纳入记忆效应。为此，我们应当写下一个时间积分，它包含所有满足对称性、由长波自由度沿着流体轨迹构建的可能算符，

$$\delta_g = \int^{\tau} d\tau' \mathcal{H}(\tau') \Big[K_\delta(\tau,\tau')\,\delta(\mathbf{x}_{\rm fl}(\tau'),\tau') + K_{\delta^2}(\tau,\tau')\,\delta^2(\mathbf{x}_{\rm fl}(\tau'),\tau')$$

$$+ K_{t^2}(\tau,\tau')\,t_{ij}t^{ij}(\mathbf{x}_{\rm fl}(\tau'),\tau) + K_{\nabla^2\delta}(\tau,\tau')\,R_*^2 \nabla^2_{\mathbf{x}_{\rm fl}} \delta(\mathbf{x}_{\rm fl}(\tau'),\tau') + \ldots \Big], \tag{122}$$

where K_i are some unknown evolution kernels and R_* is a typical length scale associated with galaxy formation physics, $R_* \sim R_{\rm vir}$, on general grounds. The bias expansion must also include stochastic contributions that are uncorrelated with the long-wavelength matter fields. In perturbation theory, the expression (122) can be simplified in the same way as we treated the time non-locality of the effective stress tensor. In particular, at leading order, one would just get

其中 K_i 是若干未知演化核，R_* 是与星系形成物理关联的特征长度标度，一般情况下为 $R_* \sim R_{\rm vir}$。偏置展开还必须包含与长波物质场不相关的随机贡献。在微扰论中，式 (122) 可以按照我们处理有效应力张量时间非定域性的相同方法简化。具体而言，在领头阶我们仅能得到

$$\delta_g = \int^{\tau} d\tau' K_\delta(\tau,\tau')\,\delta(\mathbf{x}_{\rm fl}(\tau'),\tau')$$

$$= \left[\int^{\tau} d\tau' K_\delta(\tau,\tau')\right]\delta(\mathbf{x},\tau) + \left[\int^{\tau} d\tau' K_\delta(\tau,\tau')(\tau'-\tau)\right]\frac{D}{D\tau}\delta(\mathbf{x},\tau) + \ldots$$

$$= b_1 \delta^{(1)}(\mathbf{x},\tau),$$

(123)

which is called the linear bias relation. The linear bias parameter b_1 is a Wilson coefficient, which has to be retrieved from data. Note that in general the bias coefficients receive UV contributions from loops and need to be renormalized. The EFTofLSS allows one to go beyond the leading order bias expansion (123) in a systematic and consistent fashion. A similar progress has been made for baryonic effects [16,45].

它被称为线性偏置关系。线性偏置参数 b_1 是威尔逊系数，必须从数据中提取得到。注意一般而言，偏置系数会来自圈图的紫外贡献，因此需要重整化。大尺度结构有效场论 (EFTofLSS) 允许我们以系统、自洽的方式超出领头阶偏置展开 (123)。重子效应方面也取得了类似进展 [16,45]。

Redshift Space Distortions

红移空间畸变

The observed coordinates of a galaxy are two angles fixing the position on the sky and a redshift. If the galaxies were moving exactly with the Hubble flow, their redshift could be unambiguously converted into a

radial distance. In reality, however, each galaxy has a peculiar velocity w.r.t. the Hubble flow, i.e., its apparent position is a distorted version of the actual position. This effect is called redshift space distortions.

星系的观测坐标由两个确定天球位置的角度和一个红移组成。如果星系完全随哈勃流运动，那么红移可以被明确转换为径向距离。但实际上，每个星系都存在相对于哈勃流的本动速度，也就是说，它的视位置是实际位置发生畸变后的结果。这一效应被称为红移空间畸变。

Neglecting relativistic effects, and assuming that the galaxy is far away from us, the distorted position $\mathbf{s}$ (called a position in "redshift space") is given by the actual position $\mathbf{x}$ in configuration space plus a velocity-dependent correction,

忽略相对论效应，并假设星系距离我们足够遥远，畸变后的位置 $\mathbf{s}$ (称为「红移空间」中的位置) 由构型空间中的实际位置 $\mathbf{x}$ 加上依赖速度的修正项给出，

$$x^i_{\mathrm{RS}} = x^i + \frac{v^j \hat{z}_j}{\mathcal{H}} \hat{z}_i, \tag{124}$$

where $\hat{z}_i$ is the line-of-sight direction unit vector which we choose to coincide with the z-axis. Since a galaxy distribution is simply reshuffled, the total mass remains intact, which allows us to take advantage of mass conservation,

其中 $\hat{z}_i$ 是视线方向单位矢量，我们取其与 z 轴重合。由于星系分布仅发生位置重排，总质量保持不变，因此我们可以利用质量守恒关系，

$$\left(1 + \delta_g^{(\mathrm{RS})}(\mathbf{x}_{\mathrm{RS}})\right) d^3 x_{\mathrm{RS}} = \left(1 + \delta_g(\mathbf{x})\right) d^3 x. \tag{125}$$

Using the Jacobian of the map $\mathbf{x} \to \mathbf{x}_{\mathrm{RS}}$, the galaxy density in redshift space can be simply expressed as

利用映射 $\mathbf{x} \to \mathbf{x}_{\mathrm{RS}}$ 的雅可比矩阵，红移空间中的星系密度可以简单表示为

$$\delta_g^{(\mathrm{RS})}(\mathbf{k}) = \delta_g(\mathbf{k}) + \int d^3 x e^{i\mathbf{k}\mathbf{x}} \left[\exp\left\{ik^i \hat{z}_i \left(v^j \hat{z}_j\right)/\mathcal{H}\right\} - 1\right]\left[1 + \delta_g(\mathbf{x})\right]. \tag{126}$$

Expanding the r.h.s. to linear order and using the linear theory results $v^i = -f\mathcal{H}\left[\partial_i/\Delta\right]\delta, \delta_g = b_1\delta$, we get the famous Kaiser formula [43],

将右侧展开到线性阶，并代入线性理论结果 $v^i = -f\mathcal{H}\left[\partial_i/\Delta\right]\delta, \delta_g = b_1\delta$ ，我们得到著名的凯泽公式 [43],

$$\delta_g^{(\mathrm{RS})}(\mathbf{k}) = \left(b_1 + f\frac{k_z^2}{k^2}\right)\delta(\mathbf{k}). \tag{127}$$

In order to include non-linear corrections, we need to retain higher powers of the velocity field in Eq. (126). This will generate contact operators that have uncontrolled UV sensitivity. This can be removed by coarse graining the perturbative Taylor expansion of (126), which will produce new effective operators due to smoothing just like the smoothing of the effective dark matter stress tensor produced the effective sound speed and viscosity. This procedure can be systematically carried out to any desired perturbative order in the EFT.

若要纳入非线性修正，我们需要保留式 (126) 中速度场的更高次幂项，这会产生紫外灵敏度无法控制的接触算符。对式 (126) 的微扰泰勒展开做粗粒化即可消除该问题，和有效暗物质应力张量经过平滑后产生有效声速与粘滞类似，粗粒化平滑后会产生新的有效算符。这一步骤可以在有效场论 (EFT) 框架下系统地进行，满足任意期望的微扰阶数要求。

Summary and Outlook

总结与展望

In this chapter, we have presented the basics of the EFTofLSS. We have shown that the description of the observed galaxy distribution consists of three main ingredients: non-linearities in the underlying dark matter fluid, non-linearities in the bias expansion, and non-linearities in the redshift space distortions.

在本章中，我们介绍了大尺度结构有效场论 (EFTofLSS) 的基础内容。我们已经说明，对观测得到的星系分布的描述包含三个核心组成部分: 暗物质本底流体的非线性、偏差展开中的非线性，以及红移空间畸变中的非线性。

In this chapter, we have mostly focused on the first ingredient: the non-linear evolution of dark matter in the perturbative regime. We have shown that the correct and self-consistent dark matter model in this case is a non-ideal fluid with some effective stress tensor. This stress tensor captures the long-range effects of short-scale (UV) degrees of freedom. We have also discussed in detail the non-linear evolution of the BAO, which requires a non-perturbative treatment. This treatment can be developed in the context of TSPT. In addition, TSPT provides certain insights into the UV renormalization procedure.

在本章中，我们主要关注第一个组成部分: 微扰 regime 下暗物质的非线性演化。我们已经说明，在该情形下，正确且自洽的暗物质模型是带有有效应力张量的非理想流体。该应力张量描述了小尺度 (紫外) 自由度对长程范围的影响。我们还详细讨论了重子声学振荡 (BAO) 的非线性演化，该过程需要非微扰处理，而这种处理可以在截断标准微扰论 (TSPT) 框架下构建。此外，TSPT 还为紫外重整化过程提供了若干重要启发。

Once all necessary IR and UV effects are properly accounted for, we find perfect agreement between N-body data and the EFTofLSS model for the matter power spectrum. This is not a coincidence, as the EFTofLSS is the only mathematically consistent way to build a non-linear cosmological perturbation theory for matter and galaxies. A key advantage of this approach is its systematicity, i.e., the ability to account for all non-linear clustering effects in a controlled fashion. Thus, the EFTofLSS is a powerful and efficient theoretical tool for precision large-scale structure calculations.

当所有必要的红外与紫外效应都被恰当考虑后，我们发现 N-body 模拟得到的物质功率谱数据与 EFTofLSS 模型完全吻合。这并非巧合:EFTofLSS 是唯一一种在数学上自洽的、用于构建物质与星系非线性宇宙学微扰论的方法。该方法的核心优势在于它的系统性，即可控地纳入所有非线性成团效应。因此，EFTofLSS 是进行精确大尺度结构计算的强大且高效的理论工具。

We have touched upon bias and RSD, but very briefly. We refer the interested reader to reviews for more detail. There are many other topic that we have not mentioned due to the brevity of this chapter. This include

Lagrangian EFTofLSS [20, 21, 47, 53, 69, 70], efficient evaluation of loop integrals for the EFTofLSS [26, 66], field-level EFT [67], higher-order statistics [34, 42, 54- 56], primordial non-Gaussianity [4, 5, 17, 19, 68] , massive neutrinos [13, 25, 65] , as well as applications of the EFTofLSS to the actual galaxy clustering data (e.g., [22, 28, 30, 35, 37, 38, 40, 41, 57]). We hope to explore these topics elsewhere in the future.

我们仅简要提及了偏差与红移空间畸变 (RSD)，感兴趣的读者可以参考综述获取更多细节。受本章篇幅限制，还有许多主题我们并未涉及，其中包括拉格朗日形式的 EFTofLSS [20, 21, 47, 53, 69, 70]、EFTofLSS 圈积分的高效计算方法 [26, 66]、场层面 EFT [67]、高阶统计量 [34, 42, 54-56]、原初非高斯性 [4, 5, 17, 19, 68] 、中微子质量 [13, 25, 65] ， 以及 EFTofLSS 在实际星系成团观测数据中的应用 (例如 [22, 28, 30, 35, 37, 38, 40, 41, 57])。我们希望未来能在其他工作中对这些主题展开探讨。

References

参考文献

1. A.A. Abolhasani, M. Mirbabayi, E. Pajer, JCAP 05, 063 (2016). https://doi.org/10.1088/1475- 7516/2016/05/063, [arXiv:1509.07886 [hep-th]]

2. N. Aghanim et al., [Planck], Astron. Astrophys. 641, A6 (2020); [erratum: Astron. Astrophys. 652, C4 (2021)]. https://doi.org/10.1051/0004-6361/201833910, [arXiv:1807.06209 [astro-ph.CO]]

3. V. Assassi, D. Baumann, D. Green, M. Zaldarriaga, JCAP 08, 056 (2014). https://doi.org/10.1088/1475-7516/2014/08/056, [arXiv:1402.5916 [astro-ph.CO]]

4. V. Assassi, D. Baumann, E. Pajer, Y. Welling, D. van der Woude, JCAP 11, 024 (2015). https://doi.org/10.1088/1475-7516/2015/11/024, [arXiv:1505.06668 [astro-ph.CO]]

5. V. Assassi, D. Baumann, F. Schmidt, JCAP 12, 043 (2015). https://doi.org/10.1088/1475-7516/ 2015/12/043, [arXiv:1510.03723 [astro-ph.CO]]

6. T. Baldauf, https://doi.org/10.1093/oso/9780198855743.003.0007

7. T. Baldauf, L. Mercolli, M. Mirbabayi, E. Pajer, JCAP 05, 007 (2015). https://doi.org/10.1088/ 1475-7516/2015/05/007, [arXiv:1406.4135 [astro-ph.CO]]

8. T. Baldauf, M. Mirbabayi, M. Simonović, M. Zaldarriaga, Phys. Rev. D 92(4), 043514 (2015). https://doi.org/10.1103/Phys [arXiv:1504.04366 [astro-ph.CO]]

9. D. Baumann, A. Nicolis, L. Senatore, M. Zaldarriaga, JCAP 07, 051 (2012). https://doi.org/10.1088/1475-7516/2012/07/051, [arXiv:1004.2488 [astro-ph.CO]]

10. F. Bernardeau, S. Colombi, E. Gaztanaga, R. Scoccimarro, Phys. Rept. 367, 1-248 (2002). https://doi.org/10.1016/S0370- 1573(02)00135-7, [arXiv:astro-ph/0112551 [astro-ph]]

11. D. Blas, M. Garny, T. Konstandin, JCAP 09, 024 (2013). https://doi.org/10.1088/1475-7516/ 2013/09/024, [arXiv:1304.1546 [astro-ph.CO]]

12. D. Blas, M. Garny, T. Konstandin, JCAP 01, 010 (2014). https://doi.org/10.1088/1475-7516/ 2014/01/010, [arXiv:1309.3308 [astro-ph.CO]]

13. D. Blas, M. Garny, T. Konstandin, J. Lesgourgues, JCAP 11, 039 (2014). https://doi.org/10.1088/1475-7516/2014/11/039, [arXiv:1408.2995 [astro-ph.CO]]

14. D. Blas, M. Garny, M.M. Ivanov, S. Sibiryakov, JCAP 07, 052 (2016). https://doi.org/10.1088/ 1475-7516/2016/07/052, [arXiv:1512.05807 [astro-ph.CO]]

15. D. Blas, M. Garny, M.M. Ivanov, S. Sibiryakov, JCAP 07, 028 (2016). https://doi.org/10.1088/ 1475-7516/2016/07/028, [arXiv:1605.02149 [astro-ph.CO]]

16. D.P.L. Bragança, M. Lewandowski, D. Sekera, L. Senatore, R. Sgier, JCAP 10, 074 (2021). https://doi.org/10.1088/1475-7516/2021/10/074, [arXiv:2010.02929 [astro-ph.CO]]

17. G. Cabass, M.M. Ivanov, O.H.E. Philcox, M. Simonović, M. Zaldarriaga, Phys. Rev. Lett. 129(2), 021301 (2022). https://doi.org/10.1103/PhysRevLett.129.021301, [arXiv:2201.07238 [astro-ph.CO]]

18. G. Cabass, M.M. Ivanov, M. Lewandowski, M. Mirbabayi, M. Simonović, [arXiv:2203.08232 [astro-ph.CO]].

19. G. Cabass, M.M. Ivanov, O.H.E. Philcox, M. Simonović, M. Zaldarriaga, Phys. Rev. D 106(4), 043506 (2022). https://doi.org/10.1103/PhysRevD.106.043506, [arXiv:2204.01781 [astro-ph.CO]]

20. S.F. Chen, Z. Vlah, M. White, JCAP 07, 062 (2020). https://doi.org/10.1088/1475-7516/2020/ 07/062, [arXiv:2005.00523 [astro-ph.CO]]

21. S.F. Chen, Z. Vlah, E. Castorina, M. White, JCAP 03, 100 (2021). https://doi.org/10.1088/ 1475-7516/2021/03/100, [arXiv:2012.04636 [astro-ph.CO]]

22. S.F. Chen, Z. Vlah, M. White, JCAP 02(02), 008 (2022). https://doi.org/10.1088/1475-7516/ 2022/02/008, [arXiv:2110.05530 [astro-ph.CO]]

23. J.J.M. Carrasco, M.P. Hertzberg, L. Senatore, JHEP 09, 082 (2012). https://doi.org/10.1007/ JHEP09(2012)082, [arXiv:1206.2926 [astro-ph.CO]]

24. J.J.M. Carrasco, S. Foreman, D. Green, L. Senatore, JCAP 07, 057 (2014). https://doi.org/10.1088/1475-7516/2014/07/057, [arXiv:1310.0464 [astro-ph.CO]]

25. A. Chudaykin, M.M. Ivanov, JCAP 11, 034 (2019). https://doi.org/10.1088/1475-7516/2019/ 11/034, [arXiv:1907.06666 [astro-ph.CO]]

26. A. Chudaykin, K. Dolgikh, M.M. Ivanov, Phys. Rev. D 103(2), 023507 (2021). https://doi.org/10.1103/PhysRevD.103.023507, [arXiv:2009.10106 [astro-ph.CO]]

27. A. Chudaykin, M.M. Ivanov, O.H.E. Philcox, M. Simonović, Phys. Rev. D 102(6), 063533 (2020). https://doi.org/10.1103/PhysRevD.102.063533, [arXiv:2004.10607 [astro-ph.CO]]

28. A. Chudaykin, M.M. Ivanov, M. Simonović, Phys. Rev. D 103(4), 043525 (2021). https://doi.org/10.1103/PhysRevD.103
[arXiv:2009.10724 [astro-ph.CO]]

29. M. Crocce, R. Scoccimarro, Phys. Rev. D 77, 023533 (2008). https://doi.org/10.1103/ PhysRevD.77.023533, [arXiv:0704.2783 [astro-ph]]

30. G. D'Amico, J. Gleyzes, N. Kokron, K. Markovic, L. Senatore, P. Zhang, F. Beutler, H. Gil-Marín, JCAP 05, 005 (2020). https://doi.org/10.1088/1475-7516/2020/05/005, [arXiv:1909.05271 [astro-ph.CO]]

31. V. Desjacques, D. Jeong, F. Schmidt, Phys. Rept. 733, 1-193 (2018). https://doi.org/10.1016/j.physrep.2017.12.002, [arXiv:1611.09787 [astro-ph.CO]]

32. J.F. Donoghue, M.M. Ivanov, A. Shkerin, [arXiv:1702.00319 [hep-th]]

33. M.P. Hertzberg, Phys. Rev. D 89(4), 043521 (2014). https://doi.org/10.1103/PhysRevD.89.043521, [arXiv:1208.0839 [astro-ph.CO]]

34. J. Hou, Z. Slepian, R.N. Cahn, [arXiv:2206.03625 [astro-ph.CO]]

35. M.M. Ivanov, Phys. Rev. D 104(10), 10 (2021). https://doi.org/10.1103/PhysRevD.104.103514, [arXiv:2106.12580 [astro-ph.CO]]

36. M.M. Ivanov, S. Sibiryakov, JCAP 07, 053 (2018). https://doi.org/10.1088/1475-7516/2018/ 07/053, [arXiv:1804.05080 [astro-ph.CO]]

37. M.M. Ivanov, M. Simonović, M. Zaldarriaga, JCAP 05, 042 (2020). https://doi.org/10.1088/ 1475-7516/2020/05/042, [arXiv:1909.05277 [astro-ph.CO]]

38. M.M. Ivanov, M. Simonović, M. Zaldarriaga, Phys. Rev. D 101(8), 083504 (2020). https://doi.org/10.1103/PhysRevD.101
[arXiv:1912.08208 [astro-ph.CO]]

39. M.M. Ivanov, A.A. Kaurov, S. Sibiryakov, JCAP 03, 009 (2019). https://doi.org/10.1088/1475- 7516/2019/03/009, [arXiv:1811.07913 [astro-ph.CO]]

40. M.M. Ivanov, E. McDonough, J.C. Hill, M. Simonović, M.W. Toomey, S. Alexander, M. Zaldarriaga, Phys. Rev. D 102(10), 103502 (2020). https://doi.org/10.1103/PhysRevD.102.103502, [arXiv:2006.11235 [astro-ph.CO]]

41. M.M. Ivanov, O.H.E. Philcox, M. Simonović, M. Zaldarriaga, T. Nischimichi, M. Takada, Phys. Rev. D 105(4), 043531 (2022). https://doi.org/10.1103/PhysRevD.105.043531, [arXiv:2110.00006 [astro-ph.CO]]

42. M.M. Ivanov, O.H.E. Philcox, T. Nishimichi, M. Simonović, M. Takada, M. Zaldar-riaga, Phys. Rev. D 105(6), 063512 (2022). https://doi.org/10.1103/PhysRevD.105.063512, [arXiv:2110.10161 [astro-ph.CO]]

43. N. Kaiser, Mon. Not. R. Astron. Soc. 227, 1-27 (1987)

44. J. Kim, C. Park, G. Rossi, S.M. Lee, J.R. Gott III, J. Korean Astron. Soc. 44, 217-234 (2011). https://doi.org/10.5303/JKAS [arXiv:1112.1754 [astro-ph.CO]]

45. M. Lewandowski, A. Perko, L. Senatore, JCAP 05, 019 (2015). https://doi.org/10.1088/1475- 7516/2015/05/019, [arXiv:1412.5049 [astro-ph.CO]]

46. M. Lewandowski, L. Senatore, F. Prada, C. Zhao, C.H. Chuang, Phys. Rev. D 97(6), 063526 (2018). https://doi.org/10.1103/PhysRevD.97.063526, [arXiv:1512.06831 [astro-ph.CO]]

47. J.E. McEwen, X. Fang, C.M. Hirata, J.A. Blazek, JCAP 09, 015 (2016). https://doi.org/10.1088/1475-7516/2016/09/015, [arXiv:1603.04826 [astro-ph.CO]]

48. L. Mercolli, E. Pajer, JCAP 03, 006 (2014). https://doi.org/10.1088/1475-7516/2014/03/006, [arXiv:1307.3220 [astro-ph.CO]]

49. M. Mirbabayi, F. Schmidt, M. Zaldarriaga, JCAP 07, 030 (2015). https://doi.org/10.1088/1475- 7516/2015/07/030, [arXiv:1412.5169 [astro-ph.CO]]

50. E. Pajer, M. Zaldarriaga, JCAP 08, 037 (2013). https://doi.org/10.1088/1475-7516/2013/08/ 037, [arXiv:1301.7182 [astro-ph.CO]]

51. P.J.E. Peebles, The Large-Scale Structure of the Universe. (Phillip James Edwin Peebles, Princeton University Press, 1980). ISBN: 978-0-691-08240-0. See also https://ui.adsabs.harvard.edu/abs/1980lssu.book.....P/abstract

52. J. Polchinski, Nucl. Phys. B 231, 269-295 (1984). https://doi.org/10.1016/0550- 3213(84)90287-6

53. R.A. Porto, L. Senatore, M. Zaldarriaga, JCAP 05, 022 (2014). https://doi.org/10.1088/1475- 7516/2014/05/022, [arXiv:1311.2168 [astro-ph.CO]]

54. O.H.E. Philcox, Phys. Rev. D 106(6), 063501 (2022). https://doi.org/10.1103/PhysRevD.106.063501, [arXiv:2206.04227 [astro-ph.CO]]

55. O.H.E. Philcox, M.M. Ivanov, Phys. Rev. D 105(4), 043517 (2022). https://doi.org/10.1103/ Phys-RevD.105.043517, [arXiv:2112.04515 [astro-ph.CO]]

56. O.H.E. Philcox, J. Hou, Z. Slepian, [arXiv:2108.01670 [astro-ph.CO]]

57. O.H.E. Philcox, M.M. Ivanov, M. Simonović, M. Zaldarriaga, JCAP 05, 032 (2020). https:// doi.org/10.1088/1475-7516/2020/05/032, [arXiv:2002.04035 [astro-ph.CO]]

58. O.H.E. Philcox, M.M. Ivanov, G. Cabass, M. Simonović, M. Zaldarriaga, T. Nishimichi, Phys. Rev. D 106(4), 043530 (2022). https://doi.org/10.1103/PhysRevD.106.043530, [arXiv:2206.02800 [astro-ph.CO]]

59. R. Scoccimarro, Astrophys. J. 544, 597 (2000). https://doi.org/10.1086/317248, [arXiv:astro-ph/0004086 [astro-ph]]

60. R. Scoccimarro, S. Colombi, J.N. Fry, J.A. Frieman, E. Hivon, A. Melott, Astrophys. J. 496, 586 (1998). https://doi.org/10.1086/305399, [arXiv:astro-ph/9704075 [astro-ph]]

61. A. Eggemeier, R. Scoccimarro, R.E. Smith, Phys. Rev. D 99(12), 123514 (2019). https://doi.org/10.1103/PhysRevD.99.12 [arXiv:1812.03208 [astro-ph.CO]]

62. L. Senatore, JCAP 11, 007 (2015). https://doi.org/10.1088/1475-7516/2015/11/007, [arXiv:1406.7843 [astro-ph.CO]]

63. L. Senatore, M. Zaldarriaga, JCAP 02, 013 (2015). https://doi.org/10.1088/1475-7516/2015/ 02/013, [arXiv:1404.5954 [astro-ph.CO]]

64. L. Senatore, M. Zaldarriaga, [arXiv:1409.1225 [astro-ph.CO]]

65. L. Senatore, M. Zaldarriaga, [arXiv:1707.04698 [astro-ph.CO]]

66. M. Simonović, T. Baldauf, M. Zaldarriaga, J.J. Carrasco, J.A. Kollmeier, JCAP 04, 030 (2018). https://doi.org/10.1088/147 7516/2018/04/030, [arXiv:1708.08130 [astro-ph.CO]]

67. F. Schmidt, F. Elsner, J. Jasche, N.M. Nguyen, G. Lavaux, JCAP 01, 042 (2019). https://doi.org/10.1088/1475-7516/2019/01/042, [arXiv:1808.02002 [astro-ph.CO]]

68. A. Vasudevan, M.M. Ivanov, S. Sibiryakov, J. Lesgourgues, JCAP 09, 037 (2019). https://doi.org/10.1088/1475-7516/2019/09/037, [arXiv:1906.08697 [astro-ph.CO]]

69. Z. Vlah, M. White, A. Aviles, JCAP 09, 014 (2015). https://doi.org/10.1088/1475-7516/2015/ 09/014, [arXiv:1506.05264 [astro-ph.CO]]

70. Z. Vlah, U. Seljak, M.Y. Chu, Y. Feng, JCAP 03, 057 (2016). https://doi.org/10.1088/1475- 7516/2016/03/057, [arXiv:1509.02120 [astro-ph.CO]]

71. K.G. Wilson, Phys. Rev. B 4, 3174-3183 (1971). https://doi.org/10.1103/PhysRevB.4.3174